POTENTIAL PAST AND FUTURE TREE MIGRATION RESPONSES TO CLIMATE CHANGE

BY

BAILEY DANIELLE MORRISON

DISSERTATION

Submitted in partial fulfillment of the requirements
for the degree of Doctor of Philosophy in Ecology, Evolution, and Conservation Biology
in the Graduate College of the
University of Illinois at Urbana-Champaign, 2018

Urbana, Illinois

Doctoral Committee:

        Associate Professor Jonathan A. Greenberg, Chair, Co-Director of Research
        Associate Professor Jennifer Fraterrigo, Co-Director of Research
        Professor Andrew Leakey
        Associate Professor Surangi Punyasena

ABSTRACT

Anthropogenic climate change is leading to dramatic fluctuations of essential climate dynamics and has become a major threat to modern ecosystem services and biodiversity because of its magnitude and rate of change. Climate is a well-known key constraint of species and ecosystem functions affecting distributions, extinction risk, altered disturbance regimes, biogeochemical cycling, and other ecological responses. Specifically, the ecological responses of forest and woodland vegetation to climate change are important to understand as they are important primary producers of many goods and services on which humans depend and provide supporting and regulating services for the environment. Tree species have already been found to have altered cover, biomass, density, carbon sink capabilities, fitness, extinction, invasion of non-native species, and diversity in response to modern climate change. Many conservation approaches aim to ameliorate the negative effects of environmental change within forest communities. However, conservation strategies assume the species composition of modern communities will exist with future climate change and rely on static protected area reserves. This may cause modern conservation practices to become obsolete with climate change because climate change is a dynamic process, unlike reserve practices, and species are known to respond to climate change independent of one another and their communities.

Climate surface resolution has the potential to complicate predictions of the ecological impacts of climate change since climate varies from local to global scales and this spatial variation is reflected in climate data. In Chapter 1, I investigated this issue by downscaling Last Glacial Maximum (LGM) and modern (1975-2005) 30-year averaged climate data to 60m resolution for the entire state of Alaska for 10 different climate variables, and then upsampled each variable to coarser resolutions (60m to 12km). Distributions of novel and disappeared climates were modeled to evaluate the locations and fractional area of novel and disappeared climates for each of my climate variables and resolutions. Novel and disappeared climates were primarily restricted to southern Alaska, although there were cases where some disappeared climates existed within coastal and interior Alaska. Novel and disappeared climates

increased, decreased, or had no clear relationship of fractional area with the coarse climate data, however, the use of coarser climate data increased the fractional area of novel and disappeared climates due to the removal of environmental variability and climate extremes. Results from Chapter 1 reinforce the importance of downscaling coarse climate data and suggests that studies analyzing the effects of climate change on ecosystems may overestimate the effects of climate change when using coarse climate data. Once I demonstrated the importance of scale in understanding climate change, I next investigated whether high-resolution climate metrics, specifically climate velocity, were suitable predictors of a species migration response to climate change.

Species have and will continue to shift their distributions in response to climate change, as species survival depends on the persistence of the suitability of a climatic niche space and their ability to keep pace with climatic changes in their realized niche. Many species are shifting their ranges in response to climate change. Climate velocity has become a commonly used index of the speeds and directions required for a species to keep pace with climate change. However, it is a simple measure of the rate at which climate is changing that disregards species-specific thresholds to their environment. In Chapter 2, using modern and LGM 60 m downscaled climate data for Alaska, I estimated the climate velocity for 8 different climate variables, as well as modeled LGM and modern distributions of white spruce using species distribution models. I then calculated the bioclimatic niche velocity of white spruce to estimate white spruce's migration response and ability to keep pace with post-glacial climate change. Each climate velocity estimate was compared to all others, as well as to the bioclimatic niche velocity of white spruce to determine if climate velocity was a suitable predictor of a species' migration response to climate change. I demonstrated that different climate variables yield different speeds and directions of climate, and that individual climate velocity estimates correlated poorly with the bioclimatic niche velocity as estimated for the Alaskan white spruce from the LGM to modern era. My results suggest that climate velocity alone does not provide suitable estimates of species migration responses to climate change due to climate velocity not accounting for species ecology and climatic tolerances that affect migration responses.

In the previous chapter, I found evidence that bioclimatic niche velocity was a suitable approach to understanding high-resolution species migration pressures due to climate change. I then used these concepts to test if multiple species will migrate in the same direction, or independent of each other in response to climate change. Modern conservation strategies use static protected-area techniques to protect biodiversity from environmental change. However, static and stable assumptions of community dynamics assume that species will migrate with each other in response to climate change and form similar community assemblages in the future, even though it is well accepted that species respond to climate change independent of one another due to species-specific niche constraints. In Chapter 3, I calculated the bioclimatic niche direction for 72 of California's native tree species derived from habitat suitability maps built using high-resolution downscaled climate data for the modern (1985-2015) and future (2070-2100) eras, and identified the directions of migration for each species in response to end of century climate change. Using each species' modern habitat suitability maps, I identified and classified the different forest community types that occur throughout California during the modern era, and identified whether all the species of a community at a location displayed uniform (anisotropic) migration directions, or random (isotropic) migration directions in response to climate change. While in general, individual tree species of California displayed mean northward migration directions, a number of species were estimated to have alternative migration directions in response to climate change. A vast majority of California forest community types displayed isotropic species migration directions, indicating species will migrate independently of each other. Although all community types exhibited small amounts of anisotropic species migrations, locations where species migrate together were not clustered together throughout the community's distributional range. My results indicated that the species that comprise California forest communities will migrate independently of each other, with the potential to create novel, no-analogue communities by the end of the 21st century. Additionally, my results suggested that current community conservation strategies should be revised and updated to reflect ecologists' better understanding of climate change and the impact it has on species.

Thank you, Mom and Dad, for your love and unconditional support.

Thank you, Jonathan, for being an awesome graduate adviser and for essentially being responsible for my knowledge of all facts comic book related.
I still think Marvel is better than DC.

Special thanks to Beau, the best wiener-beagle a human could ever be blessed with. You've been with me for all my highs and lows, as well my entire university experience for the past 13 years. I look forward to you being by my side for our next journey into post-doctoral life!

TABLE OF CONTENTS

INTRODUCTION

Earth's climate has continuously changed throughout its history, and species have been challenged to adapt (Davis & Shaw, 2001), alter phenology (Cleland, Chuine, Menzel, Mooney, & Schwartz, 2007), shift ranges (Davis & Shaw, 2001), and/or seek climatic refuges (Ashcroft, 2010; Dobrowski, 2011) to track environmental change in space and time (Burrows et al., 2011). However, modern climate change has become a major threat to ecosystem services and biodiversity because of its magnitude, rate of change, and the potential to eliminate extant climates as well as create novel conditions globally (Williams & Jackson, 2007). If modern climate change exceeds organisms' ability to respond, distributional shifts, community structures, and ecosystem functions may be greatly altered (Ackerly et al., 2010).

Many species have already responded by altering the timing of their life cycles or shifting their geographic distributions (Chen, Hill, Ohlemuller, Roy, & Thomas, 2011; Colwell, Brehm, Cardelus, Gilman, & Longino, 2008; Parmesan & Yohe, 2003), with many studies suggesting that species will shift towards higher latitudes or elevations in response to warming climates. For example, a meta-analysis conducted by Chen et al. (2011) found that the distribution of species in recent decades has shifted to higher elevations at a median rate of 11.0 m/decade, and to higher latitudes at a median rate of 16.9 km/decade. However, more recent analyses emphasize the need to move away from the expectation that species will move to cooler temperatures (Crimmins, Dobrowski, Greenberg, Abatzoglou, & Mynsberge, 2011; Dobrowski et al., 2013), as different species have individual responses to climate change. Therefore, it is important to understand how species have, are, or will migrate in response to climate change in order to plan effective conservation management strategies that preserve Earths biodiversity.

This dissertation focuses on addressing: 1) how does the spatial resolution of gridded climate data affect estimates of novel and disappeared climates, 2) is climate velocity a suitable predictor of species migration responses to climate change, and 3) do species of a forest community migrate in the same direction, or independently of on another in response to climate change? These questions are addressed by

1

developing fine resolution downscaled climate datasets for Alaska and California combined with species distribution models to produce spatially explicit estimates of the migration speeds and directions required for vegetative species to keep pace with climate change.

Chapter 1 examines the question of where novel and disappeared climates are found in Alaska from the Last Glacial Maximum (LGM) to modern era, and how choice in climate data resolution affects the fractional area of estimated novel and disappeared climates in Alaska. The analysis uses advanced statistical downscaling techniques to create the finest available gridded climate dataset in Alaska (60 m), and upsampled this dataset to coarser scales to estimate and compare the fractional area of novel and disappeared climates at different resolutions. Downscaled climate datasets incorporate many spatial features known to influence climate at finer scales (e.g. elevation gradients, coastal effects, temperature inversions, and rain shadows) that are undetectable in coarse resolution climate data. The downscaling models were developed with the specific goal of capturing these fine-scale spatial features known to influence climate across a wide variety of climate variables for both the Last Glacial Maximum (~21,000 ya) and modern (1985-2005) eras. Once I demonstrated the importance of scale in understanding climate change, I next investigate whether high-resolution climate metrics, specifically climate velocity, is a suitable predictor of a species migration response to climate change.

Climate velocity has commonly been used to infer migration rates of biota, however, all climate velocity analyses acknowledge that the measure does not incorporate species information, nor is an estimate of biological migration rates (Burrows et al., 2011; Carroll, Parks, Dobrowski, & Roberts, 2018; Loarie et al., 2009). Chapter 2 examines whether climate velocity, a measure of the rate and direction of climate change, is a suitable measure of a species migration response to climate change, by developing a species calibrated measure of climate velocity using an Environmental Limiting Factor (ELF) model of Alaskan white spruce (*Picea glauca*), "bioclimatic niche velocity", to compare to estimates of eight different climate velocity estimates. Climate velocity and ELFs are sensitive to the resolution of gridded climate data, therefore I reused my downscaled Alaska climate dataset from Chapter 1 to minimize

overestimating white spruce distributions and low velocities (Dobrowski et al., 2013; Franklin et al., 2013).

Once I demonstrated that bioclimatic niche velocity was a suitable predictor of a species response to climate change I next investigate how multiple species of forest communities will respond to climate change. Community conservation strategies rely on species of communities migrating in the same direction, as well as maintaining the same species assemblages of the modern era (Hannah et al., 2002), even though species are known to have independent responses to climate change (Hutchinson, 1957; Jackson & Overpeck, 2000). In Chapter 3, I present a study which uses the bioclimatic niche velocity introduced in Chapter 2 to estimate the migration direction of 72 endemic California tree species to end-of-century climate change. The goal of Chapter 3 is to determine if species of a community will migrate in the same direction, or independently of one another in response to climate change. use bioclimatic niche velocity to estimate the migration directions of 72 tree species endemic to California to examine whether species of a forest community type will migrate in similar directions, or independent direction in response to climate change.

REFERENCES

Ackerly, D. D., Loarie, S. R., Cornwell, W. K., Weiss, S. B., Hamilton, H., Branciforte, R., & Kraft, N. J. B. (2010). The geography of climate change: implications for conservation biogeography. *Diversity and Distributions, 16*(3), 476-487. doi:10.1111/j.1472-4642.2010.00654.x

Ashcroft, M. B. (2010). Identifying refugia from climate change. *Journal of Biogeography, 37*(8), 1407-1413.

Burrows, M. T., Schoeman, D. S., Buckley, L. B., Moore, P., Poloczanska, E. S., Brander, K. M., . . . Richardson, A. J. (2011). The Pace of Shifting Climate in Marine and Terrestrial Ecosystems. *Science, 334*(6056), 652-655. doi:10.1126/science.1210288

Carroll, C., Parks, S. A., Dobrowski, S. Z., & Roberts, D. R. (2018). Climatic, topographic, and anthropogenic factors determine connectivity between current and future climate analogs in North America. *Global change biology*.

Chen, I. C., Hill, J. K., Ohlemuller, R., Roy, D. B., & Thomas, C. D. (2011). Rapid Range Shifts of Species Associated with High Levels of Climate Warming. *Science, 333*(6045), 1024-1026. doi:10.1126/science.1206432

Cleland, E. E., Chuine, I., Menzel, A., Mooney, H. A., & Schwartz, M. D. (2007). Shifting plant phenology in response to global change. *Trends in Ecology & Evolution, 22*(7), 357-365.

Colwell, R. K., Brehm, G., Cardelus, C. L., Gilman, A. C., & Longino, J. T. (2008). Global warming, elevational range shifts, and lowland biotic attrition in the wet tropics. *Science, 322*(5899), 258-261. doi:10.1126/science.1162547

Crimmins, S. M., Dobrowski, S. Z., Greenberg, J. A., Abatzoglou, J. T., & Mynsberge, A. R. (2011). Changes in Climatic Water Balance Drive Downhill Shifts in Plant Species' Optimum Elevations. *Science, 331*(6015), 324-327. doi:10.1126/science.1199040

Davis, M. B., & Shaw, R. G. (2001). Range shifts and adaptive responses to Quaternary climate change. *Science, 292*(5517), 673-679.

Dobrowski, S. Z. (2011). A climatic basis for microrefugia: the influence of terrain on climate. *Global Change Biology, 17*(2), 1022-1035. doi:10.1111/j.1365-2486.2010.02263.x

Dobrowski, S. Z., Abatzoglou, J., Swanson, A. K., Greenberg, J. A., Mynsberge, A. R., Holden, Z. A., & Schwartz, M. K. (2013). The climate velocity of the contiguous United States during the 20th century. *Global change biology, 19*(1), 241-251. doi:10.1111/gcb.12026

Franklin, J., Davis, F. W., Ikegami, M., Syphard, A. D., Flint, L. E., Flint, A. L., & Hannah, L. (2013). Modeling plant species distributions under future climates: how fine scale do climate projections need to be? *Global change biology, 19*(2), 473-483. doi:10.1111/gcb.12051

Hannah, L., Midgley, G., Lovejoy, T., Bond, W., Bush, M., Lovett, J., . . . Woodward, F. (2002). Conservation of biodiversity in a changing climate. *Conservation biology, 16*(1), 264-268.

Hutchinson, G. (1957). Concluding remarks Cold ssring Harbor Symp. *Quant, 22*, 66-77.

Jackson, S. T., & Overpeck, J. T. (2000). Responses of plant populations and communities to environmental changes of the late Quaternary. *Paleobiology, 26*(4), 194-220. doi:Doi 10.1666/0094-8373(2000)26[194:Roppac]2.0.Co;2

Loarie, S. R., Duffy, P. B., Hamilton, H., Asner, G. P., Field, C. B., & Ackerly, D. D. (2009). The velocity of climate change. *Nature, 462*(7276), 1052-U1111. doi:10.1038/nature08649

Parmesan, C., & Yohe, G. (2003). A globally coherent fingerprint of climate change impacts across natural systems. *Nature, 421*(6918), 37-42.

Williams, J. W., & Jackson, S. T. (2007). Novel climates, no-analog communities, and ecological surprises. *Frontiers in Ecology and the Environment, 5*(9), 475-482. doi:10.1890/070037

CHAPTER 1: SPATIAL SCALE AFFECTS NOVEL AND DISAPPEARED CLIMATE CHANGE PROJECTIONS IN ALASKA

1.1 ABSTRACT

The formation of novel and disappeared climates between the Last Glacial Maximum (LGM) and the present is important to consider in order to understand the expansion and contraction of species niches and distributions, as well as the formation and loss of communities and ecological interactions over time. Our choice in climate data resolution has the potential to complicate predictions of the ecological impacts of climate change, since climate varies from local to global scales and this spatial variation is reflected in climate data. To address this issue, I downscaled LGM and modern (1975-2005) 30-year averaged climate data to 60m resolution for the entire state of Alaska for 10 different climate variables, and then upsampled each variable to coarser resolutions (60m to 12km). I modeled the distributions of novel and disappeared climates to evaluate the locations and fractional area of novel and disappeared climates for each of my climate variables and resolutions. Generally, novel and disappeared climates were located in southern Alaska, although there were cases where some disappeared climates existed within coastal and interior Alaska. Climate resolution affected the fractional area of novel and disappeared climates in three patterns: as the spatial resolution of climate became coarser, the fractional area of novel and disappeared climates 1) increased, 2) decreased, or 3) had no explainable relationship. Generally, the use of coarser climate data increased the fractional area of novel and disappeared climates due to decreased environmental variability and removal of climate extremes. Coarse climate data did decrease the fractional area of disappeared T_{min} climates, however this pattern was an artifact of computational aggregation error from upsampling my downscaled climate products. My results reinforce the importance of downscaling coarse climate data and suggest that studies analyzing the effects of climate change on ecosystems may overestimate or underestimate their conclusions when utilizing coarse climate data.

1.2 INTRODUCTION

Post-glacial climate change provides a useful context and natural experimentation for assessing biotic responses to global climate change (Davis, 1990; Overpeck, Bartlein, & Webb, 1991; Webb III, 1992). The late quaternary, which includes the LGM 21,000 years ago, matches the magnitude of predicted anthropogenic climate change and contains the largest manifestation of natural climate change preserved in the geologic record (Mix, Bard, & Schneider, 2001; Overpeck et al., 1991). Our awareness and understanding of past ecological responses to climate change is important as it enables ecologists to predict the potential responses of ecosystems to anthropogenic climate change now and in the future.

Niche theory predicts that n-dimensional changes in the environment (e.g. precipitation, temperature, etc.) will cause shifts in species distributions and the formation of novel species assemblages, since every species responds individualistically to its abiotic and biotic environment (Hutchinson, 1957; Jackson & Overpeck, 2000). This assumption has been supported by large changes in species ranges where past climates lacked modern analogs, leading to the formation of novel LGM species associations and biomes with no modern equivalent (Williams & Jackson, 2007). Therefore, variations of climate in space and time (e.g. LGM vs. Modern n-dimensional environment) are thought to be an important factor in understanding the formation of novel and disappeared climates, as well as the expansion and contraction of a species' niche and distribution (Ackerly et al., 2010; Jackson & Overpeck, 2000; Williams & Jackson, 2007). Novel climates are climatic environments with no-analog conditions in the past, whereas disappeared climates are climatic environments with no-analog conditions today (Ackerly et al., 2010; Fitzpatrick & Hargrove, 2009; Glassberg, 2014; Hobbs et al., 2006; Ohlemuller, 2011; Radeloff et al., 2015; Williams & Jackson, 2007).

A key aspect of quantifying climate, including the identification of novel and disappeared climates, is the choice of spatial resolution. Spatial resolution has the potential to complicate the prediction of ecological impacts of climate change because climate varies dramatically at local scales and this variation is undetectable in coarse resolution climate data (Bellard, Bertelsmeier, Leadley, Thuiller, & Courchamp, 2012; Dobrowski, Abatzoglou, Greenberg, & Schladow, 2009; Franklin et al., 2013; Seo,

Thorne, Hannah, & Thuiller, 2009). Long term climate patterns observed across the globe are a result of a combination of many different processes that occur at varying spatial scales. Most modeled climate data (regional and general circulation models) is coarse scale (>50 km) and these datasets are unlikely to incorporate many spatial features known to influence climate at finer scales, (e.g. elevation gradients, coastal effects, temperature inversions, and rain shadows) (C. Daly, 2006; Dobrowski et al., 2009; Levin, 1992).

Spatial variability in climate can be nested into macroclimates (global), mesoclimates (regional), topoclimates (landscape), and microclimates (local) (Ackerly et al., 2010; Geiger, Aron, & Todhunter, 2009). Macroclimates are the broad patterns of atmospheric circulation across >50 km scales, such as the North-South rainfall gradient along the state of Alaska. Mesoclimates are variations at 1-50 km reflecting marine air and mountain range properties, such as rain shadow effects. Topoclimates include landscape scale effects such as aspect, slope, elevation, and terrain that affect surface radiation, wind, and cold air drainage at the 10 m to1 km scale. Lastly, microclimates have the finest scale variability and are determined by vegetation cover and fine scale surface features (<10 m). Finer spatial scales (topo and micro) create unique combinations of climate variables within a very limited area (Ackerly et al., 2010), and can provide significant processes that buffer against larger regional and global climate trends (e.g. temperature inversions) (Randin et al., 2009; Willis & Bhagwat, 2009). For example, mesoscale PRISM mean global temperature variability is limited to 3°C, while a finer toposcale mean global temperature surface at 30 m found a global temperature variability as high as 8°C (Ackerly et al., 2010; C. Daly, 2006).

I selected climate surfaces commonly used in climate change and ecological analyses to identify and determine where novel, disappeared, and shared climates are distributed across the state of Alaska from the LGM to modern era. To help clarify the effect of climate grid resolution on estimations of novel and disappeared climates, I analyzed how the amount of fractional area of novel, disappeared, and shared climates vary with climate grid spatial resolution by statistically downscaling coarse-scale climate models

at scales ranging from 60 m to 12 km. I compared modeled distributions and fractional area of novel, disappeared, and shared climates across nine Alaskan ecoregions to ask the following specific questions:

1. Where are novel, disappeared, and shared climates located in Alaska from the LGM to modern era?

2. How does the fractional area of novel, disappeared, and shared climates differ depending on the resolution of modeled climate grid data used for analysis?

1.3 METHODS

1.3.1 Overview:

The first step of my analysis was to perform a topographically-mediated downscaling of coarse-scale modern and LGM climate surfaces to a resolution of 60 m for the modern and LGM periods. Next, I up-sampled these surfaces to coarser resolutions. Finally, I performed my analysis investigating the impacts of scale on the distribution of shared, novel, and disappeared climates throughout Alaska. Study Area:

Alaska, USA, is an ideal location for understanding the potential impacts of scale on climate change as polar regions currently experience the highest rates of warming globally, and by the end of the 21st century will be at least 40% higher than the global mean (Larsen et al., 2014). There is agreement between several coupled atmosphere-ice-ocean climate models that global warming should be enhanced in the Arctic (Raisanen, 2001). Additionally, Alaska has a diverse and complex physiography and presence of long-term meteorological stations.

The total land area in Alaska is approximately 151,773.3 km^2, with over 54,563 km of tidal shoreline, including islands, and stretches in latitude by nearly 20°. 17 of the 20 highest mountain peaks of North America are in Alaska, with the highest elevation at Mt. McKinley (6,150 m.a.s.l), and lowest at the Pacific Ocean coastline (0 m.a.s.l). Presently, there are approximately 100,000 glaciers covering 75,109.9 km^2 (5% of the total land area of Alaska), however, during the LGM, glaciers covered an

estimated 30% of the state. Present mean temperature is 16.8 °C during the summer, and -11.0 °C during the winter.

1.3.2 Climate downscale:

Input data:

Weather station data: Spatially explicit monthly weather station data was collected from the National Oceanic and Atmospheric Administration's (NOAA) Global Historical Climatology Network (GHCND) (Menne, Durre, Vose, Gleason, & Houston, 2012). I compiled records from 415 stations across the period of 1975-2005, although the period of record for each station varies. Missing data fields as well as extreme outliers were removed from the weather dataset by identifying observations > 3 standard deviations from the means of all observations across time for minimum temperature (T_{min}), maximum temperature (T_{max}), mean temperature (T_{ave}), and total monthly precipitation (P) (Aggarwal, 2015).

Digital Elevation Map and Transforms: An elevation surface was assembled for the entire state of Alaska using United States Geologic Surveys (USGS) 1 arc-second (~60 m) digital elevation maps (DEM) (USGS, 2016). The digital elevation map (DEM) was resampled and reprojected to Alaska Albers Equal Area Conic, ensuring grid cells of exactly 60 m. From this dataset, I calculated slope, aspect, and the topographic convergence index (TCI) for Alaska (Wolock & McCabe, 1995). TCI was calculated with TauDEM using a D-infinity flow accumulation algorithm (Tesfa et al., 2011). Regions where slope was 0° were given a placeholder value of 0.001 when calculating TCI to avoid divide-by-zero issues.

General circulation model climate data: Coarse-scale (1°) general circulation model (GCM) climate grids were collected from the National Center for Atmospheric Research's (NCAR) Community Climate System Model version 4 (CCSM4) for near surface (2 m) T_{min}, T_{max}, T_{ave}, precipitation, short wave radiation (I_{cloud}) and wind (U, V) (Gent et al., 2011; Kluzek, 2011). All climate surfaces were pooled into two 30-year averages, ~18,000-18,030 ya (t_1) for the LGM and 1975-2005 (t_2) for modern climate. All GCM surfaces were reprojected to the Alaska Albers Equal Area Conic projection and resampled to 60 m

resolution using bilinear interpolation. The wind speed vector surfaces were converted to wind speed and direction.

Downscaling models:

Shortwave irradiance: Solar radiation can regulate temperature in complex terrains as topography produces varying solar angles and can reduce terrain winds that diminish boundary layer mixing during the winter months (C. Daly, 2006; Dobrowski et al., 2009; Urban, Miller, Halpin, & Stephenson, 2000). Therefore, solar radiation is an important physiographic parameter to consider when downscaling temperature to topo and microscales. Mean monthly daily clear sky irradiance at a location x,y ($I_{(x,y,t)}$, W/m^2) was modeled using the r.sun algorithm (Suri & Hofierka, 2004) running under GRASS GIS 7.1. This algorithm uses topographic elevation, slope, aspect, and geographic latitude as inputs referenced against solar angles. GRASS GIS's r.sun algorithm is a complex and flexible solar radiation model that has been found to outperform other similar products (SolarFlux, Solei, Solar Analyst, and SRAD) because it performs especially well for large areas at fine resolutions with complex terrain and can be used for long-term calculations at different scales (Jaroslav, 2013; Ruiz-Arias, Tovar-Pescador, Pozo-Vázquez, & Alsamamra, 2009). To create "true sky" clouded irradiance surfaces for both the LGM and today, I acquired coarse modeled surface downwelling shortwave radiation (100 km) that was calculated by the Coupled Model Intercomparison Project (CMIP5, Modern) the Paleoclimate Modeling Intercomparison Project (PMIP5, LGM) (Taylor, Stouffer, & Meehl, 2012). These groups calculate surface downwelling shortwave radiation using additional modeled climate surfaces produced from the same CCSM4 LGM and modern historical runs used in my temperature and precipitation downscale models. To transform my high resolution "clear-sky" irradiance to "true-sky" irradiance, I calculated the ratio of true-sky to clear-sky irradiance for each month for both the LGM and today, and then applied each corresponding ratio to each monthly high resolution clear-sky irradiance surface to create twelve monthly LGM and Modern "true-sky" surface radiation surfaces that are capable of considering coarse atmospheric properties (e.g. cloud cover) of each era with my clear-sky radiation surfaces. I then summarized my monthly radiation surfaces into an annual average radiation surface to compute novel and disappeared radiation climates for

later analysis. Mean radiation was created by computing the yearly average of all monthly radiation surfaces for both the LGM and modern eras at 60 m resolution.

Temperature and precipitation: For minimum, maximum and average temperature, as well as precipitation, I used an empirical downscaling approach as described in Dobrowski et al. (2009). This approach calibrates a downscaling model in which the high-resolution climate variable is a function of the coarse scale climate and various topographic predictors (EQ 1.1). I used the following general downscaling approach:

$$EQ\ 1.1:\ Observed\ Climate_{x,y,t}^{High\ Res} = f(CCSM\ Climate_{x,y,t}^{Coarse\ Res} + Physiographic_{x,y}^{High\ Res})$$

where *observed Climate* at location (x,y) at time t represents my high resolution weather station data. *CCSM Climate* at the same (x,y) locations and time t represents my coarse GCM modeled climate. *Physiographic Inputs* at the same (x,y) locations, and when applicable time t, represents my high resolution modeled physiographic surfaces (e.g. elevation, cold-air pooling, radiation, etc.). I assume the topographic impacts on climate do not change in time, only in space, so the only varying predictors in my model are coarse scale climate and radiation inputs. My other topographic-based predictors remain constant (e.g. TCI).

I calibrated these models using weather station data to represent the high-resolution climate linked with the GCM climate grids that corresponds to the date of the weather measurement. I initially used a random forest algorithm to determine variable importance of all model predictors, including my precipitation topographic surfaces at a variety of spatial scales (60 m, 500 m, 1 km, and 5 km) for variable selection (Breiman, 2001). Using the most important variables, I produced three models for temperature (T_{min}, T_{max}, T_{ave}) calibrated using 80% of the available weather station data (43,768 observations) (Madsen & Thyregod, 2010). The remaining 20% of weather station data (10,943 observations) was used for model validation, in which I calculated the root mean square error (RMSE), Pearson's correlation coefficient, and percent bias. I created a precipitation model employing similar methods previously used to create my temperature models, however, the precipitation model was trained using a stratified sampling procedure

(vs. 80% dataset) to ensure an equal proportion of measured weather station precipitation values were represented in the training dataset since the majority of weather observations recorded 0 mm/month precipitation. The training dataset was stratified in ~310 mm width bins from randomly sampling 80% of the original precipitation dataset. I then randomly sampled 5,000 precipitation values from each bin to create the final training dataset. My testing dataset was comprised from the remaining 20% of the original precipitation dataset.

Generalized linear models (GLM) were chosen to generate all downscale models. GLMs are advantageous for downscaling because they can extrapolate beyond the range of the model's training data, which is necessary when predicting LGM climates as the range of climates is likely different than the modern climate. Additionally, GLMs can handle more complicated situations; for example, they do not require a normal distribution of the response variable (Madsen & Thyregod, 2010). A variety of tests/exploratory models were created to check that all GLM assumptions were met. To ensure that all input predictors were independent of one another, all variables were plotted against one another to verify that there were no significant relationships between each variable. A correlation threshold of 0.95 was used as a cutoff value preventing too great a multicollinearity between any pair of predictors. Additionally, an exploratory generalized additive model (GAM) was created to produce partial plots for each independent variable to verify linear behavior of all model inputs, although this method was not chosen for the final models to avoid spline interpolations on my predictors (Venables & Ripley, 2002). Lastly, each model's residuals were examined to ensure that the residuals were normally distributed. The residuals were plotted against the predicted fitted values to ensure a homogenous structure of each model's variance.

Temperature model: The model I used to downscale T_{min}, T_{max}, and T_{ave} was found to be a function of elevation at x,y ($Z_{(x,y)}$), mean monthly daily clear sky irradiance at a location x,y ($I_{(x,y,t)}$), and topographic convergence ($C_{(x,y)}$) which is a proxy for local convective forcings such as cold-air pooling (EQ 1.2) (Dobrowski, 2011; Dobrowski et al., 2009; Katurji & Zhong, 2012). The final model form was:

$$EQ\ 1.2{:}\ T_{(x,y,t,t')} = T'_{(x,y,t,t')} + Z_{(x,y)} + C_{(x,y)} + I_{(x,y,t)} + \varepsilon,$$

where $T_{(x,y,t,\ t')}$ represents observed high resolution temperature (min, max, average) at a given station (x,y) and month (t), and $T'_{(x,y,t,\ t')}$ is coarse modeled surface temperature (min, max, average). The coldest T_{min} month (December for LGM, and January for modern) was used to represent the coldest annual temperatures. Likewise, the hottest month for T_{max} (July for both LGM and modern) was used to represent the hottest annual temperatures.

Precipitation model: The model to downscale precipitation was found to require topographic predictors at a variety of scales, not just the high resolution 60 m predictors. Specifically, I used elevation at location x,y $(Z_{(x,y)})$ at 60 m; topographic slope at location x,y at 1 km resolution $(m_{x,y})$; wind speed $(m/s,\ \omega_{(x,y,t,t')})$ and wind direction at a given location (x,y) $(degrees,\ \theta_{(x,y,t')})$ and month (t) at 100 km, and the angular difference between geographic direction and topographic aspect to act as an orographic effect proxy (i.e. rain shadow) at 500 m resolution $(\Delta_{x,y,t,t'})$. Elevation and slope exhibited slight nonlinear trends which were corrected by applying a log transformation to each of the two predictor variables. A cubic root transformation was applied to $(P_{x,y,t,t'})$ and $(P'_{x,y,t,t'})$ so the model could not predict values below 0 mm/month (EQ 1.3). The final model form was:

$$EQ\ 1.3{:}\ (P_{x,y,t,t'})^{1/3} = (P'_{x,y,t,t'})^{1/3} + \log(Z_{x,y}) + \log(m_{x,y}) + \omega_{x,y,t,t'} + \theta_{x,y,t,t'} + \Delta_{x,y,t,t'} + \varepsilon$$

Potential evapotranspiration (PET): Plants must use energy and water to grow and reproduce, therefore the primary effects of climate on plants is regulated by the interactions of energy and water (Stephenson, 1990). Through water balance equations, energy is represented by potential evapotranspiration (PET) and available water (Stephenson, 1998). PET was calculated at monthly time steps at 60 m for the LGM and modern era using the Penman-Monteith method which utilizes my downscaled temperature, elevation, wind speed, and cloud-corrected irradiance surfaces as inputs (Allen, Pereira, Raes, & Smith, 1998; Monteith, 1965; Penman, 1948). This method determines a reference evapotranspiration from climate data and represent climatic water balance rather than physiological evapotranspiration. PET was calculated by using a standard hypothetical reference crop of height 0.12 m with a fixed surface stomatal

resistance of 70 s m^{-1} and albedo of 0.23. Annual PET for the LGM and modern era was summarized by computing the summation of all monthly surfaces for each era.

Actual evapotranspiration and water deficit: The interactions of PET and available water can be described with additional water balance parameters: Actual Evapotranspiration (AET) and Water Deficit (DEF). AET is defined as the evaporative water loss from a site covered by a standard crop, given the prevailing water availability, and represents biologically available usable energy and water at a site independent of actual vegetation. Water deficit refers to climatic water deficit, not soil water deficit, and represents the amount of evaporative demand that was not met by available water (Stephenson, 1998).

AET and DEF were calculated at monthly time scales at 60 m for the LGM and modern era, by using a snow hydrology model that models additional water and energy parameters that influence available water at a site (Dobrowski et al., 2013). Downscaled precipitation, mean temperature, and radiation were used to estimate the fraction of precipitation arising as either rainfall, snowfall, snowpack, or snowmelt during a given month at 60 m resolution for both the LGM and modern eras (Dingman, 2002; Dobrowski et al., 2013). These products were then used to calculate AET and DEF in combination with PET and a coarse soil water holding capacity surface (Dunne & Willmott, 1996) to determine the available plant extractable water from rainfall or snowmelt from the previous month (Dobrowski et al., 2013). A spatially constant available soil water holding capacity (AWC) value of 5.0 cm (the mean AWC of Alaska) was used rather than a spatially varying AWC due to a lack of high-resolution AWC products in Alaska (Dunne & Willmott, 1996). The model first determines the amount of maximum potential available soil water at a site. If there is an excess of soil water, AET is the same as PET because evapotranspiration is not limited by water availability. However, if available water is less than the sites maximum potential available water, AET will be less than PET (AET = PET − DEF), because maximum water evaporative demand cannot be met by the available amount of water present at the site. I created annual summaries of each surface (AET, DEF, Snow, and Rain) by computing the summation all monthly surfaces, for each climate variable, for each individual era.

1.3.3 Climate aggregation and reclassification:

To understand how climate grid resolution can potentially affect the distribution of novel and disappeared climates in Alaska, I aggregated each 60 m annual climate surface to coarser resolutions. Aggregation surfaces were created using a standard average pixel aggregation of each 60 m annual climate surface using the following resolutions:120 m, 240 m, 800 m (e.g. PRISM), 1 km (e.g. NASA Nex & WorldClim), 2 km, 3 km, 4 km, 5 km, 10 km, and 12 km (e.g. CMIP)(Christopher Daly, Gibson, Doggett, Smith, & Taylor, 2004; Fick & Hijmans, 2017; Thrasher et al., 2013). Table 1.1 lists the final annual surfaces and grid units for my novel and disappeared climate analysis.

Table 1.1: Summary of annual downscaled (60 m) climates for the LGM and modern eras used in novel and disappeared climate analysis.

Climate Variable	Units	Min	Max	Mean	SD
LGM					
Annual AET	mm	0.0	651.7	184.9	88.1
Annual Deficit	mm	0.0	420.6	22.5	33.1
Annual PET	mm	0.3	667.4	207.4	93.9
Annual Rain	mm	0.0	3452.9	231.2	223.2
Annual Snow	mm	0.2	5494.4	782.2	439.2
Mean Radiation	w	0.0	261.0	131.0	23.4
T_{max}	°C	-21.0	30.5	16.9	8.1
T_{min}	°C	-36.1	4.3	-21.9	3.4
Modern					
Annual AET	mm	0.0	445.4	183.5	49.0
Annual Deficit	mm	0.0	314.4	11.5	15.0
Annual PET	mm	1.7	463.5	195.0	52.0
Annual Rain	mm	0.0	4424.7	505.6	330.0
Annual Snow	mm	0.0	3420.5	717.2	263.1
Mean Radiation	w	0.0	209.7	97.8	17.1
T_{max}	°C	-13.2	31.3	21.0	3.7
T_{min}	°C	-34.7	6.6	-18.1	5.4

Annual climate variables at each of the 11 spatial resolutions were binned to simplify the ranges of possible climate values for analysis. I computed the 5th and 95th percentiles of each 60 m annual climate variable and removed these values as outliers in each surface. The range of each 60 m annual

climate variable was determined and used to create 25 equal sized bins for each variable to reassign pixel

values. Bin widths were computed for each surface using the following equation:

$$EQ\ 1.4: Bin\ Width = \frac{(MaxRange(LGM||Modern) - (MinRange(LGM||Modern))}{Max\ Bin\ Value}$$

Where *MaxRange(LGM||Modern)* is the maximum value of between the LGM or modern climate surface

at 60 m, *MinRange(LGM||Modern)* is the minimum value between the LGM or modern climate surface at

60 m, and *Max Bin Value* is the maximum bin class value (25). To reclassify each annual climate surface

at all resolutions, the bin widths were applied to each LGM and modern climate surface using the

following equation:

$$EQ\ 1.5: Bin\ Class = \frac{Ceiling(\text{Climate Value}_{x,y,t} - Min(\text{Climate Surface}_t))}{Bin\ Width}$$

Where *Climate Value$_{x,y,t}$* is the climate surfaces value at location *x,y* and at time *t* (LGM or modern),

Min(Climate Surface$_t$) is the minimum value of the climate surface at time t. Pixels that fell within the

removed 1st and 99th ranges were reclassified to either the lowest (0) or highest (25) bins for final
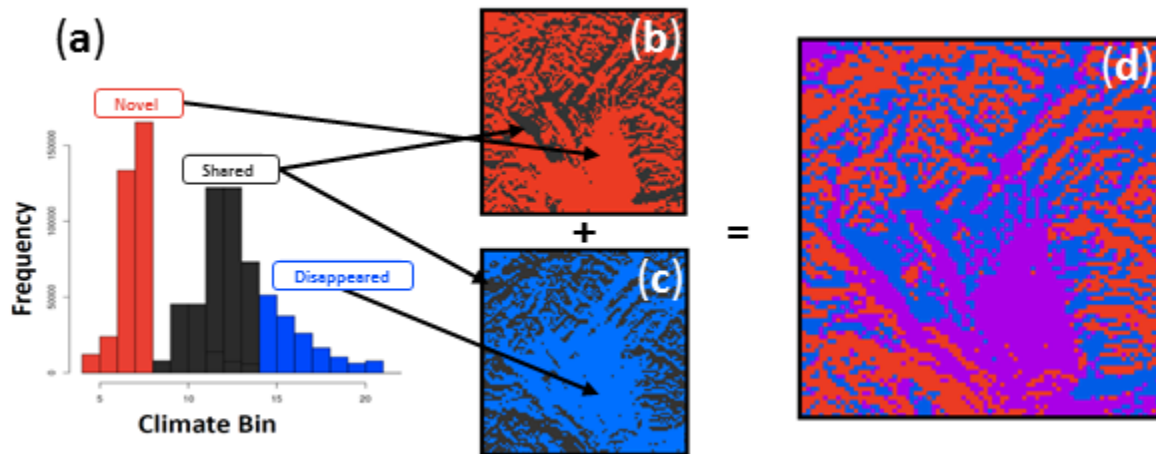
reclassification.

1.3.4 Novel and disappeared climate distributions:

Novel and disappeared climate distributions for each climate surface were computed at all

resolutions and eras from the reclassified climate surfaces. Novel climates were defined as modern

climate bins that did not exist during the LGM and disappeared climates as LGM climate bins that did not

exist in the modern period (Figure1.1a). Using these definitions, I then determined which bins constituted

novel, disappeared, or shared climates for each climate variable and era. Pixels for each climate surface,

resolution, and era were reclassified to 1) novel, 2) disappeared, 3) shared, or 4) novel and disappeared

climates based on each variable's novel and disappeared bin definitions. If a specific climate existed only

during the LGM, the climate range was considered "disappeared" (blue pixels) (Figure1.1c). If a specific

climate exists only in the modern era, the climate range was considered "novel" (red pixels) (Figure1.1b).

If a specific climate existed during both time periods, the climate was considered "shared" (black pixels),

as that specific range of climate could be found either during the LGM or modern era within the extent of Alaska (Figure 1.1 b&c). Lastly, it is possible for a specific climate range to be both novel and disappeared at the same location. For instance, during the LGM, minimum temperatures at some locations were so cold they are not observed in the modern era. However, in the exact same location during the modern era, minimum temperatures may have warmed so much due to anthropogenic climate change that they were not present during the LGM. If a specific climate was both novel and disappeared at the same location, the climate range was considered "both" (purple pixels) (Figure 1.1d).

The locations of novel and disappeared climates were summarized by computing the fractional area of novel, disappeared, and shared climates for the entire state of Alaska, as well as the fractional area among nine "Level 2" Alaskan ecoregions defined by the U.S. Geologic Survey (Gallant, Binnian, Omernik, & Shasby, 1995).

I quantified the amount of novel, disappeared, or shared climate at a given spatial resolution, and used a Spearman's rank correlation coefficient to determine whether the relationship between novel, disappeared, or shared fractional climate and spatial resolution was positive, negative, or no apparent relationship.

Figure 1.1: Classification process for "novel", "disappeared", "shared", and "both" climates. 2 km climate surfaces were used for visualization purposes for this figure, as "both" climates are almost nonexistent at 60 m resolution. Novel climates are red, disappeared climates are blue, shared climates are black, and both novel and disappeared climates are purple. (**a**) Histogram of LGM and Modern radiation climate bin ranges to define novel, disappeared, and shared climate bins. (**b**) Novel/Shared climate locations at 10km. (**c**) Disappeared/Shared climate locations at 10km. (**d**) Union of maps B and C. Purple pixels are intersection locations where climate was both novel and disappeared at 10km.

1.4 RESULTS

1.4.1 Downscale model evaluations:

All temperature model (T_{min}, T_{max}, T_{ave}) assumptions of GLMs methods were met. Correlation coefficients (0.86, 0.86, 0.89), root mean square error (RMSE, 5.36, 5.96, 4.92 °C), and percent bias (-0.041, -0.032, -0.37) for the final GLM for T_{min}, T_{max}, and T_{ave} models suggests that all models were well calibrated (Figure 1.2 a-c). Independent variables ($T_{Coarse,}$ elevation, TCI, and radiation) for all three temperature models had significant p-values of <0.001, confirming the importance of all model predictors. In all three models, coarse modeled temperature, followed closely by radiation, were the most significant contributors to model performance. Elevation and TCI, while still important, were less significant as determined by exploratory random forest model variable importance plots (Figure 1.3 a-c).

All model assumptions of the precipitation GLM were met. The Pearson's correlation coefficient (0.59), RMSE (0.90 mm), and percent bias (0.91) for the precipitation model indicated that the basic

GLM model was well calibrated (Figure 1.2d). As expected, my precipitation model correlation was lower than my temperature downscale models because downscaling procedures modeling precipitation are less well understood than downscale temperature methods. However, the precipitation model's correlation falls within the range of reported correlation values from other previously downscale precipitation products, indicating that my model is well calibrated to current precipitation model standards (Cannon, 2011; Maraun et al., 2010; Wetterhall, Bardossy, Chen, Halldin, & Xu, 2006; Widmann, Bretherton, & Salathé Jr, 2003). Independent precipitation variables (P_{coarse}, log(elevation), log(slope), wind direction, and orographic effects) had significant p-values of $<<0.001$, again, validating my choice in predictors. Wind speed was the least significant predictor for my precipitation model with a p-value of 0.0961, however, wind speed was still somewhat beneficial in predicting precipitation patterns across Alaska. Overall, elevation was the most significant predictor of precipitation, followed by slope, coarse modeled precipitation, orographic effects, wind speed, and lastly, wind direction as the weakest predictor as indicated by my random forest variable importance plots (Figure 1.3d).
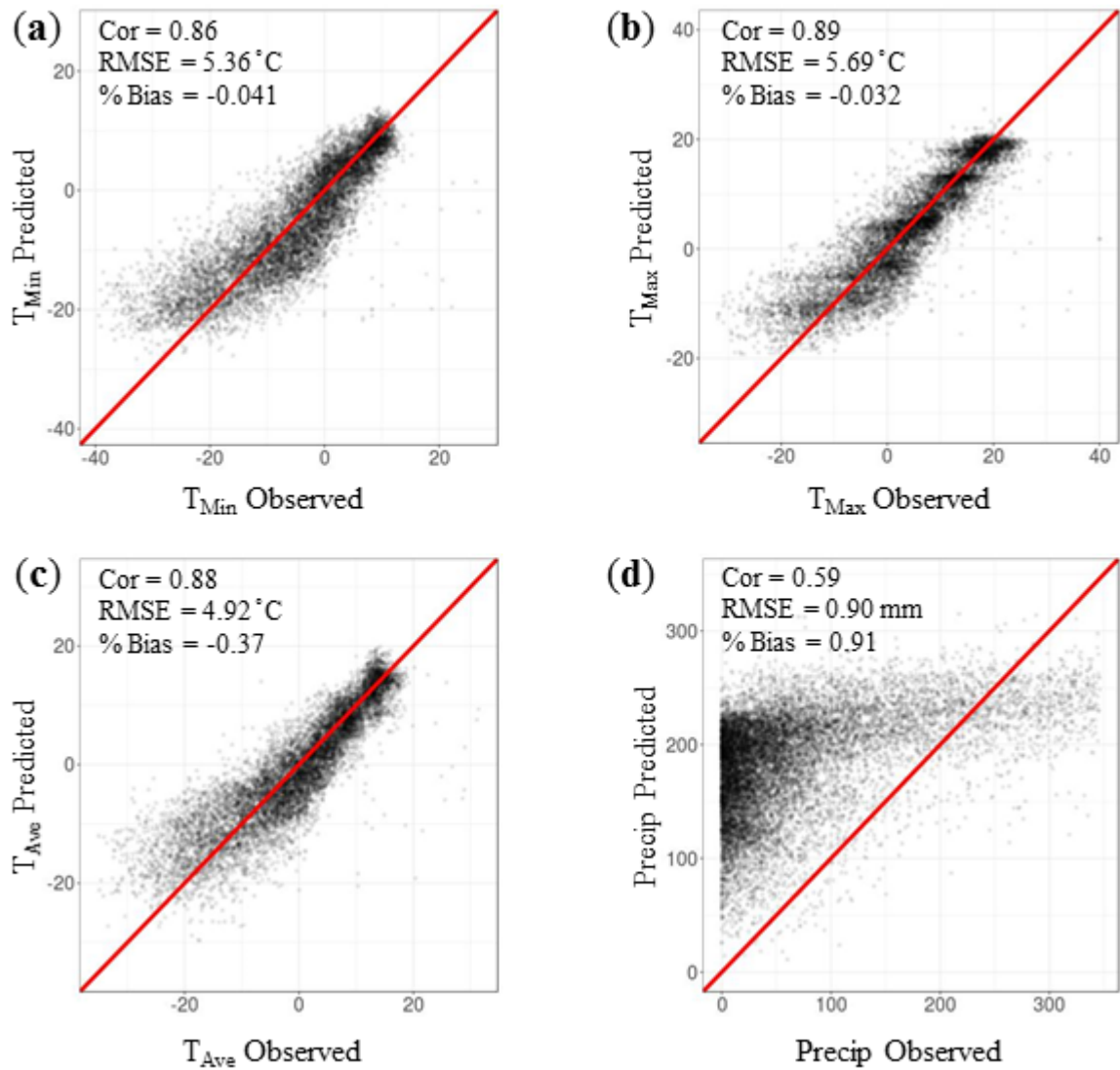
Figure 1.2: Downscale model evaluations. All plots are observed weather station data vs. predicted downscaled climate values, with correlation, RMSE, % Bias, and a 1:1 red correlation line to represent at hypothetical perfect correlation between observed and predicted values. (**a**) T_{min} Model, (**b**) T_{max} Model, (**c**) T_{ave} Model, (**d**) Precipitation Model performance.
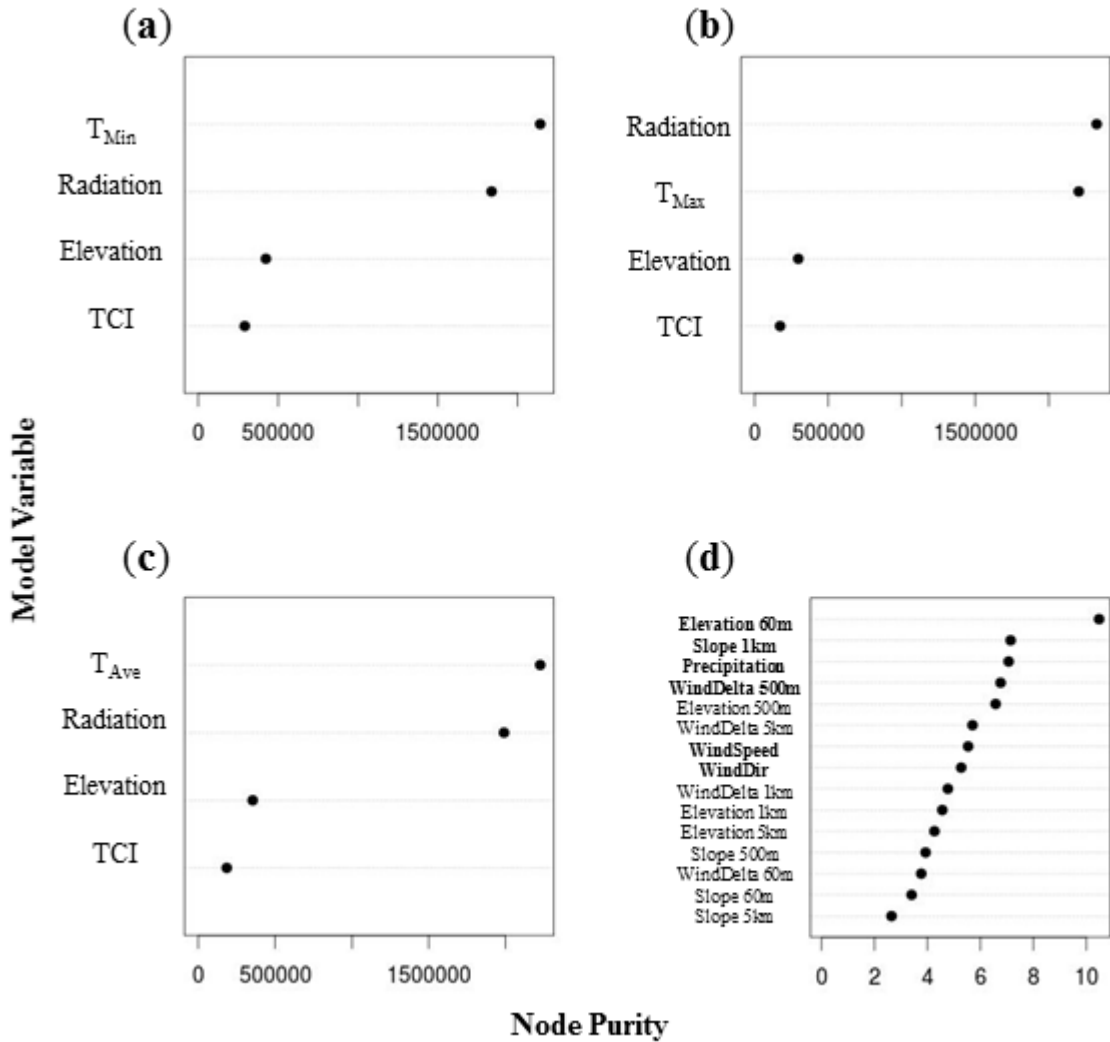
Figure 1.3: Variable importance plots for downscaled climate models based on random forest model preliminary investigations. (**a**) T_{min} Model, (**b**) T_{max} Model, (**c**) T_{Ave} Model, (**d**) Precipitation model. Bold precipitation model variables indicate variables selected from random forest importance and spatial resolution.

1.4.2 Downscaled novel and disappeared climate distributions:

Disappeared climates were defined as LGM climates that did not exist during the modern era.

Seven of the eight downscaled climate surfaces contained disappeared climates across Alaska, with rain

being the exception. Overall, disappeared climates covered 55.9% of Alaska from the LGM to modern

era. T_{max} displayed the highest amount of disappeared climates in Alaska, covering 33.6% of the state

alone, while water deficit displayed the lowest amount of disappeared climates at 2.9% (Table 1.2). For most ecoregions, disappeared climates covered <30% of Alaska, although >30% of some coastal ecoregions were covered by disappeared climates, especially for T_{max} (Figure 1.4). Ecoregions most affected by disappeared maximum temperature climates were the Coast Mountain Transition (85.0%) and Pacific Mountain Transition (82.5%). The Coastal Rainforest ecoregion displayed the largest amount of disappeared snow climates in the state, covering 40.0% of the region (Figure 1.4). Western Alaska also experienced disappeared climates in the Aleutian Meadows and Bering Taiga ecoregions due to disappeared PET climates, however, the fraction of disappeared climates were not as high as the southern portion of the state at 37.1 and 43.9% respectively (Figure 1.4). The Bering Tundra ecoregion contained the least amount of disappeared climates for all climate variables, containing <10% of disappeared climates for the entire region. All other ecoregions and climate variables contained varying amounts of disappeared climates across Alaska (Figure 1.4).
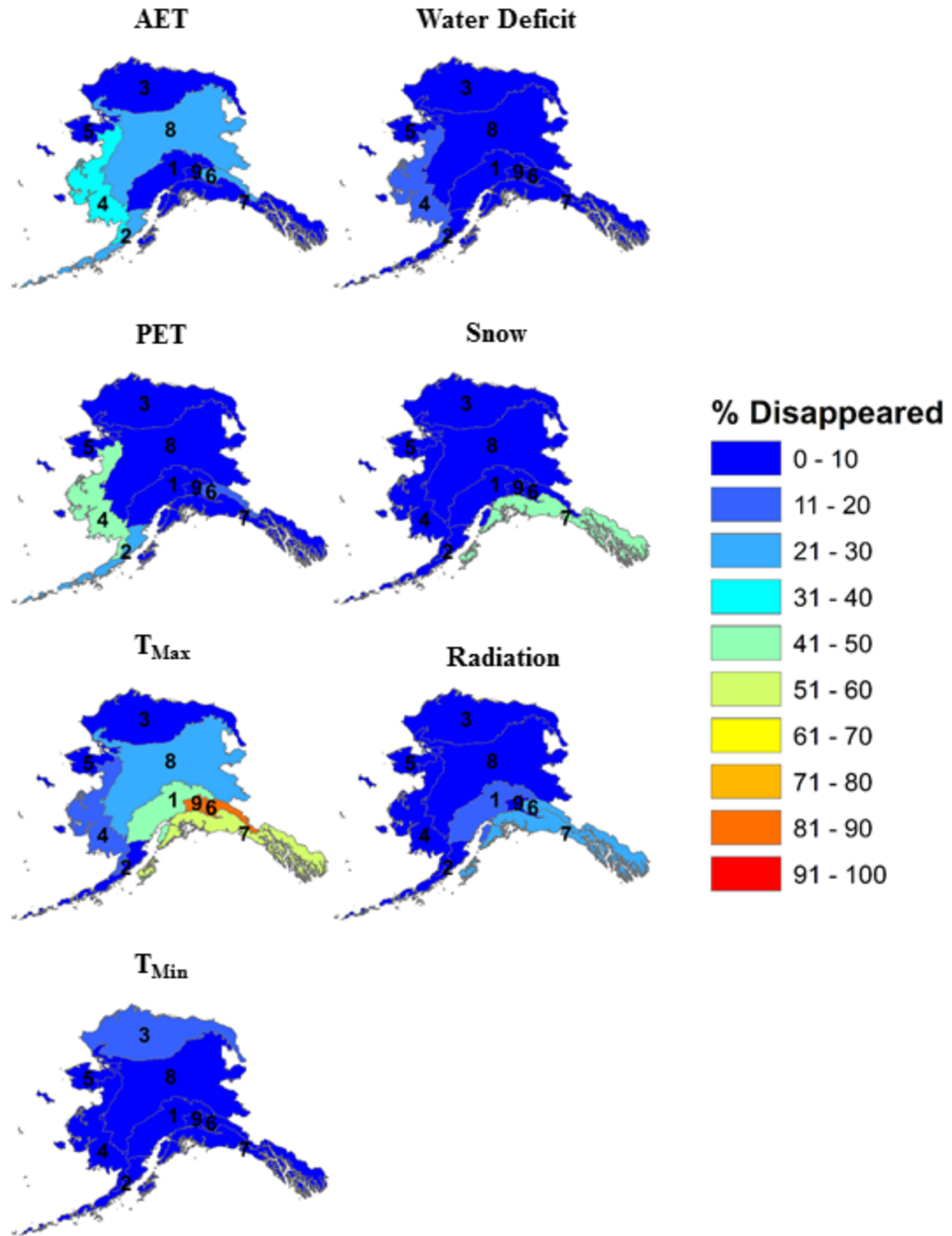
Figure 1.4: Fractional area coverage of disappeared climates for the nine "Level 2" Alaskan ecoregions. [1] Alaska Range Transition, [2] Aleutian Meadows, [3] Arctic Tundra, [4] Bering Taiga, [5] Bering Tundra, [6] Coast Mountain Transition, [7], Coastal Rainforests, [8] Intermontane Boreal, [9] Pacific Mountain Transition.

Novel climates were defined as modern climates that did not exist during the LGM. Of the eight downscaled climate surfaces, only radiation, rain, and T_{min} contained novel climates in Alaska. Novel climates were less common than disappeared climates in Alaska, covering <10.0% across all of Alaska from the LGM to modern era. T_{min} displayed the highest amounts of novel climates in Alaska, covering 5.5% of the state, while radiation displayed the smallest amount of novel climates at 2.0% (Table 1.2). Most ecoregions were covered by <10% of novel climates for all three climate variables, except for the Aleutian Meadows and Coastal Rainforests ecoregions of Alaska from T_{min} climates (Figure 1.5). T_{min} contained the largest amounts of novel climates for both ecoregions, at 56.9% and 24.8%, respectively. While less than novel T_{min} climates, novel rain also affected these ecoregions covering 29.7% and 17.6%, respectively (Figure 1.5). Radiation contained some novel climates in Alaska, however all ecoregions in Alaska had <4% novel radiation climates present in Alaska from the LGM to modern era (Figure 1.5).
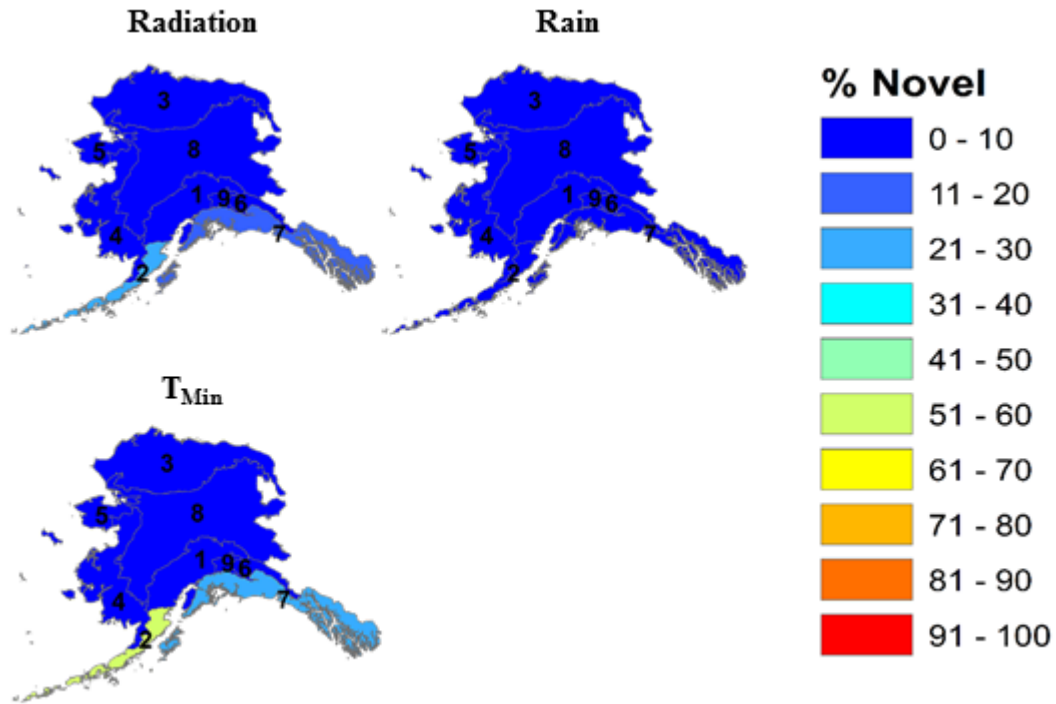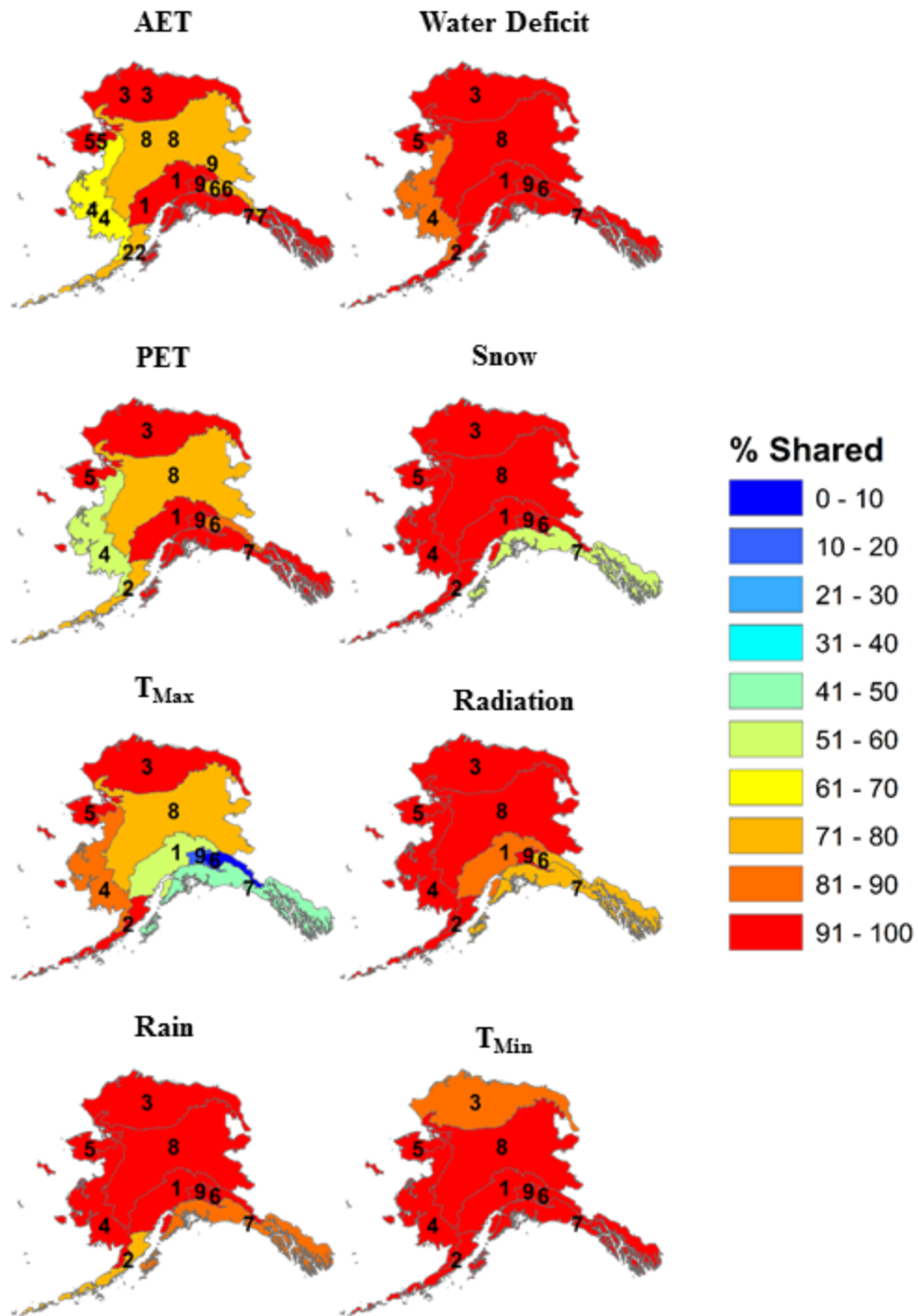
Figure 1.5: Fractional area coverage of novel climates for the nine "Level 2" Alaskan ecoregions. [1] Alaska Range Transition, [2] Aleutian Meadows, [3] Arctic Tundra, [4] Bering Taiga, [5] Bering Tundra, [6] Coast Mountain Transition, [7], Coastal Rainforests, [8] Intermontane Boreal, [9] Pacific Mountain Transition.

Shared climates were defined as climates that existed during both the LGM and modern eras. As expected, all eight climate surfaces contained shared climates throughout Alaska, since no climate surface was classified as 100% novel or disappeared. Overall, shared climates generally covered more of Alaska than novel or disappeared climates, with a minimum fractional area of 40.6%. Shared water deficit climates covered 97.1% of the state, indicating water deficit climates have changed least in Alaska (Table 1.2). Additionally, shared T_{max} climates covered 66.4% of Alaska, indicating that T_{max} climates have changed the most in the state from the LGM to modern era (Table 1.2). This was expected as water deficit contained no novel climates and the lowest amount of disappeared climates, while T_{max} contained no novel climates, but the largest amount of disappeared climates in Alaska. While all Alaskan ecoregions

contained various amounts of shared climates, there were isolated cases where ecoregions were <80% shared, although this was expected whenever high novel or disappeared climates covered the same ecoregion and climate variable (Figure 1.6). The Arctic Tundra, Bering Tundra, and Intermontane Boreal ecoregions contained the highest overall shared climate distributions in Alaska at 84.9%, 98.28%, and 75.3%, indicating that these ecoregions are generally less affected by post-glacial climate change (Figure 1.6). The Coast and Pacific Mountain Transition ecoregions experienced the lowest amounts of shared climates at 15.0% and 17.5%, indicating that these ecoregions are generally more affected by post-glacial climate change (Figure 1.6).

Figure 1.6: Fractional area coverage of shared climates for the nine "Level 2" Alaskan ecoregions. [1] Alaska Range Transition, [2] Aleutian Meadows, [3] Arctic Tundra, [4] Bering Taiga, [5] Bering Tundra, [6] Coast Mountain Transition, [7], Coastal Rainforests, [8] Intermontane Boreal, [9] Pacific Mountain Transition.

While it is possible for downscaled novel and disappeared climates to exist at the same location from the LGM to modern era, only a very small fraction of T_{min} climates displayed this phenomenon in Alaska at 60 m resolution and was determined to be insignificant as it only covered <0.001% (39.6 km^2) of Alaska. At coarser resolutions there was a noticeable increase in climates classified as "both" novel and disappeared for some climate surfaces at a location, however this portion of the results concentrates on my high resolution downscaled climate surfaces ("both" climates vs. spatial resolution is discussed in the next section).

Table 1.2: Percent cover (based on fractional area) for novel, disappeared, and shared climates for each climate variable in Alaska from the LGM to modern era.

Type	AET	Water Deficit	PET	Snow	T_{max}	Rad	T_{min}	Rain
% Novel	0.0%	0.0%	0.0%	0.0%	0.0%	2.0%	5.5%	3.7%
% Disappeared	15.6%	2.9%	15.6%	6.0%	33.6%	13.0%	6.3%	0.0%
% Shared	84.4%	97.1%	84.4%	94.0%	66.4%	85.1%	88.2%	96.3%
% Both	0.0%	0.0%	0.0%	0.0%	0.0%	0.0%	0.0%	0.0%

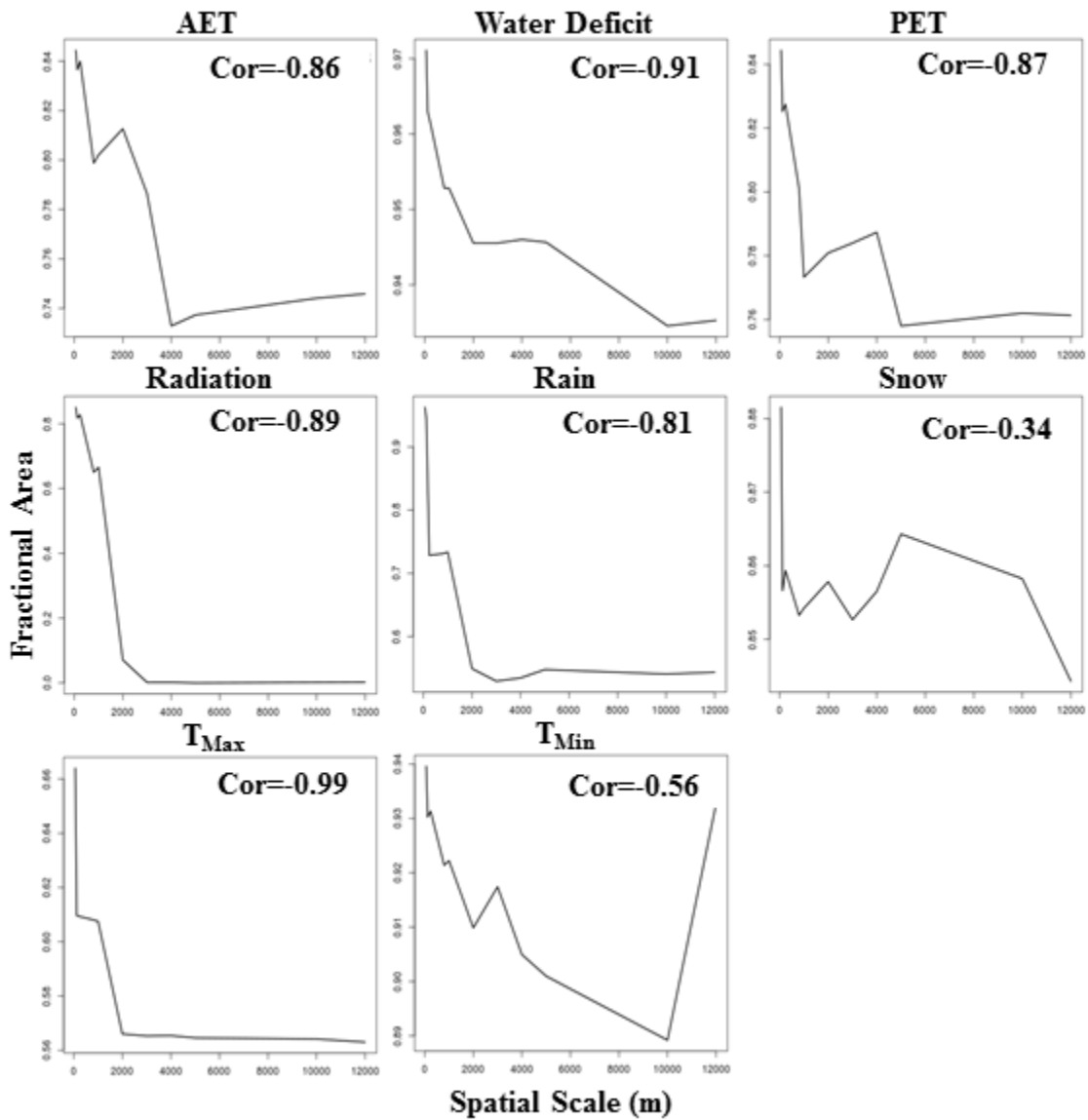**1.4.3 No-analogue climates vs. spatial resolution:**

As spatial resolution becomes coarser, the fractional area of novel and disappeared climates generally increases, while the fractional area of shared climates generally decreases. All disappeared climate surfaces, except minimum temperature, had moderate (0.40 to 0.59) to very strong (0.80 to 1.00) Spearman's rank correlations between spatial resolution and fractional area, indicating that as the spatial resolution of climate becomes coarse, the fractional area of disappeared climates increases (Figure 1.7). All novel climate surfaces had a strong (0.60 to 0.79) to very strong (0.80 to 1.00) Spearman's rank correlation coefficient between spatial resolution and fractional area, indicating that as spatial resolution of climate becomes coarser, the fractional area of novel climates increases as well (Figure 1.8). All climate variables had a negative relationship between fractional area of shared climate and spatial resolution, as expected. The strengths of Spearman's rank correlations varied from moderate (-0.40 to 0.59) to very strong (-0.80 to -1.00) (Figure 1.9).
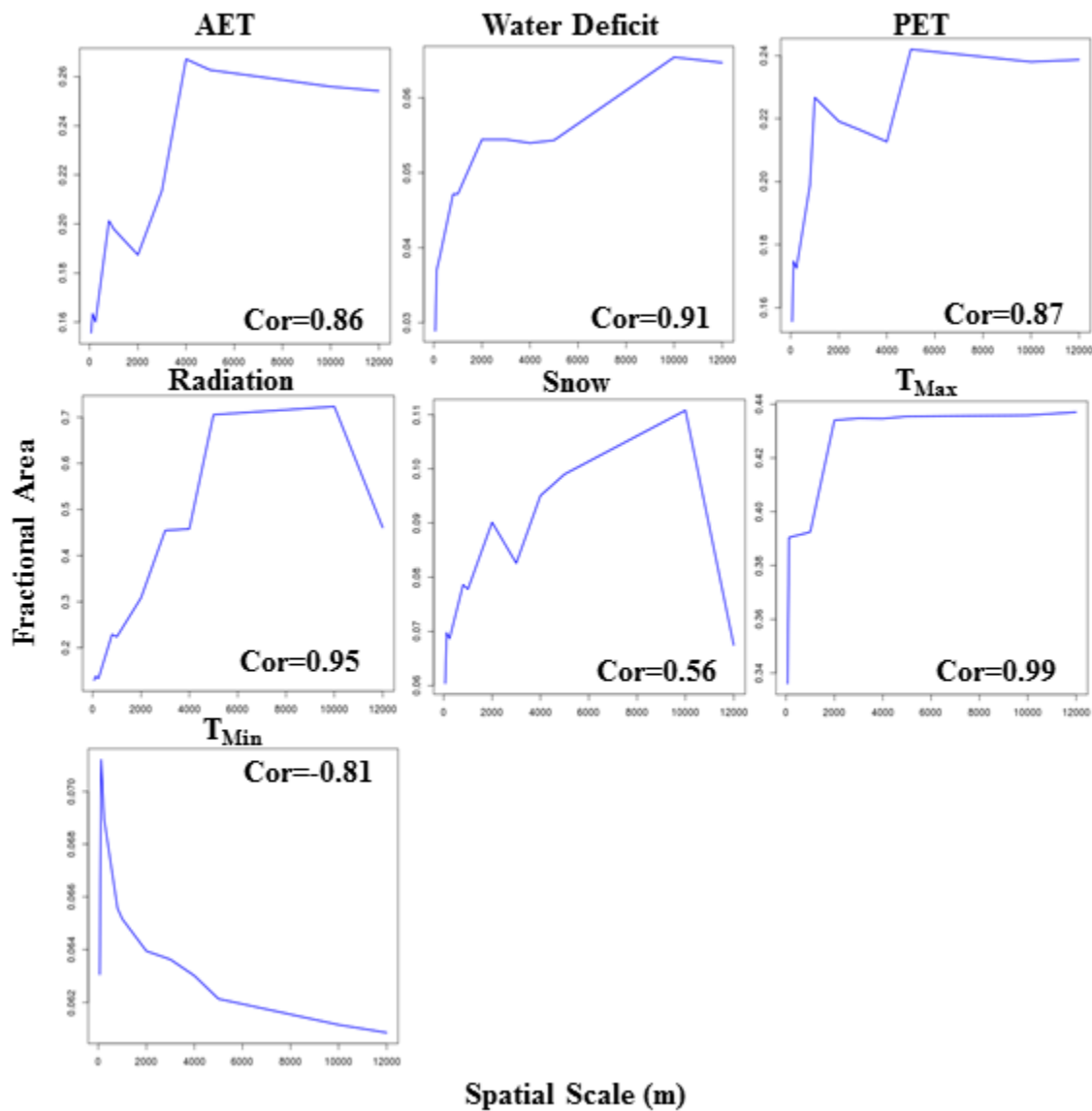
Figure 1.7: Disappeared climate vs. spatial scale plots. Spatial scale (60 m -12 km) plotted against fractional area of disappeared climates for each climate variable. The Spearman's Rank correlation coefficient is included on each plot.
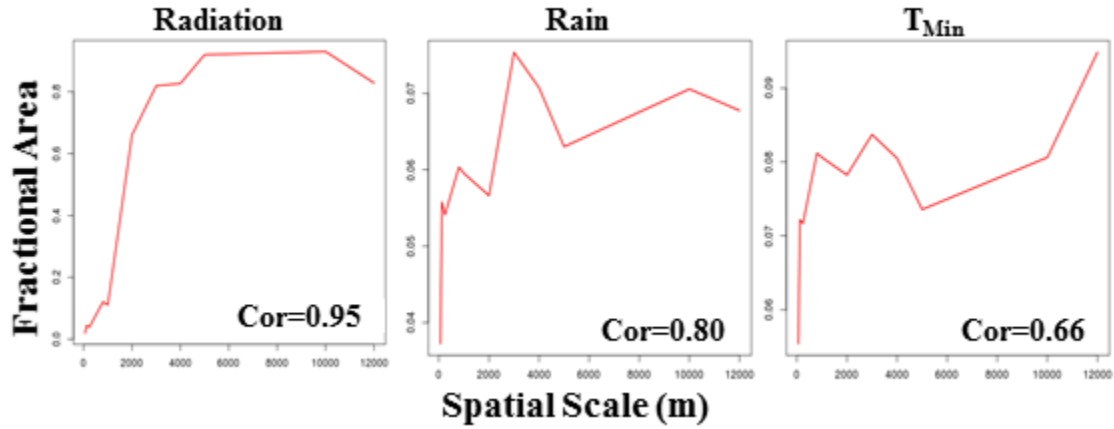
Figure 1.8: Novel climate vs. spatial scale plots. Spatial scale (60 m -12 km) plotted against fractional area of novel climates for each climate variable. The Spearman's Rank correlation coefficient is included on each plot.

Figure 1.9: Shared climate vs. spatial scale plots. Spatial scale (60 m -12 km) plotted against fractional area of shared climates for each climate variable. The Spearman's Rank correlation coefficient is included on each plot.

An exception to the previous patterns, disappeared T_{min}, produced a very strong (0.80 to 1.0) negative Spearman's rank correlation of 0.81 (Figure 1.7). The negative relationship of this correlation coefficient suggests that as spatial resolution becomes coarser, the amount of fractional disappeared T_{min} climates decreases.

The relationship between spatial resolution and fractional area of "both" novel and disappeared

climates at the same locations was less clear than novel, disappeared, and shared climates (Figure 1.10).

While "both" climates were virtually nonexistent at 60 m resolution for all climate surfaces except T_{min}

climates, the occurrence of "both" climates noticeably increased for rain and radiation climate surfaces at

coarser resolutions. T_{min} climate surfaces did not have any noticeable increase in both novel and

disappeared T_{min} climates occurring in the same location at any resolution. "Both" climates for radiation

displayed a very strong Spearman's rank correlation between spatial scale and fractional area, indicating

that as radiation climate becomes coarser, the amount of both novel and disappeared climates at the same

location will increase. However, rain and T_{min} had extremely low correlations, indicating that an increased

occurrence of both novel and disappeared climates at the same will not always occur as climate resolution

becomes coarser (Figure 1.10).

Figure 1.10: "Both" climate vs. spatial scale plots. Spatial scale (60 m -12 km) plotted against fractional area of "both" climates for each climate variable. The Spearman's Rank correlation coefficient is included on each plot.
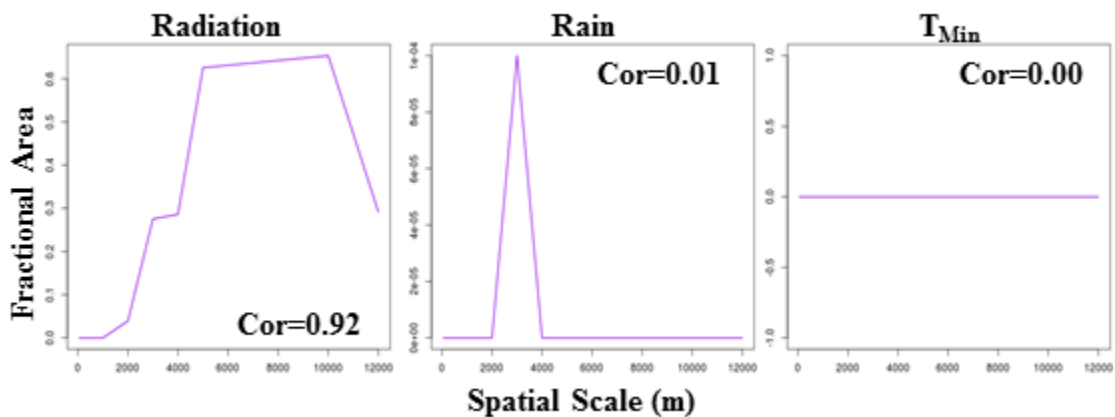
1.5 DISCUSSION

As climate changes, either from natural processes and/or human activity, novel and disappeared

climates will arise (Jackson & Overpeck, 2000; Williams & Jackson, 2007). Long term climate patterns

that affect observed novel and disappeared climates, whether in the past, present, or future, arise not only

from geographic and temporal changes in the environment, but also as a result of atmospheric and topographic processes that occur across many spatial scales (Ackerly et al., 2010).

Determining how climate resolution affects climate change predictions is necessary to avoid under or overestimating the potential impacts of climate change for ecological analyses dependent on gridded climate data. I downscaled climate data at 11 spatial resolutions spanning three orders of magnitude to include climate data at resolutions used for previous climate-change impact projections to identify the distribution and abundance of novel, disappeared, and shared climates across Alaska, as well as how the spatial resolution of climate data used affects these estimates of climate (e.g. PRISM, BioClim, NASA Nex, CMIP) (Christopher Daly et al., 2004; Fick & Hijmans, 2017; Thrasher et al., 2013). I found that novel and disappeared climates primarily affected Southern Alaska. Additionally, climate data generally increased the fractional area of novel and disappeared climates as the resolution became coarser, however, it was also possible, although rare, to decrease the fractional area or have no apparent relationship between the fractional area of novel and disappeared climates and climate data resolution.

1.5.1 Novel, disappeared, and shared climate distributions:

All my downscaled climate surfaces, except rain, contained disappeared climates across Alaska. Rain was the only surface that did not contain disappeared climate because 1) rain values cannot reach lower than 0 mm of precipitation (unlike temperature), and 2) environmentally, warm modern climates produce more rain and less snow, which can only extend the upper limit of possible modern rain values. Therefore, the combination of these two effects produced no unique rain values for my LGM climate surfaces. Overall, disappeared climates primarily affected the south-eastern Coast Mountain and Pacific Mountain Transition ecoregions, where modern climate has significantly warmed causing the extremely low maximum temperature climates of the LGM to disappear. Disappeared snow climates primarily affected the Southern Coastal Rainforest ecoregion, where more precipitation now falls as rain, as opposed to snow during the LGM, causing high levels of LGM snow climates to disappear for the modern

era. While the fractional area of disappeared climates in Western Alaska were not as high as Southern Alaska, the Aleutian Meadows and Bering Taiga ecoregions experienced some disappeared AET and PET climates, likely as a result of higher radiation climates during the LGM than the modern era. There is some evidence from paleoclimate simulations that suggests less atmospheric water vapor reduced the amount of low-level clouds and increased the amount of high-level clouds, which could result in increased surface radiation while still producing a cooling effect over arctic regions during the LGM (Webb, Rind, Lehman, Healy, & Sigman, 1997).

Only three of my eight downscaled climate surfaces contained novel climate distributions in Alaska. These surfaces included radiation, rain, and minimum temperature, however, novel climates were a rarer occurrence than disappeared climates. Less novel climates, when compared to disappeared climates, is likely an artifact of possible climate ranges of Alaska, since I considered only Alaska as my reference area of interest for this study, which ignores all other possible climate ranges across Earth. Additionally, as with disappeared rain climates, novel rain, snow, radiation, AET, PET, and water deficit climates are environmentally restricted. Therefore, due to natural post-glacial and/or anthropogenic climate change, only the southernmost portion of Alaska could experience significant amounts of novel climates. Modern climate change has led to increasingly warmer minimum temperatures in the southern Aleutian Meadows and Coastal Rainforest ecoregions. Consequently, this has eliminated extremely cold minimum temperatures that were present during the LGM, while simultaneously increasing the amount of rainfall in the state due to more precipitation being converted to rain over snow. Additionally, these ecoregions are along the southern-most portions of the state, which are lowest in latitude and should therefore be warmer than any other region of Alaska.

Since novel and disappeared climates identify areas most affected by climate change, shared climates fundamentally capture regions that have been least affected by post-glacial climate change. Novel and disappeared climates largely affected Southern Alaska, resulting in lower fractional areas of shared climates in the south, and higher fractional areas in the North. As expected, the most northern ecoregions of the state, the Arctic Tundra, Bering Tundra, and Intermontane Boreal ecoregions, contained

the largest amount of shared climates, while the southernmost ecoregions, the Coast and Pacific Mountain Transition ecoregions, contained the least amount of shared climates.

The occurrence of both novel and disappeared climates existing at the same location on my downscaled climate surfaces was virtually non-existent. T_{min} contained a few pixels (11) classified as both novel and disappeared, however, this phenomenon was deemed insignificant because it covered such a small fraction of Alaska's area. At larger spatial resolutions, there are instances where some climate variables have a substantial increase in both novel and disappeared climates occurring at the same location. However, areas where both novel and disappeared climates occurred at the same location at resolutions >60 m were not considered for analysis on the distribution of novel and disappeared climates.

Novel and disappeared climates are an important characterization of climate change that help identify the vulnerability of ecoregions, since they can push species beyond their ideal climate space and lead to ecologically risky scenarios such as migration, range shifts, and extinction. The Aleutian Meadows and Coastal Rainforests of Alaska stood out as the most vulnerable ecoregions to post-glacial climate change. These two regions generally experienced both large amounts of novel and disappeared climates across all climate variables when compared to all other ecoregions in Alaska. Ecoregions with large shared climate distributions may have important implications for identifying glacial refugia because they represent regions that have experienced the least climate change through time and contain the most stable climates in Alaska. The Bering Tundra was the least vulnerable Alaskan ecoregion to post-glacial climate change, as all variables in the region contained extremely low fractional areas of novel or disappeared climates.

While I have identified the least and most climatically vulnerable ecoregions to post-glacial climate change, large variations in the abundance and distribution of novel and disappeared climates will also affect the significance of each climate variable on a refugia as specified by the optimal niche species. Situations arose where one to few climate variables contained substantial amounts of novel or disappeared climates, while many others contained low to no novel or disappeared climates. This is important for two reasons: First, if an ecoregion contained significant fractional areas of novel or disappeared climates, it

35

does not necessarily imply that all climate variables within the same ecoregion experienced high amounts of novel or disappeared climates. For instance, the Coast Mountain Transition ecoregion in Alaska contained the largest fractional area of disappeared T_{Max} climates. Most other climate variables within the same ecoregion contained low amounts of disappeared climates (Figure 1.4).

Second, large fractional areas of novel or disappeared climate does not necessarily equate to ecological significance for a species (e.g. niche theory). For example, a species may have a large temperature threshold (generalist) with a low snow threshold (specialist). Even with the significant warming of the LGM (85.0% disappeared T_{max}), T_{max} climates may still fall within the optimal range of the species. However, while changes to LGM snow climates were low (2.3% disappeared snow), this change may be ecologically risky for the species if the changes fall outside its optimal snow range. In this case, disappeared snow climates are significant to a species, not disappeared T_{max} climates, even though there was a far greater fractional area of disappeared T_{max} climates. This suggests that disappeared or novel climates may only be important if they are a limiting factor or extend beyond the optimal niche for a species (De Baar, 1994; Vandermeer, 1972). If the change in climate is a limiting factor, the risk of distribution shifts or extirpation may increase for a species. However, if the change in climate is not limiting, the existence of novel and disappeared climates may have minimal impacts on a species.

1.5.2 Climate grid resolution and fractional area patterns:

In my study, the amount of novel and disappeared climate distributions was affected by climate grid resolution in two primary ways. First, as climate data becomes coarser, there is a positive relationship between the fractional area of novel and disappeared climates and spatial resolution. This pattern occurs for two reasons: 1) coarser climate data reduced environmental variability, which in turn removes the extreme ranges of climate, and 2) there are fewer climates that fall within the shared climate bin definition, resulting in fewer climates classified as shared while simultaneously increasing the frequency of novel or disappeared climates simply due to the coarser scales (Figure 1.11). As expected, all shared climates displayed a negative relationship between climate resolution and fractional area (Figure 1.9).

Shared climates should display a negative relationship because as the fractional area of novel and disappeared climates increases with spatial resolution, the fractional area of shared climates must decrease because it accounts for areas not classified as either novel or disappeared. Previous studies by Franklin et al. (2013), Heikkinen, Luoto, Kuussaari, and Toivonen (2007), and Seo et al. (2009) found similar results modeling species distributions, finding that coarse climate data predicts larger suitable habitats compared to finer resolution climate data. My study confirms this trend, although my analysis is focused solely on the distribution of climate as opposed to the distribution of species.
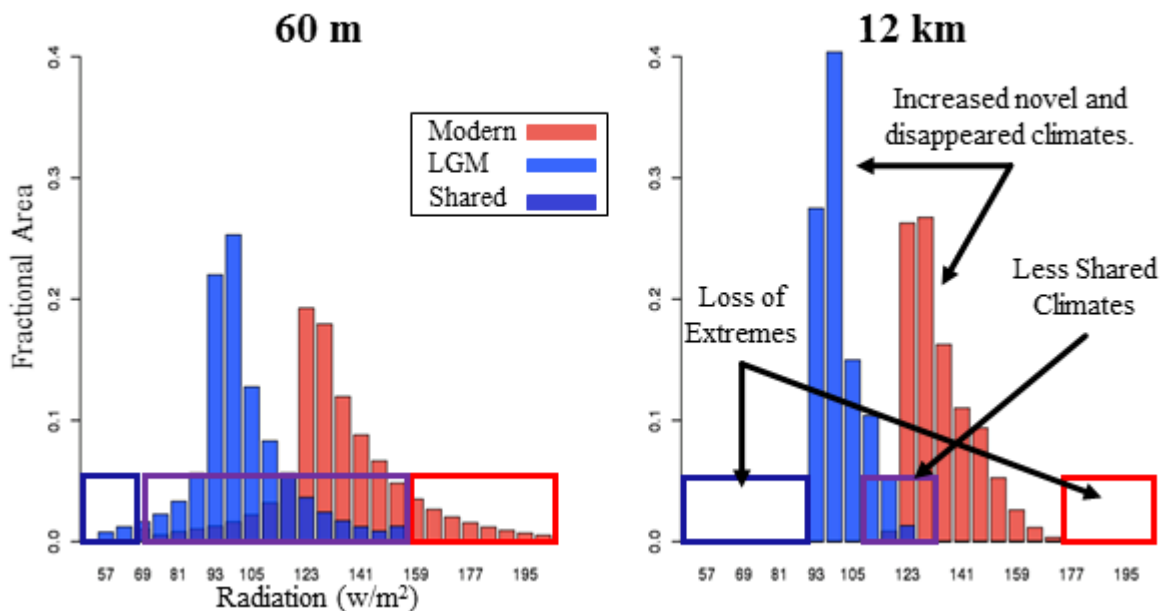
Figure 1.11: Coarser resolutions can increase the amount of novel and disappeared climates in Alaska. Modern climate ranges are red bars, LGM climate ranges are blue bars, and the overlap of modern and LGM climates are dark blue bars. The red boxes are novel climate bins, blue boxes are disappeared climate bins, and purple boxes are shared climate bins.

The positive relationship between spatial resolution and novel and disappeared climate distributions suggests that the use of coarse grid climate data may have led to the overestimation of novel and disappeared climate distributions in previous analyses, and thereby cause overestimates of potential impacts of climate change. This may lead to significant errors when trying to determine where post-

37

glacial climate change has occurred. Additionally, this error can be propagated into other analyses that depend on climate grid data, such as species distribution models, which implies that these studies may also over or underestimate predicted species ranges, refugial locations, and other climate-species analyses (Franklin et al., 2013; Randin et al., 2009; Trivedi, Berry, Morecroft, & Dawson, 2008).

Second, as climate data becomes coarser, there can be a negative relationship between spatial resolution and the amount of novel and disappeared climates, although this trend only occurred with my T_{min} disappeared climate surfaces. This pattern can occur when novel or disappeared climates are extremely spatially heterogeneous (i.e. patchy) (Figure 1.12). At coarser resolutions, my T_{min} climate aggregation scheme successively grouped similar temperatures together at each progressively coarser resolution (Wu, 1999). Because my 60 m disappeared T_{min} surface was extremely patchy, successively aggregating the surface to coarser resolutions averaged out the few pixels classified as disappeared T_{min} climates and progressively reclassified coarser T_{min} disappeared climates to T_{min} shared climates. Randin et al. (2009) reported a similar negative pattern when comparing the distribution of alpine species, however Randin's study considered climate resolution with varying study extents. The combination of climate resolution and study extent was found to cause a negative relationship between the amount of suitable alpine species habitats and climate resolution/extent as their species distribution models were unable to capture the full environmental niche of alpine species at regional scale climate resolutions or limited study extents. Therefore, the negative pattern between alpine species distributions and climate data resolution from Randin et al. (2009) was not a product of heterogeneously complex climate surfaces.
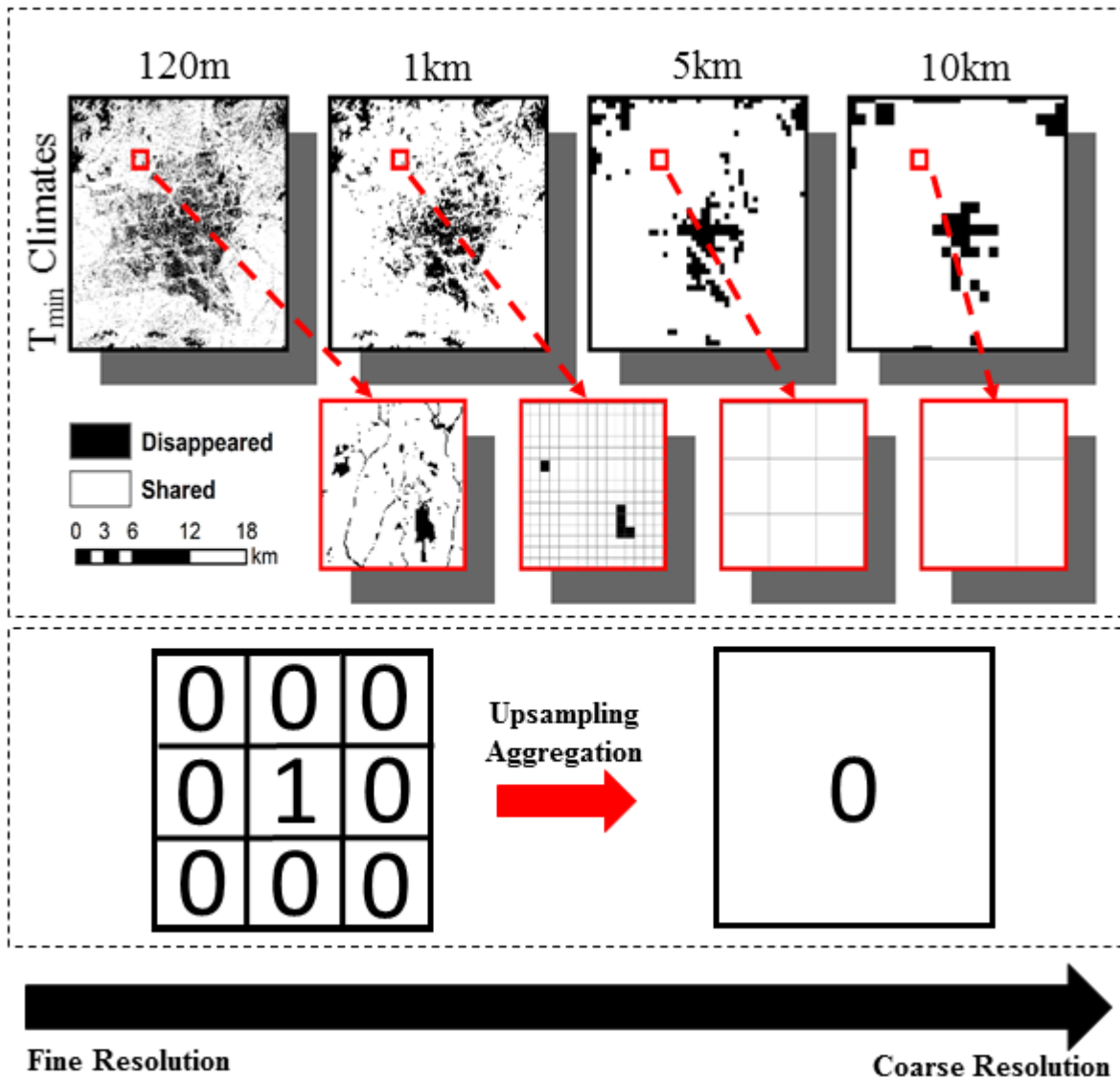
Figure 1.12: Coarser resolutions can decrease the amount of novel and disappeared climates in Alaska. Disappeared T_{min} at 120m displays regions with patchy, but random spatial distributions, while coarse disappeared T_{min} climates display clustered distributions. Isolated patches of disappeared T_{min} climates at high resolutions will be reclassified to shared T_{min} climates when upsampling T_{min} climates to coarser scales using standard pixel aggregation methods.

Although a negative relationship between fractional area and spatial resolution occurred on only one climate surface, this phenomenon suggests it is possible to underestimate the amount of novel and disappeared climates when using coarse gridded climate products. Again, significant errors may arise

when estimating post-glacial climate change distributions leading to serious underestimations of novel and disappeared climate distributions, the potential impacts of climate change, and potentially propagating this error into other climate dependent analyses. However, this pattern is less likely to occur since it depends on the patchiness of novel and disappeared climates as opposed to gridded climate data's ability to capture landscape scale processes influencing climate patterns.

No significant relationship between fractional area of novel and disappeared climates and spatial resolution is possible and this pattern did not visibly arise within my study. There were some cases where the Spearman's rank correlation was 'moderate', although this does not necessarily indicate a relationship. However, while all surfaces displayed moderate to strong correlations, there was a fair amount of variation in fractional area as spatial resolution became coarser. This suggests that there may be significant thresholds occurring at various spatial scales. The exact causes of this variation are still unclear, but I hypothesize that this variation may be a result of distortion caused by aliasing artifacts when up-sampling my 60 m downscaled climate surfaces to coarser scales (Haines-Young & Chopping, 1996; Kennie & McLaren, 1988), or may be caused by Moiré fringes (Gustafsson, 2000) producing overlooked oscillations across a landscape. While Moiré fringes are a well-known issue affecting raster image processing and visualization, to the best of my knowledge, no studies have investigated whether naturally occurring processes and phenomenon known to influence climate or other Earth systems, generate spatial Moiré distributions.

1.5.3 Conclusions:

It is important to understand how climate change through time affects the distribution and abundance of novel and disappeared climates, as well as how choice in gridded climate data resolution affects our estimations of climate change. If my 60 m downscaled climate surfaces accurately reflect physiographic processes affecting climate at multiple scales, my fine scale climate products should improve estimations of novel and disappeared climate distributions, compared to coarser climate products, especially in areas with high topographic complexity.

1.6 REFERENCES

Ackerly, D. D., Loarie, S. R., Cornwell, W. K., Weiss, S. B., Hamilton, H., Branciforte, R., & Kraft, N. J. B. (2010). The geography of climate change: implications for conservation biogeography. *Diversity and Distributions, 16*(3), 476-487. doi:10.1111/j.1472-4642.2010.00654

Aggarwal, C. C. (2015). *Outlier analysis.* Paper presented at the Data mining.

Allen, R. G., Pereira, L. S., Raes, D., & Smith, M. (1998). *Crop evapotranspiration-Guidelines for computing crop water requirements-FAO Irrigation and drainage paper 56* (Vol. 300): Irrigation and Drainage.

Bellard, C., Bertelsmeier, C., Leadley, P., Thuiller, W., & Courchamp, F. (2012). Impacts of climate change on the future of biodiversity. *Ecology Letters, 15*(4), 365-377. doi:10.1111/j.1461-0248.2011.01736

Breiman, L. (2001). Random forests. *Machine learning, 45*(1), 5-32.

Cannon, A. J. (2011). Quantile regression neural networks: Implementation in R and application to precipitation downscaling. *Computers & Geosciences, 37*(9), 1277-1284.

Daly, C. (2006). Guidelines for assessing the suitability of spatial climate data sets. *International Journal of Climatology, 26*(6), 707-721. doi:10.1002/joc.1322

Daly, C., Gibson, W., Doggett, M., Smith, J., & Taylor, G. (2004). *Up-to-date monthly climate maps for the conterminous United States.* Paper presented at the Proc., 14th AMS Conf. on Applied Climatology, 84th AMS Annual Meeting Combined Preprints, Amer. Meteorological Soc., Seattle, WA.

Davis, M. B. (1990). Climatic change and the survival of forest species. *The earth in transition: patterns and processes of biotic impoverishment. Cambridge: Cambridge University Press. p*, 99-111.

De Baar, H. (1994). von Liebig's law of the minimum and plankton ecology (1899–1991). *Progress in Oceanography, 33*(4), 347-386.

Dingman, S. (2002). Water in soils: infiltration and redistribution. Physical hydrology. In: upper saddle river, New Jersey: Prentice-Hall, Inc.

Dobrowski, S. Z. (2011). A climatic basis for microrefugia: the influence of terrain on climate. *Global Change Biology, 17*(2), 1022-1035. doi:10.1111/j.1365-2486.2010.02263.x.

Dobrowski, S. Z., Abatzoglou, J., Swanson, A. K., Greenberg, J. A., Mynsberge, A. R., Holden, Z. A., & Schwartz, M. K. (2013). The climate velocity of the contiguous United States during the 20th century. *Global change biology, 19*(1), 241-251. doi:10.1111/gcb.12026

Dobrowski, S. Z., Abatzoglou, J. T., Greenberg, J. A., & Schladow, S. G. (2009). How much influence does landscape-scale physiography have on air temperature in a mountain environment? *Agricultural and Forest Meteorology, 149*(10), 1751-1758. doi:10.1016/j.agrformet.2009.06.006

Dunne, K., & Willmott, C. J. (1996). Global distribution of plant-extractable water capacity of soil. *International Journal of Climatology, 16*(8), 841-859

Fick, S. E., & Hijmans, R. J. (2017). WorldClim 2: new 1-km spatial resolution climate surfaces for global land areas. *International Journal of Climatology, 37*(12), 4302-4315.

Fitzpatrick, M. C., & Hargrove, W. W. (2009). The projection of species distribution models and the problem of non-analog climate. *Biodiversity and Conservation, 18*(8), 2255-2261. doi:10.1007/s10531-009-9584-8

Franklin, J., Davis, F. W., Ikegami, M., Syphard, A. D., Flint, L. E., Flint, A. L., & Hannah, L. (2013). Modeling plant species distributions under future climates: how fine scale do climate projections need to be? *Global change biology, 19*(2), 473-483. doi:10.1111/gcb.12051

Gallant, A. L., Binnian, E. F., Omernik, J. M., & Shasby, M. B. (1995). *Ecoregions of Alaska*: US Government Printing Office.

Geiger, R., Aron, R. H., & Todhunter, P. (2009). *The climate near the ground*: Rowman & Littlefield.

Gent, P. R., Danabasoglu, G., Donner, L. J., Holland, M. M., Hunke, E. C., Jayne, S. R., . . . Zhang, M. H. (2011). The Community Climate System Model Version 4. *Journal of Climate, 24*(19), 4973-4991. doi:10.1175/2011jcli4083.1

Glassberg, D. (2014). Place, Memory, and Climate Change. *Public Historian, 36*(3), 17-30. doi:10.1525/tph.2014.36.3.17

Gustafsson, M. G. (2000). Surpassing the lateral resolution limit by a factor of two using structured illumination microscopy. *Journal of microscopy, 198*(2), 82-87.

Haines-Young, R., & Chopping, M. (1996). Quantifying landscape structure: a review of landscape indices and their application to forested landscapes. *Progress in Physical Geography, 20*(4), 418-445.

Heikkinen, R. K., Luoto, M., Kuussaari, M., & Toivonen, T. (2007). Modelling the spatial distribution of a threatened butterfly: Impacts of scale and statistical technique. *Landscape and Urban Planning, 79*(3-4), 347-357. doi:10.1016/j.landurbplan.2006.04.002

Hobbs, R. J., Arico, S., Aronson, J., Baron, J. S., Bridgewater, P., Cramer, V. A., . . . Zobel, M. (2006). Novel ecosystems: theoretical and management aspects of the new ecological world order. *Global Ecology and Biogeography, 15*(1), 1-7. doi:10.1111/j.1466-822x.2006.00212

Hutchinson, G. (1957). Concluding remarks Cold ssring Harbor Symp. *Quant, 22*, 66-77.

Jackson, S. T., & Overpeck, J. T. (2000). Responses of plant populations and communities to environmental changes of the late Quaternary. *Paleobiology, 26*(4), 194-220. doi:10.1666/0094-8373

Jaroslav, H. (2013). Topographic Solar Radiation Modeling for Environmental Applications. In *Solar Energy* (pp. 715-730): Springer.

Katurji, M., & Zhong, S. Y. (2012). The Influence of Topography and Ambient Stability on the Characteristics of Cold-Air Pools: A Numerical Investigation. *Journal of Applied Meteorology and Climatology, 51*(10), 1740-1749. doi:10.1175/Jamc-D-11-0169.1

Kennie, T., & McLaren, R. (1988). Modelling for digital terrain and landscape visualisation. *The Photogrammetric Record, 12*(72), 711-745.

Kluzek, E. (2011). CCSM research tools: CLM4. 0 user's guide documentation.

Larsen, J. N., Anisimov, O. A., Constable, A., Hollowed, A. B., Maynard, N., Prestrud, P., . . . Stone, J. M. R. (2014). *Polar Regions. Climate Change 2014: Impacts, Adaptations, and Vulnerability. Part B: Regional Aspects. Contribution of Working Group II to the Fifth Assessment Report of the Intergovernmental Panel on Climate Change* (V. R. Barros, C. B. Field, D. J. Dokken, M. D. Mastrandrea, K. J. Mach, T. E. Bilir, M. Chatterjee, K. L. Eb, Y. O. Estrada, R. C. Genova, B. Girma, E. S. Kissel, A. N. Levy, S. MacCracken, P. R. Mastrandrea, & L.L.White Eds.). Cambridge, United Kingdom and New York, NY, USA: Cambridge University Press.

Levin, S. A. (1992). The Problem of Pattern and Scale in Ecology. *Ecology, 73*(6), 1943-1967. doi:10.2307/1941447

Madsen, H., & Thyregod, P. (2010). *Introduction to general and generalized linear models*: CRC Press.

Maraun, D., Wetterhall, F., Ireson, A., Chandler, R., Kendon, E., Widmann, M., . . . Themeßl, M. (2010). Precipitation downscaling under climate change: Recent developments to bridge the gap between dynamical models and the end user. *Reviews of Geophysics, 48*(3).

Menne, M. J., Durre, I., Vose, R. S., Gleason, B. E., & Houston, T. G. (2012). An Overview of the Global Historical Climatology Network-Daily Database. *Journal of Atmospheric and Oceanic Technology, 29*(7), 897-910. doi:10.1175/Jtech-D-11-00103.1

Mix, A. C., Bard, E., & Schneider, R. (2001). Environmental processes of the ice age: land, oceans, glaciers (EPILOG). *Quaternary Science Reviews, 20*(4), 627-657.

Monteith, J. L. (1965). *Evaporation and environment.* Paper presented at the Symp. Soc. Exp. Biol.

Ohlemuller, R. (2011). Running Out of Climate Space. *Science, 334*(6056), 613-614. doi:10.1126/science.1214215

Overpeck, J. T., Bartlein, P. J., & Webb, T. (1991). Potential magnitude of future vegetation change in eastern North America: comparisons with the past. *Science, 254*(5032), 692-695.

Penman, H. L. (1948). *Natural evaporation from open water, bare soil and grass.* Paper presented at the Proceedings of the Royal Society of London A: Mathematical, Physical and Engineering Sciences.

Radeloff, V. C., Williams, J. W., Bateman, B. L., Burke, K. D., Carter, S. K., Childress, E. S., . . . Usinowicz, J. (2015). The rise of novelty in ecosystems. *Ecological Applications, 25*(8), 2051-2068.

Raisanen, J. (2001). CO2-induced climate change in CMIP2 experiments: Quantification of agreement and role of internal variability. *Journal of Climate, 14*(9), 2088-2104.

Randin, C. F., Engler, R., Normand, S., Zappa, M., Zimmermann, N. E., Pearman, P. B., . . . Guisan, A. (2009). Climate change and plant distribution: local models predict high-elevation persistence. *Global change biology, 15*(6), 1557-1569. doi:10.1111/j.1365-2486.2008.01766

Ruiz-Arias, J., Tovar-Pescador, J., Pozo-Vázquez, D., & Alsamamra, H. (2009). A comparative analysis of DEM-based models to estimate the solar radiation in mountainous terrain. *International Journal of Geographical Information Science, 23*(8), 1049-1076.

Seo, C., Thorne, J. H., Hannah, L., & Thuiller, W. (2009). Scale effects in species distribution models: implications for conservation planning under climate change. *Biology Letters, 5*(1), 39-43. doi:10.1098/rsbl.2008.0476

Stephenson, N. L. (1990). Climatic Control of Vegetation Distribution - the Role of the Water-Balance. *American Naturalist, 135*(5), 649-670. doi:10.1086/285067

Stephenson, N. L. (1998). Actual evapotranspiration and deficit: biologically meaningful correlates of vegetation distribution across spatial scales. *Journal of Biogeography, 25*(5), 855-870. doi:10.1046/j.1365-2699.1998.00233.x

Suri, M., & Hofierka, J. (2004). A New GIS-based Solar Radiation Model and Its Application to Photovoltaic Assessments. *Transactions in GIS, 8*(2), 15. doi:10.1111/j.1467-9671.2004.00174

Taylor, K. E., Stouffer, R. J., & Meehl, G. A. (2012). An overview of CMIP5 and the experiment design. *Bulletin of the American Meteorological Society, 93*(4), 485-498.

Tesfa, T. K., Tarboton, D. G., Watson, D. W., Schreuders, K. A. T., Baker, M. E., & Wallace, R. M. (2011). Extraction of hydrological proximity measures from DEMs using parallel processing. *Environmental Modelling & Software, 26*(12), 1696-1709. doi:10.1016/j.envsoft.2011.07.018

Thrasher, B., Xiong, J., Wang, W., Melton, F., Michaelis, A., & Nemani, R. (2013). Downscaled climate projections suitable for resource management. *Eos, Transactions American Geophysical Union, 94*(37), 321-323.

Trivedi, M. R., Berry, P. M., Morecroft, M. D., & Dawson, T. P. (2008). Spatial scale affects bioclimate model projections of climate change impacts on mountain plants. *Global change biology, 14*(5), 1089-1103. doi:10.1111/j.1365-2486.2008.01553

Urban, D. L., Miller, C., Halpin, P. N., & Stephenson, N. L. (2000). Forest gradient response in Sierran landscapes: the physical template. *Landscape Ecology, 15*(7), 603-620. doi:10.1023/A:1008183331604

USGS. (2016). *The National Map*. Retrieved from: http://nationalmap.gov/3DEP/3dep_prodserv.html

Vandermeer, J. H. (1972). Niche Theory. *Annual review of Ecology and Systematics, 3*, 29.

Venables, W., & Ripley, B. (2002). Statistics and computing.

Webb III, T. (1992). Past change in vegetation and climate: Lessons for the future. *Global warming and biological diversity*, 59-75.

Webb, R. S., Rind, D. H., Lehman, S. J., Healy, R. J., & Sigman, D. (1997). Influence of ocean heat transport on the climate of the Last Glacial Maximum. *Nature, 385*(6618), 695.

Wetterhall, F., Bardossy, A., Chen, D. L., Halldin, S., & Xu, C. Y. (2006). Daily precipitation-downscaling techniques in three Chinese regions. *Water Resources Research, 42*(11). doi:Artn W11423

10.1029/2005wr004573

Widmann, M., Bretherton, C. S., & Salathé Jr, E. P. (2003). Statistical precipitation downscaling over the northwestern United States using numerically simulated precipitation as a predictor. *Journal of Climate, 16*(5), 799-816.

Williams, J. W., & Jackson, S. T. (2007). Novel climates, no-analog communities, and ecological surprises. *Frontiers in Ecology and the Environment, 5*(9), 475-482. doi:10.1890/070037

Willis, K. J., & Bhagwat, S. A. (2009). Biodiversity and climate change. *Science, 326*(5954), 806-807.

Wolock, D. M., & McCabe, G. J. (1995). Comparison of single and multiple flow direction algorithms for computing topographic parameters in TOPMODEL. *Water Resources Research, 31*(5), 1315-1324.

Wu, J. (1999). Hierarchy and scaling: extrapolating information along a scaling ladder. *Canadian journal of remote sensing, 25*(4), 367-380.

CHAPTER 2: IS CLIMATE VELOCITY AN ADEQUATE MEASURE OF SPECIES MIGRATION RESPONSES TO CLIMATE CHANGE?

2.1 ABSTRACT

Many species are shifting their ranges in response to climate change. Species survival will not only depend on the persistence of suitable bioclimatic niche space, but their ability to keep pace with shifts in their niche space. Climate velocity has become a commonly used index of the speeds required for a species to keep pace with climate change. However, climate velocity is a simple measure of the rate at which climate is changing that disregards species-specific thresholds to their environment. I computed the climate velocity for eight climate variables using 60 m downscaled climate data in Alaska for the Last Glacial Maximum (LGM) and modern era. With the same climate variables, I then estimated LGM and modern distributions of white spruce (*Picea glauca*). I calculated the bioclimatic niche velocity of white spruce by using the model structure of climate velocity hybridized with white spruce distribution maps to estimate white spruce's migration response to keep pace with post-glacial climate change. I then compared all climate velocity estimates to each other and to my white spruce migration velocity estimates to determine if climate velocity is a suitable predictor of a species' migration response to climate change. I show that different climate variables yield different rates and direction of climate velocity, and that individual climate velocity estimates correlate poorly with the bioclimatic niche velocity as estimated for the Alaskan white spruce from the LGM to modern era. My results suggest that climate velocity alone does not provide suitable estimates of species migration responses to climate change due to climate velocity not accounting for species ecology and climatic tolerances that affect migration responses. My results may help explain unexpected or conflicting observational evidence of climate-driven species range shifts.

2.2 INTRODUCTION

The influence of climate change on Earth's biota partly depends on the rate at which climate is changing and its interactions with a species' ability to migrate to favorable habitat (Sandel et al., 2011). Threats to global biodiversity from climate change make it important to identify the rates and directions species have, are, or will need to migrate in response to climate change (Chen, Hill, Ohlemuller, Roy, & Thomas, 2011). Shifts in species and biome ranges are expected to cause the rearrangement of ecosystems including the creation of novel communities across the globe (Pereira et al., 2010; Williams, Jackson, & Kutzbacht, 2007). Many species have already responded to climate change by altering the timing of their life cycles or shifting their geographic distributions towards higher latitudes or elevations (Chen et al., 2011; Colwell, Brehm, Cardelus, Gilman, & Longino, 2008; Parmesan & Yohe, 2003). In recent years, climate velocity has become proposed as a practical approach to estimate the rate and direction with which an organism would need to migrate to maintain an isocline for a given climate variable (Dobrowski et al., 2013), with studies projecting large shifts in the distribution of terrestrial biomes, including some biome types requiring displacements of more than 1 km yr^{-1} to track anthropogenic climate change (Loarie et al., 2009).

Climate velocity is a spatially explicit measure of the local rate of displacement of climatic conditions over the Earth's surface and is derived from the ratio of temporal and spatial gradients of a climate variable (M. T. Burrows et al., 2011; Dobrowski et al., 2013; Loarie et al., 2009). Because climate velocity integrates shifts in climate with local spatial topo-climate gradients, it can capture important buffering effects of climatic heterogeneity as well as varying bioclimatic consequences, making it a more biologically relevant measure than traditional climate anomaly surfaces (Sandel et al., 2011). For example, locally homogeneous climate landscapes will experience higher climate velocities than heterogeneous ones, as a species may need to migrate a considerable distance to track a 1°C increase in temperature on flat terrain, yet only need to migrate a short distance to track a similar temperature change uphill in mountainous terrain. Therefore, species in homogeneous environments are not only likely to

experience higher climate velocities but may be required to have strong dispersal abilities to track temperature changes as opposed to species in heterogeneous environments (Sandel et al., 2011).

While climate velocity has been asserted as an important index for proxying the rate at which species will need to migrate to track climate change, three major criticisms exist: 1) climate velocity lacks complex multi-climate interactions (Dobrowski et al., 2013; Loarie et al., 2009), 2) climate velocity lacks sensitivity to the resolution of gridded climate surfaces used to compute its spatial and temporal gradients (Loarie et al., 2009), and 3) climate velocity lacks species-specificity (Loarie et al., 2009), and are reviewed as follows:

First, climate change involves complex interactions among multiple climate factors (Cubasch et al., 2013). However, many previous ecological analyses utilizing climate velocity focus on observed and predicted changes in temperature because there is less uncertainty in the direction and magnitude of temperature change than other climate variables (Loarie et al., 2009; Murphy et al., 2004). While our understanding of temperature change may be better than other climate variables, I must consider that climate is more than just temperature, and that species are limited by any number of climate and non-climate variables (Vandermeer, 1972). Therefore, the rate and directions estimated by climate velocity will vary depending on variables resulting in counterintuitive movements and/or multiple or opposing influences on biota (Dobrowski et al., 2013).

Second, estimates of climate velocity have been found to be sensitive to the spatial grain used in climate change analyses (Loarie et al., 2009). This can significantly affect conclusions drawn from climate velocity used to estimate potential extinction risk for species, because spatio-temporal patterns of climate in heterogeneous environments are complex, and the scale of climate used in analyses should reflect the scale at which vegetation (or other organismal types) actually experience their environment (Dobrowski, Abatzoglou, Greenberg, & Schladow, 2009; Urban, Miller, Halpin, & Stephenson, 2000). Therefore, the resolution of climate data used in analyses should match the scale in which organisms migrate and experience climate. For example, Loarie et al. (2009) chose to use climate surfaces at 1 km resolution because many species and large temperature changes occur at the kilometer scale. Similarly,

studies focusing on landscape scale or smaller scale (< 1 km) population migrations should use climate data at resolutions less than 1 km.

Lastly, and perhaps most importantly, while climate velocity can be used to correlate patterns of species endemism and biotic specialization with climate change (Dobrowski et al., 2013), it simply estimates the rate and direction of climate change, and is therefore not a measure of a species migration rate (Loarie et al., 2009). Climate velocity can be used to understand range edge expansions and contractions, ecotones, and to estimate general distance responses all species may need to migrate to avoid extinction due to climate change. However, individual species are adapted to their environments leading to specialized tolerances, and therefore will respond to climate change with a wide diversity of responses driven by internal species trait differences and external drivers of change (Chen et al., 2011). Thus, different species should be expected to exhibit distinct, individualistic responses to climate velocity (Ackerly et al., 2010). For species with small climate tolerances, climate velocity estimates may approximate the rate of migration needed to avoid extinction, while climate velocity estimates for species with large tolerances will tend to underestimate migration speeds required to potentially avoid extinction (Loarie et al., 2009). Additionally, species do not all migrate at the same pace or direction of movement or experience the same expansion and contraction of their ranges. No assumptions should be made about the tolerances of individual species, as the implications of climate change will depend on individual critical thresholds, breadth of tolerance, and limiting factors of a species (Loarie et al., 2009).

With the latter issue in mind, I used the concept of bioclimatic velocity (Serra-Diaz et al., 2014) to test the effectiveness of climate velocity when actual species information is used. Bioclimatic velocity uses the same model structure as climate velocity but integrates species-specificity and multivariate climate via a species distribution modeling (SDM) framework. As with climate velocity, I summarize the speed at which a species must migrate by deriving the ratio of temporal and spatial gradients of a species' potential distribution; i.e. the rate and direction the species must migrate to keep the same probability of occurrence. SDMs correlate combinations of abiotic environmental variables (i.e. the fundamental niche) most closely associated with the known presence/absence information of a species, then use this

relationship to identify and project past, present, or future suitable environments on a landscape (Soberon & Peterson, 2005). Thus, the geographic distribution of a species estimated from SDMs is a spatial reflection of a species-specific climatic niche. In this analysis, I am interested in species responses to climate change, and focus on the bioclimatic niche of species (i.e. potential niche) rather than all environmental change (i.e. fundamental niche). Therefore, bioclimatic niche velocity is a measure of the rate and direction a species needs to move to keep pace with climate change and remain in a similar, suitable environment.

Since previous studies claim that climate velocity is well suited to assess the effects of climate on biota and the dispersal capacity of organisms (M. T. Burrows et al., 2011; Dobrowski et al., 2013; Hamann, Roberts, Barber, Carroll, & Nielsen, 2015; Loarie et al., 2009; Ohlemuller, 2011; Sandel et al., 2011), climate velocity should predict similar migration responses of a species as bioclimatic niche velocity. Therefore, in this study I ask:

Is climate velocity a suitable predictor of a species' response to climate change?

To address this question, I used 60m resolution downscaled climate surfaces as my environmental predictors, modeled LGM and modern Alaskan climate velocities, and modeled the bioclimatic niche velocity of the white spruce (*Picea glauca*). I refer to bioclimatic velocity (Serra-Diaz et al., 2014) as bioclimatic niche velocity because it is more clear than Serra-Diaz et al. (2014) terminology since it differentiates that I am estimating white spruce migration from a potential distribution, not their realized niche. Rather than using traditional central tendency type models to derive a species' distributions (Guisan & Thuiller, 2005), I utilized environmental limiting factor (ELF) methods (M. Austin, 2007; Cade & Noon, 2003; Greenberg, Santos, Dobrowski, Vanderbilt, & Ustin, 2015; Sankaran et al., 2005) to quantify the potential niche of a species and to avoid issues with unmeasured factors (Cade & Noon, 2003; Huston, 2005; Thomson, Weiblen, Thomson, Alfaro, & Legendre, 1996). I chose white spruce because it is one of the most dominant and widespread tree species in boreal and sub-boreal Alaska and has survived in Alaska from the LGM to modern era despite drastic changes to the regions' climate over geologic time (Abrahamson, 2014). I compared climate velocity to the calibrated bioclimatic niche

velocity to determine if climate velocity adequately predicts a species' response to climate change. If

climate velocity is a suitable predictor of species' responses to climate change, then climate velocity

should correlate with the magnitude and direction calculated from the white spruce distributions.

2.3 METHODS

2.3.1 White spruce sample data:

I collected spatially explicit presence data for white spruce in Alaska from LANDFIRE's

Reference Database (LFRDB), which includes natural community occurrences and canopy cover for

species across the state (LANDFIRE, 2016). LFDRB aggregates data from sources such as USFS Forest

Inventory Analysis Vegetation Data (Smith, 2002), USGS national Gap Analysis Program (USGS-GAP,

2018), and NPS Inventory and Monitoring (Marion, 1991). Species occurrences for this dataset have been

collected at both plot and individual levels, depending on where the source samples were collected. Of the

44,475 reported species occurrences in Alaska, 3,084 of the observations reported white spruce present. If

the observation stated white spruce as present, but did not report a % tree cover estimate, the observation

was dropped from my database. I considered the remaining 41,391 occurrences that did not report white

spruce present as pseudoabsence observations and were assigned a percent cover of 0% (Figure 2.1).
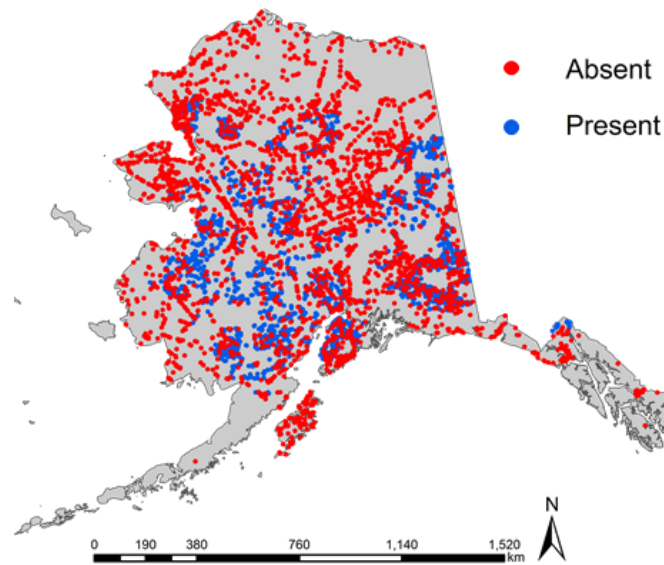
Figure 2.1: Map of white spruce presence-absence sample locations. Blue points are locations where white spruce was recorded as present. Red points are pseudoabsence locations where no white spruce was recorded.

2.3.2 Climate surfaces:

I used a set of 30-year average 60m downscaled climate surfaces that included the mean temperature of the warmest month (T_{max}), the mean temperature of the coldest month (T_{min}), annual rain, snow, actual and potential evapotranspiration (AET, PET), climatic water deficit (Def), and mean "true-sky" surface radiation (Rad) for the LGM (~21,000 ya) and modern era (1975-2005). Further details on the dataset used, and the development of all products, are provided in Chapter 1 methods. Table 2.1 summarizes the Alaska-wide values of this dataset. In addition to my climate surfaces, I compiled 60m resolution for surfaces of glacier presence based on the Alaska PaleoGlacier Atlas (Manley & Kaufman, 2002), proximity to water bodies (Clearinghouse, 1990, 1998), and elevation using the United States Geologic Surveys (USGS) 1 arc-second digital elevation maps (DEM) (USGS, 2016).

Table 2.1: Statistical summary list of initial climate and physical environmental surfaces used for climate velocity and ELF model for the Alaskan LGM and modern eras.

Environmental Variable	Units	Min	Max	Mean	SD
LGM					
Annual AET	mm	0.0	651.7	184.9	88.1
Annual Deficit	mm	0.0	420.6	22.5	33.1
Annual PET	mm	0.3	667.4	207.4	93.9
Annual Rain	mm	0.0	3452.9	231.2	223.2
Annual Snow	mm	0.2	5494.4	782.2	439.2
Mean Radiation	w	0.0	261.0	131.0	23.4
T_{max}	°C	-21.0	30.5	16.9	8.1
T_{min}	°C	-36.1	4.3	-21.9	3.4
Glacier Presence	NA	0	1	0.08	0.27
Proximity to Water	km	0	81.6	0.75	0.66
Elevation	m.a.s.l.	-25.5	6150.3	441.9	543.8
Modern					
Annual AET	mm	0.0	445.4	183.5	49.0
Annual Deficit	mm	0.0	314.4	11.5	15.0
Annual PET	mm	1.7	463.5	195.0	52.0
Annual Rain	mm	0.0	4424.7	505.6	330.0
Annual Snow	mm	0.0	3420.5	717.2	263.1
Mean Radiation	w	0.0	209.7	97.8	17.1
T_{max}	°C	-13.2	31.3	21.0	3.7
T_{min}	°C	-34.7	6.6	-18.1	5.4
Glacier Presence	NA	0	1	0.01	0.09
Proximity to Water	km	0	81.6	0.75	0.66
Elevation	m.a.s.l.	-25.5	6150.3	441.9	543.8

2.3.3 Environmental limiting factor model (ELF):

Tree cover-bioclimate database: I fused my white spruce % tree cover database with the modern environmental predictor values extracted from the position of the vegetation plots. The final database contained 44,475 observations across Alaska describing white spruce's environmental envelope.

Environmental limiting factor analysis: I followed similar methods as described in Greenberg et al. (2015) to perform an environmental limiting factor (ELF) analysis to estimate the fundamental niche of white spruce tree cover. First, for each environmental variable, I modeled the maximum potential % tree cover

across the possible range of values for each specific environmental variable using quantile regression. I

applied a log-odds transformation to the tree cover values in my database (Warnes, Bolker, & Lumley,

2014), with a minimum of 0% tree cover. White spruce can have 100% cover in Alaska, however my

database only reported a maximum of 90%, which was used as the maximum value cap in my log-odds

transformation. Every hull model was created using the following general quantile regression formula:

$$EQ\ 2.1:\ \textit{Log-Odds(Maximum Tree Cover}_{x,y,t}) = f(B_{Spline}(\textit{Climate}_{v,x,y,t}), q = 0.99)$$

Where *Maximum Cover*$_{x,y,t}$ represents estimated maximum potential tree cover at location (x,y) during

either the LGM or modern era (t), *Climate*$_{v,x,y,t}$ represents the potential limiting bioenvironmental variable

(v) at location (x,y) during the LGM or modern era (t) with a B-Spline function applied, and q represents

the percentile limit for the quantile regression model requirement. I chose a percentile of 99% to capture

only maximum tree cover values of white spruce for the entire range of possible environmental values.

Once modeled, I inverse log-odds transformed *Maximum Tree Cover*$_{x,y,t}$ back to its original 0-90% value

range. Unlike the rest of the environment variables, for glacier presence/absence I classified a location

with a glacier present as 0% tree cover, and locations with no glaciers present as 90% tree cover.(Helm &

Collins, 1997).
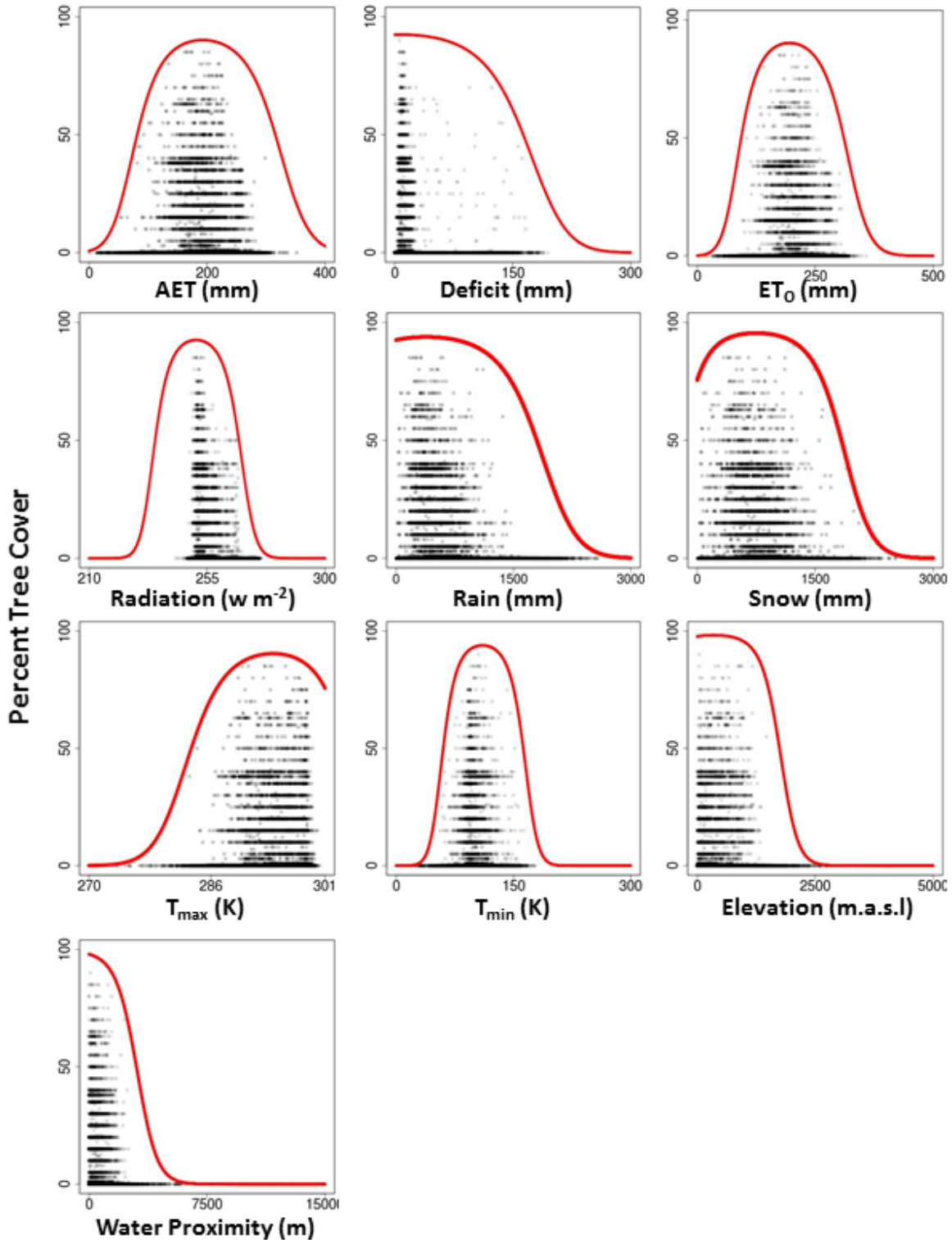
Figure 2.2: ELF scatterplots for the range of each climate variable vs. the range of white spruce tree cover used to create and model my ELF maximum tree cover hull models. Black scatterplot dots represent sample data from tree cover-bioclimate database. Red lines represent hull modeled tree cover for a given climate value from climate variable's hull model.

Model validation: I validated my ELF models by binning each environmental variable into 100 equal

sized bins across its possible range and extracting the maximum tree cover value within each

environmental bin. This created a unique N=100 validation dataset for each environment variable with

close to maximum tree cover values that could be validated using Pearson's correlation, root mean

squared error (RMSE), and percent bias statistics. All hull models had a Pearson's correlation coefficient

value > 0.70, indicating strong positive relationships between my modeled maximum tree cover and

sampled maximum tree cover data (Table 2.2). RMSE values were variable among all my

bioenvironmental variables for my ELF models with my water proximity surfaces having the lowest tree

cover error of 6.29%, and radiation containing the largest error at 33.35% (Table 2.2). All models, except

radiation, had negative % biases, which indicates my models underpredicted maximum potential % tree

cover somewhat (Table 2.2). While the snow-tree cover hull model had a positive % bias of 1.72, this was

extremely low and considered acceptable because one validation point was greater than the modeled

maximum tree cover response at the top of the bell curve (Figure 2.2).

Table 2.2: Summary statistic results for each ELF Hull quantile regression model for all climate variables
used to estimate LGM and modern white spruce potential % tree cover.

Environmental Variable	Correlation	RMSE	% Bias
AET	0.87	21.98	-12.74
Deficit	0.82	26.89	-17.03
PET	0.93	17.10	-10.36
Radiation	0.74	33.35	-22.59
Rain	0.83	25.10	-14.74
Snow	0.97	8.49	1.72
T$_{max}$	0.89	20.96	-11.16
T$_{min}$	0.70	34.94	-25.42
Elevation	0.92	17.14	-8.44
Water Proximity	0.93	6.29	-1.26

Potential tree cover and limiting factor surfaces: Once all hulls were modeled for each environmental

variable and white spruce tree cover, I applied the models to each corresponding environmental variable

for the LGM and modern era producing 11 modern maximum tree cover surfaces and 11 LGM maximum

potential tree cover surfaces. I stacked the 11 maximum potential tree cover surfaces for both eras and 1) determined the minimum potential tree cover value (limiting value) across all variables for each pixel and 2) determined which environmental variable was responsible for limiting white spruce maximum tree cover at each pixel, producing two potential maximum tree cover surfaces (LGM and modern), and two limiting factor surfaces (LGM and modern). If one environmental variable was found to be the limiting factor, that pixel was reclassified as the limiting factor. If more than one variable was responsible for limiting tree cover, the pixel was reclassified as "multi", indicating that more than one environmental factor corresponded with limiting tree cover.

2.3.4 Climate and bioclimatic niche velocity calculations:

I calculated climate velocity following the methods of Dobrowski et al. (2013) and M. T. Burrows et al. (2011) on climate surfaces between the LGM and modern eras for T_{min}, T_{max}, rain, snow, radiation, AET, PET, and water deficit. Climate velocity vectors were calculated as follows:

$$EQ\ 2.2:\ V_{c,x,y} = \left(\frac{d_c/d_t}{d_c/d_x}, \frac{d_c/d_t}{d_c/d_y} \right) = \left(\frac{|Modern_c - LGM_c|/18,000\ years}{atan(slope(Modern_c))} \right) = \frac{meters}{year}$$

where $V_{c,xy}$ represents the speed component of climate velocity, d_c/d_t is the change in climate variable over time (temporal gradient, unit/yr) and d_c/d_{xy} is the change in the same climate variable over distance (spatial gradient, unit/m) (Michael T Burrows et al., 2014).

Bioclimatic niche velocity vectors were derived using nearly identical methods as climate velocity vectors but using the modern and LGM ELF surfaces. The following formula was used to derive the speed component of bioclimatic niche velocity:

$$EQ\ 2.3:\ V_{p,x,y} = \left(\frac{|Modern_p - LGM_p/18,000\ years|}{atan(slope(Modern_p))} \right) = \frac{meters}{year}$$

where d_p/d_t is the change in tree cover or SDM probability over time (temporal gradient, % tree cover/yr) and d_p/d_{xy} is the change in tree cover or SDM probability over distance (spatial gradient, % tree cover/m). The final white spruce bioclimatic niche velocity surfaces (speed and direction) were computed where the

LGM ELF potential % tree cover was greater than 0, and the habitat suitability at a location decreased between the LGM and modern eras (i.e. potential % tree cover decreased in the modern era). Regions where white spruce could not persist during the LGM indicate areas where Alaska's climate did not fall within white spruce's climatic niche. While biologically relevant, the information ultimately cannot produce bioclimatic niche velocity estimates. Additionally, regions where white spruce's habitat suitability increased from the LGM to modern era indicate areas where the climate has remained within white spruces climatic niche, and therefore places no pressure on white spruce to migrate due to post-glacial climate change.

**2.3.5 Climate vs. bioclimatic niche velocity analysis:**

To quantify the strength of the relationship between both measures, I computed the Pearson's correlation coefficient between my estimated bioclimatic niche velocity and every climate variable's individual speed and direction for the entire state of Alaska. Additionally, I computed the standard deviation between all climate velocity surfaces for speed and direction to determine how individual climate velocity measurements correspond to one another. As the directional components of climate and bioclimatic velocity are circular, I used circular mean, standard deviation, and correlation functions to compute directional statistics in this analysis with the I "circular" R package (Agostinelli & Lund, 2013; Jammalamadaka & Sarma, 1988).

2.4 RESULTS

2.4.1 White spruce distributions:

White spruce had greater distributions during the modern era than the LGM (Figure 2.3). My modern white spruce tree cover estimates suggest that a vast majority of Alaska's terrestrial surface is climatically suitable for white spruce based on the environmental variables I chose, and as data shows 94.1% of Alaska supports white spruce tree cover >0% (Figure 2.3). 69.2% of Alaska was also climatically suitable for white spruce to survive the LGM with tree cover >0% (Figure 2.3). Overall,

78.9% of the land area of Alaska became more suitable for white spruce, 18.9% became less suitable for

white spruce, and 2.1% had no change in suitability for white spruce from the LGM to modern era (Figure

2.3).
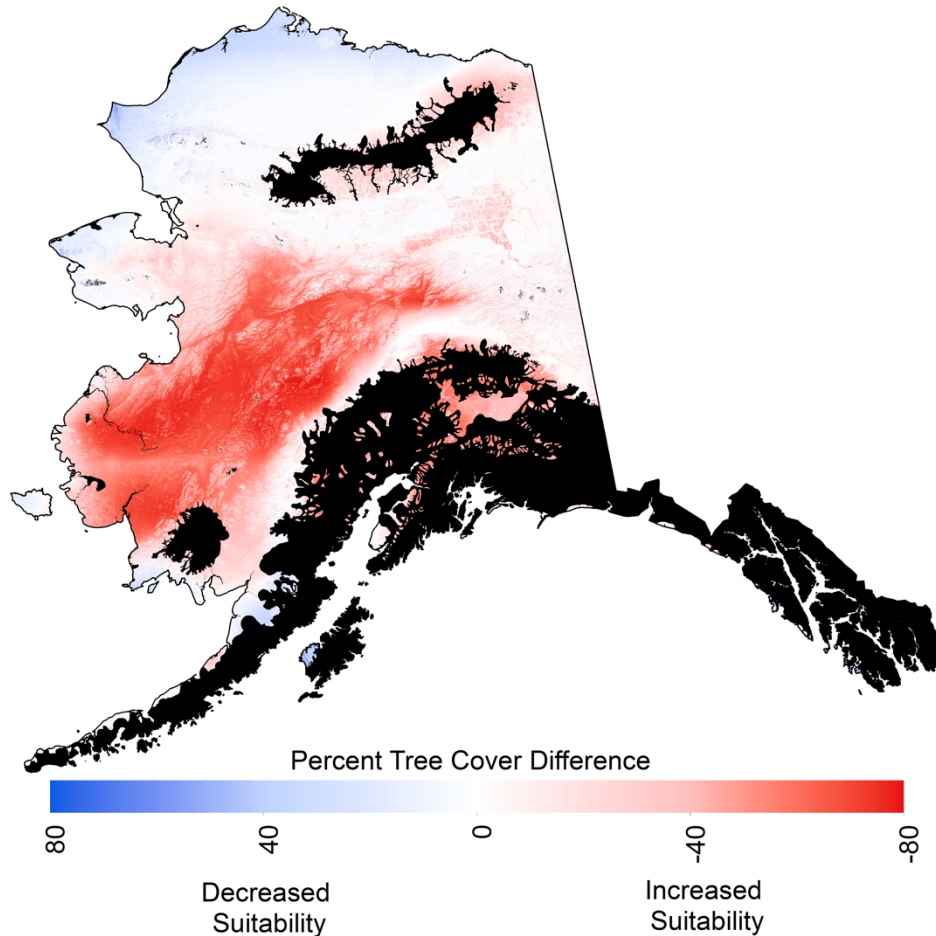
Figure 2.3: Difference between LGM and modern white spruce potential % tree cover distributions for all of Alaska where LGM distributions were > 0 % tree cover. Red regions indicate areas where modern tree cover is greater than LGM tree cover, and similarly, blue regions indicate areas where LGM tree cover was greater than modern tree cover. Increased tree cover is assumed synonymous with increased habitat suitability. Black regions indicate areas where white spruce did not occur during the LGM and were not considered for this analysis.

White spruce distributions were limited by all climate variables used as predictors in my ELF

models, suggesting that all climate variables have influence on white spruce distributions in Alaska

during both the LGM and modern eras (Figure 2.4).
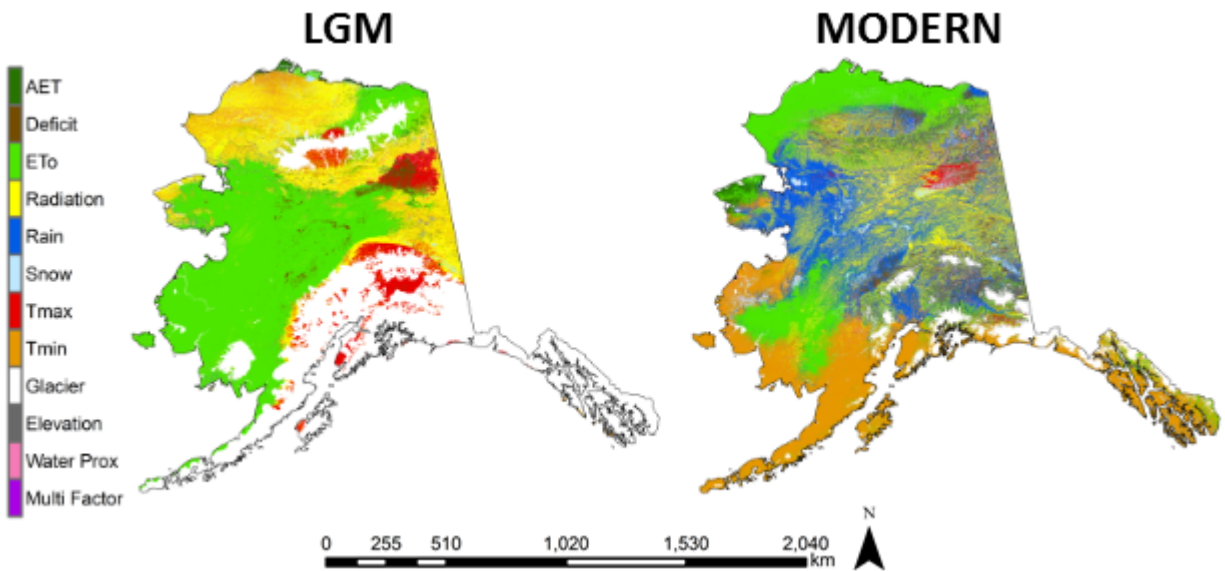
Figure 2.4: Spatially explicit maps of climatic factors most limiting white spruce across Alaska during the LGM (left) and modern (right) eras.

2.4.2 Climate velocity trends:

Mean climate speeds ranged from 0.02 m/yr to 1.68 m/yr (Table 2.3). The mean speed between all climate speeds by pixel was 0.30 m yr^{-1} with a standard deviation of 1.1 m yr^{-1}. The standard deviation of climate speeds ranged from 0.05 to 9.37 m yr^{-1} (Table 2.3). The mean standard deviation between all climate speeds by pixel was 0.52 m yr^{-1}, with a standard deviation of 2.29 m yr^{-1} (Figure 2.5a).

Table 2.3: Climate and bioclimatic niche velocity mean and standard deviation summary statistics for speed and direction.

Variable	Speed (m yr^{-1})		Direction (Degrees)	
	Mean	Stdev	Mean	Stdev
AET	0.13	0.22	193.82°	2.75°
Deficit	0.07	0.14	191.23°	2.85°
PET	0.15	0.23	188.24°	2.56°
Radiation	1.68	9.37	25.16°	2.66°
Rain	0.15	0.41	7.54°	3.25°
Snow	0.02	0.05	162.19°	3.33°
T_{max}	0.79	1.79	125.32°	2.74°
T_{min}	0.22	0.32	357.24°	2.93°
Species	**0.49**	**1.31**	**353.45°**	**2.86°**

Mean directions for AET, deficit, and PET were primarily south, radiation, rain, and T_{min} were north, and snow and T_{max} climate velocities were southeast (Table 2.3, Figure 2.6). The mean direction between all climate directions by pixels was 180.51° (south), with a standard deviation of 53.50°. The standard deviation of climate speeds ranged from 2.56 to 3.33° (Table 2.3). The mean standard deviation between all climate speeds by pixel was 87.87°, with a standard deviation of 18.48° (Figure 2.5b)
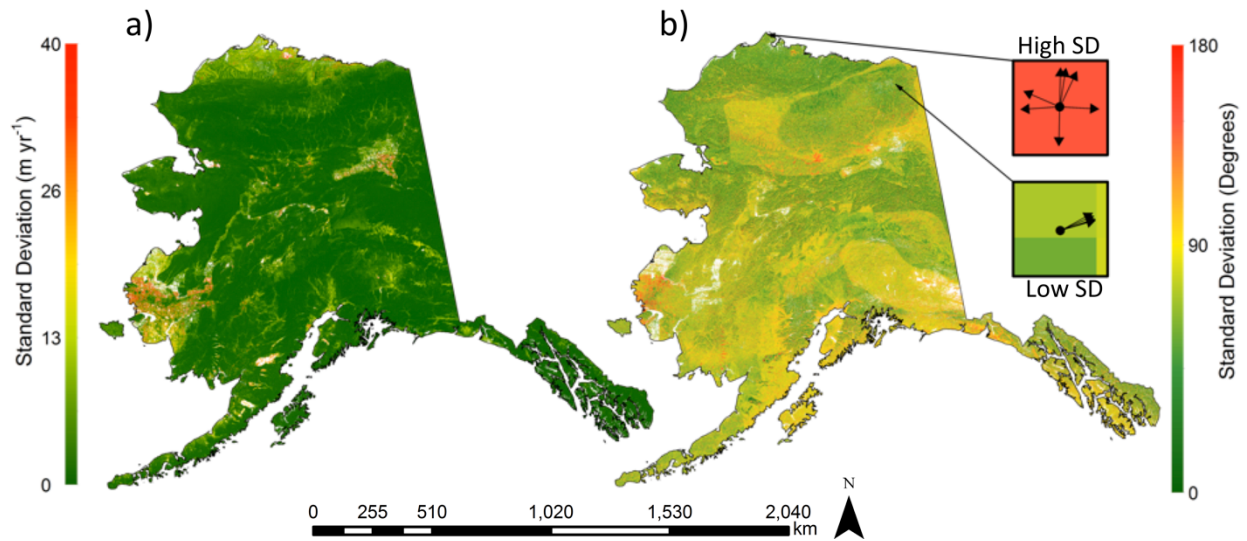
Figure 2.5: The standard deviation of climate velocity speed and directions. **a)** climate speed. **b)** climate direction. In both inset maps, each arrow represents the direction climate is changing for each climate variable.
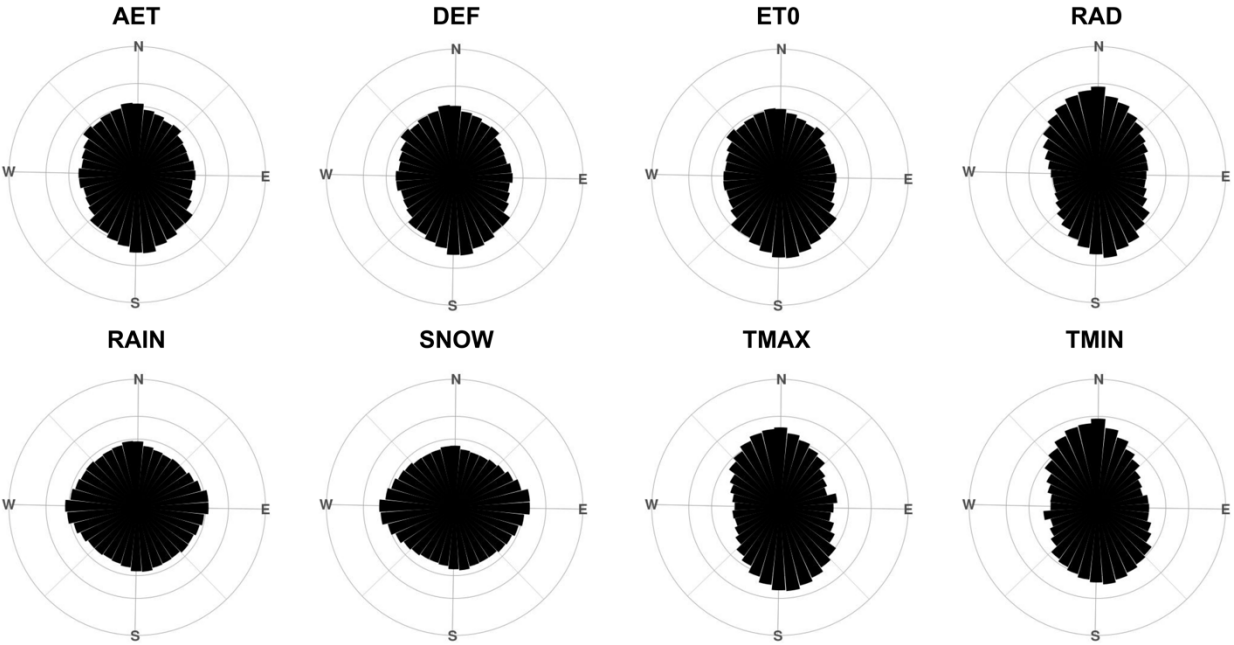
Figure 2.6: Climate direction histograms broken into 36 equal sized bins of 10°. Inner circles represent fraction of climate velocity pixels within bin from 0-5%.

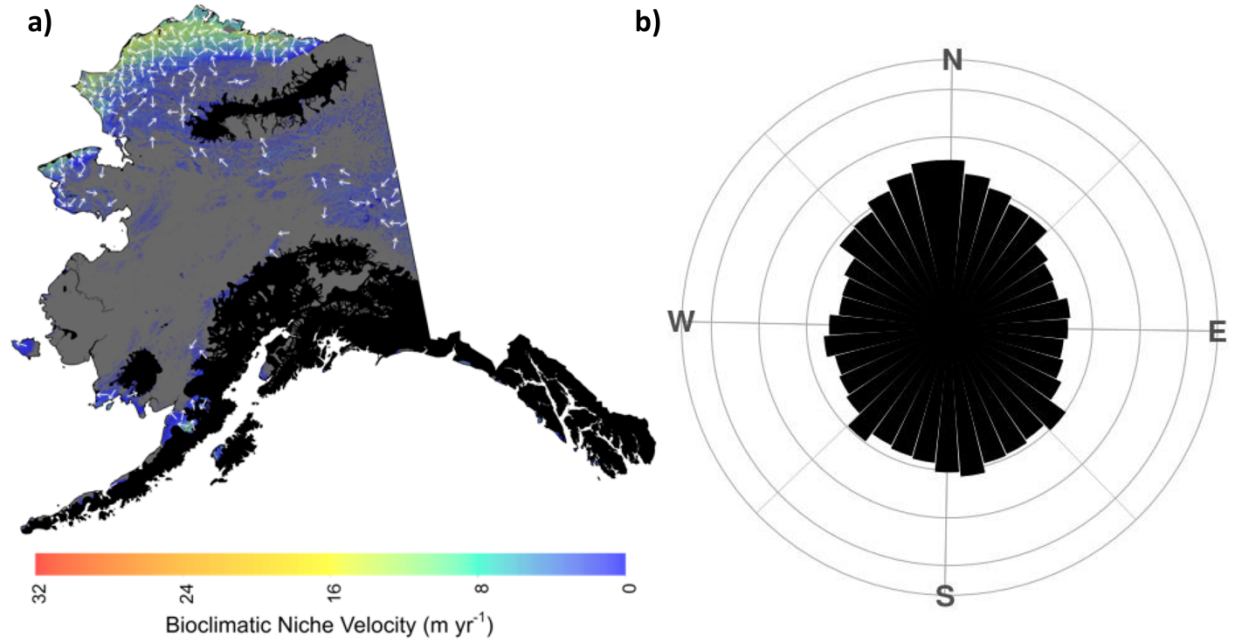### 2.4.3 Bioclimatic niche velocity trends:

Of the 69.2% of Alaska's land area that was potentially inhabited by white spruce during the LGM (Figure 2.3), 54.6% of this area experienced an increase in white spruce habitat suitability, and 14.6% of this area experienced a decrease in white spruce habitat suitability from the LGM to modern era (Figure 2.7a). Within the 14.6% land area where white spruce experienced a decrease in habitat suitability, white spruce bioclimatic niche speed averaged 0.49 m yr^{-1}, and standard deviation of 1.31 m yr^{-1} (Table 2.3, Figure 2.7a). On average, white spruce was required to move north (353.45°) to keep pace with climate change, with a standard deviation of 2.86° (Table 2.3, Figure 2.7b).

Figure 2.7: The bioclimatic niche velocity of white spruce from the LGM to modern era in Alaska. **a)** The bioclimatic niche speed of white spruce. Black background indicates regions where white spruce existed in the modern era, but not the LGM. Grey regions indicate regions where potential % tree cover increased from the LGM to modern era. **b)** The bioclimatic niche direction of white spruce. Fraction of direction is summarized in 10° bins from 0°-360°. Inner circle lines represent the % of pixels in each 10° directional bin in 2% intervals.

2.4.4 Bioclimatic niche vs. climate velocity:

Bioclimatic niche speed was higher than climate speed for all climate variables except Radiation and T_{max} (Table 2.3). When correlated with bioclimatic niche speeds, climate speeds had a Pearson's correlation coefficient ranging from 0.002 (snow) to 0.390 (PET) (Figure 2.8) with a mean correlation coefficient across all climate variables of 0.20.
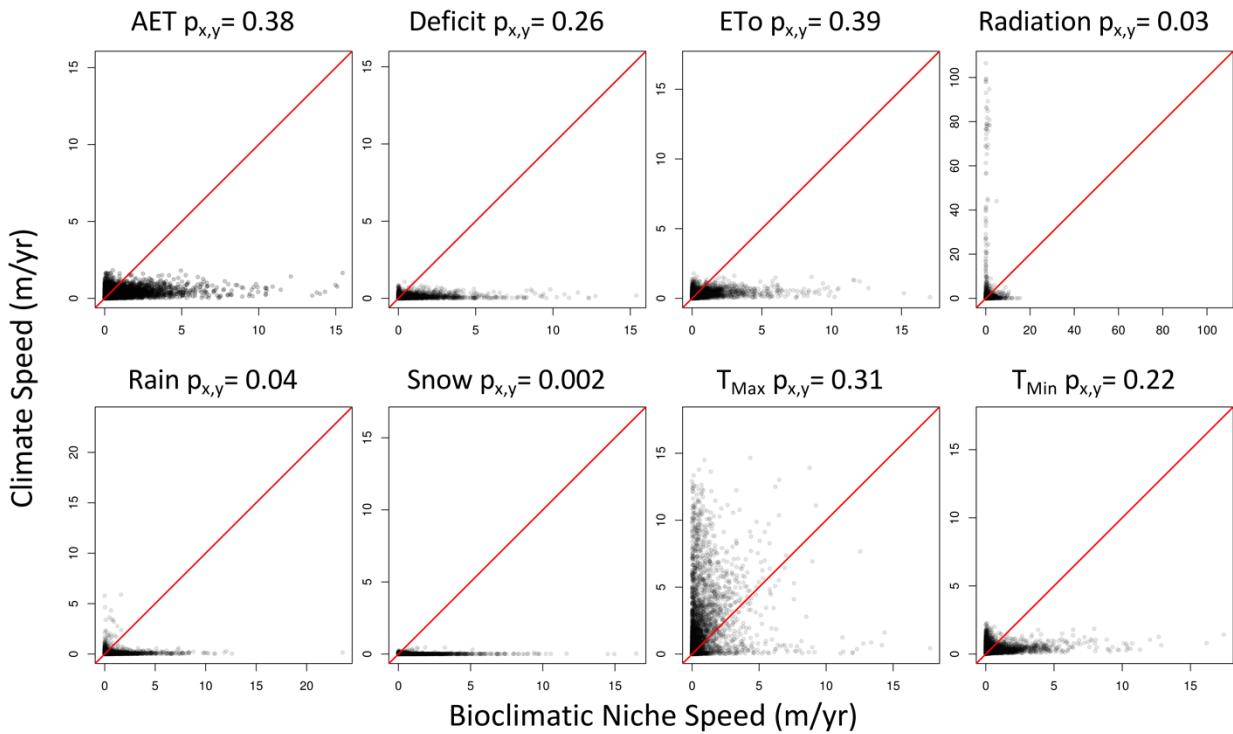
Figure 2.8: Density scatterplots of climate vs. bioclimatic niche speeds with correlation coefficient values for each climate-bioclimatic niche velocity pair.

When bioclimatic niche velocity was correlated with direction, climate directions had a Pearson's correlation coefficient ranging from -0.17 (PET) to 0.39 (T_{max}) with a minimum absolute correlation of 0.005 (snow) (Figure 2.9). The mean absolute correlation across all climate variables was 0.13.
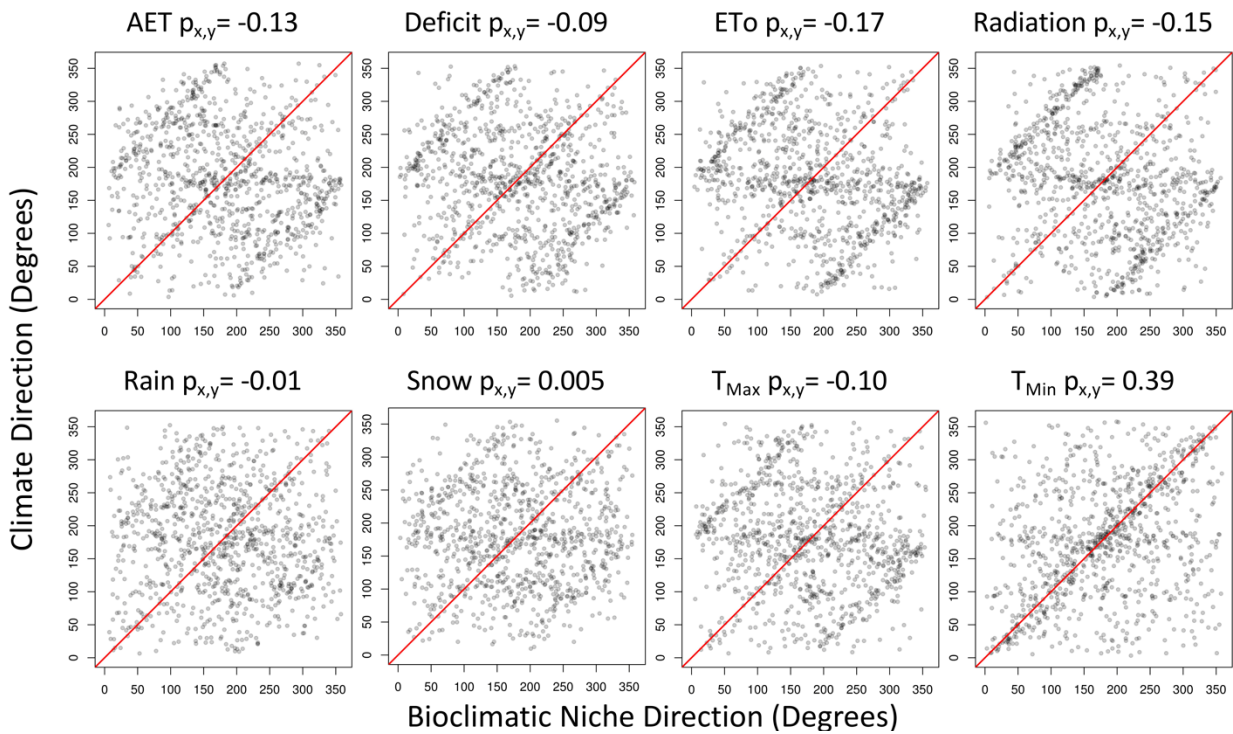
Figure 2.9: Density scatterplots of climate vs. direction with correlation coefficient values for each climate-bioclimatic niche velocity pair.

2.5 DISCUSSION

2.5.1 Validity of white spruce migration response to post-glacial climate change:

Underlying this analysis is the assumption that the bioclimatic niche velocity is closer to true estimates of a species migration response to climate change than climate velocity, minimally assuming that my ELF models of white spruce are accurate. The quality of my ELF climate hull models used to estimate white spruce maximum potential % tree cover performed well (Figure 2.2, Table 2.3) and indicate that my final ELF white spruce surfaces for the LGM and modern era more than adequately estimate the potential maximum tree cover of white spruce at a location based on the most limiting climatic factor. ELF models can be limited by the number of samples used in an analysis (Littell, Peterson, & Tjoelker, 2008; Rehfeldt, Crookston, Warwell, & Evans, 2006), however, I used a large number of modern white spruce samples (n > 40,000), scaled to the extent of Alaska, and which captured

rare climatic thresholds of the climate variables used in this analysis. Additionally, my white spruce

bioclimatic velocity estimates correspond with Alaskan white spruce LGM paleobotany analyses,

suggesting that my bioclimatic niche velocity estimates may be capturing accurate rates and direction of

white spruce migration following the LGM. For example, my bioclimatic niche velocity speeds are within

a reasonable range to spruce migration estimates from the LGM to modern era using fossil evidence (300-

400 m/yr) (Fastie, 1995), and modeled wind dispersed rates for wind dispersed conifer species (30-80

m/yr) from the LGM to modern era (Clark, Lewis, & Horvath, 2001). Additionally, the locations of low

white spruce bioclimatic velocities correspond with phylogeographic analyses of LGM Alaskan white

spruce refugial locations (Anderson, Hu, & Paige, 2011; Zazula, Telka, Harington, Schweger, &

Mathewes, 2006). Since refugia are locations that preserve local habitat where species can persist during

periods of regionally adverse climate (Gavin et al., 2014), low climate velocities indicate regions where

climate changes slowly, producing less pressure for a species to migrate, and more likely to harbor

refugia. Migration rates estimated from fossil data has been criticized as many of these studies have

estimated migration rates that exceed the dispersal capabilities of many plants (Provan & Bennett, 2008).

However, the rates reported by both Fastie (1995) and Clark et al. (2001) are within reason, providing

migration rates that accommodate changes in climate and the possibility of climatic refugia.

2.5.2 Climatic niche requirements complicate climate velocity interpretations:

       I demonstrated that climate velocity estimates did not predict similar rates and directions to one

another throughout Alaska (Figure 2.5), suggesting that different climate variables used to derive climate

velocity will not necessarily estimate similar rates or directions to one another, or a species migration

response to climate change. This has two implications for studies relying on climate velocity to estimate

species migration responses to climate change.

       First, many climate velocity studies focus on a single climate variable (e.g. temperature) to derive

potential migration responses to climate change (Ackerly et al., 2010; M. T. Burrows et al., 2011;

Dobrowski et al., 2013; Loarie et al., 2009; Pinsky, Worm, Fogarty, Sarmiento, & Levin, 2013; Sandel et

al., 2011) and do not necessarily consider how relevant that single climate variable is to a species migration response to climate change. If climate velocities derived from different climate variables produced similar rates and directions, using climate variables of no biological consequence to estimate climate velocity would have no impact on estimated migration responses, as they would be similar. However, I show that different climate variables produce different climate velocities, reiterating the importance of identifying the most critical climate variable(s) of a species to estimate accurate migration responses to climate change for that species (Figure 2.5, Table 2.3). Therefore, climate velocities derived from inconsequential climate variables will likely lead to inaccurate estimates of a species' response to climate change. My results are consistent with previous studies highlighting the importance of using biologically relevant climate variables in climate change studies. For example, Crimmins, Dobrowski, Greenberg, Abatzoglou, and Mynsberge (2011) reported Sierra Nevada tree species are tracking changes in climatic water balance downhill, rather than cooler temperatures uphill, and Dobrowski et al. (2013) reported similar down-slope trends from evaporative demand climate velocities. Therefore, climate variables need to be species-relevant in climate velocity analyses as different climate variables estimate different migration responses to climate change.

Second, even if a species-relevant climate variable is used to estimate climate velocity, many species climatic niche are comprised of several climate variables (Woodward, 1987), with many species climatic variables influencing their response to climate change through migration (Hutchinson, 1957; Jackson & Overpeck, 2000). Simple univariate climate velocities will inaccurately estimate species migrations responses for species that are spatially and temporally controlled by a complex array of climate variables. In my analysis, all climate variables used to derive ELF tree cover surfaces influenced the distribution and the migration response of Alaskan white spruce to post-glacial climate change (Figure 2.4). Therefore, it would be inappropriate to assume that not including all of the eight climate velocity estimates in this analysis would adequately estimate the migration response of white spruce. Dobrowski et al. (2013) reiterates this concern using climatic water balance variables (e.g. AET and water deficit) that indirectly combine biologically relevant and physically based variables that characterize the concurrent

availability of both water and energy for biota, as well as temperature velocity that captures important life history on plants freezing. They found that while climatic water balance and temperature velocities displayed similar speeds, AET and water deficit typically moved in opposing directions to temperature velocity.

2.5.3 Inconsequential estimates of climate velocity:

In addition to the differences between climate velocity estimates, I also showed that all climate velocities in this analysis had poor correlations with bioclimatic niche velocity (Figures 2.8 & 2.9), suggesting that climate velocity and bioclimatic velocity do not estimate similar species migration responses to climate change. The difference between speed and direction estimates of climate velocity and bioclimatic niche velocity can be explained because climate velocity produces migration estimates at locations that are meaningless where a species does not need to migrate to suitable climates.

First, unlike bioclimatic niche velocity, climate velocity analyses do not remove regions where a species does not occur (M. T. Burrows et al., 2011; Dobrowski et al., 2013; Loarie et al., 2009). Climates that falls within the empty environmental space of a species niche is never suitable for the species at any point in time, and will not permit successful species migration (Jackson & Overpeck, 2000), making species migration responses derived from climate velocity at these locations misleading. For example, Alaskan white spruce did not occur at all pixels within the boundary of Alaska during either the LGM or modern era (Figure 2.3) and did not produce bioclimatic niche velocities in these regions. However, all climate variables produced climate velocities that predict migration response for white spruce in these unoccupied regions, suggesting that spruce will respond to climate change in these regions. Second, unlike bioclimatic niche velocity, climate velocity is incapable of identifying locations where climate becomes more or less suitable for a species, producing velocities in locations with no climatic pressure to migrate. For example, locations where the climatic suitability for a species decreases over time implies the species faces pressure to migrate to more climatically suitable habitat. Conversely, locations where habitat suitability increases for a species places no climatic pressure for a species to migrate, as it is

67

already suitable, again making velocities at these locations misleading (Figure 2.10) (Jackson &

Overpeck, 2000). Both of these realizations reinforce Serra-Diaz et al. (2014) statement concerning the

importance of transforming physical climate space to biotic climate space to help guide the location and

timing of species migration responses to climate change to set conservation priorities and successful

management actions (Hannah, Midgley, & Millar, 2002; Mawdsley, O'malley, & Ojima, 2009).
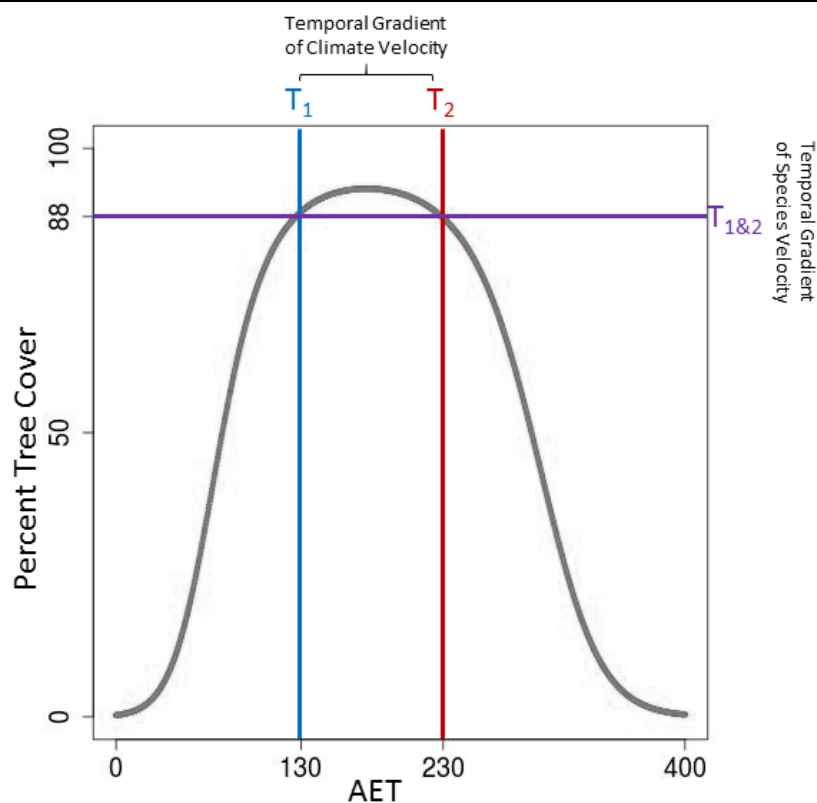
Figure 2.10: Climate velocity does not identify locations where a species habitat suitability increases or decreases and will estimate rates and direction where a species has no need to migrate. The graph depicts the white spruce maximum tree cover across all possible values of LGM and modern AET climate values. T_1 represent the end of the LGM, approximately 18,000 ya, while T_2 represents the modern era, 0 ya. If the spatial gradient of AET from the LGM (T_1) to modern (T_2) is > 0, a 100 mm AET change from T_1 to T_2 results in the temporal gradient of AET velocity to be 0.005 mm/yr. If the spatial gradient of white spruce tree cover from T_1 to T_2 is > 0, the same 100 mm change in AET produces a bioclimatic niche velocity of 0 mm/yr. In this example, a 100 mm change in AET from T_1 to T_2 leads to no change in the habitat suitability of white spruce, indicating no climatic pressure to migrate to other "more suitable" AET climates.

2.5.4 Limitations and future directions of bioclimatic niche velocity:

While bioclimatic niche velocity is an alternate method to estimate a species migration response to climate change, uncertainties and limitations exist. Similar errors and uncertainties inherent to climate velocity will be propagated into bioclimatic niche velocity estimates since bioclimatic niche velocity is derived using the same model structure as climate velocity. Previously recognized concerns of climate velocity, such as the uncertainty of the spatial and temporal gradient of climate velocity (Loarie et al., 2009), sensitivity to the spatial grain of the analysis (Dobrowski et al., 2013; Loarie et al., 2009; Serra-Diaz et al., 2014), and analyses at spatial scales relevant to dispersal capacity of a species (Loarie et al., 2009; Wiens, 1989) will also occur in bioclimatic niche velocity.

Similarly, since bioclimatic niche velocity depends on surfaces such as ELF models or SDMs, any assumptions, errors, or limitations of ELF/SDM models can propagate into bioclimatic niche velocity calculations, such as evolutionary capacity, measured and unmeasured biotic factors, dispersal ability/accessibility, as well as modeling techniques (Araujo & Guisan, 2006; Soberon & Peterson, 2005). Since the goal of this analysis was to develop a species informed measure of climate velocity, I did not work on improving SDM modeling techniques previously acknowledged, or address the accuracy of my white spruce distribution surfaces (Araujo & Guisan, 2006; M. Austin, 2007; M. P. Austin & Van Niel, 2011; Buckley et al., 2010; Franklin et al., 2013; Soberon & Peterson, 2005; Wiens, Stralberg, Jongsomjit, Howell, & Snyder, 2009). However, the more accurate an SDM is to a species realized niche, the more likely bioclimatic velocity will accurately estimate species migration responses to climate change. Further research is needed to understand how the limitations of SDMs influence and affect conclusions drawn from bioclimatic niche velocity analyses.

2.5.5 Conclusions:

Climate velocity has been proposed as an important index to understand the rate species may be required to move to keep pace with climate change. However, climate velocity is a simple univariate measure of climate change which does not include any actual species specific information yet is still used

to infer species responses to climate change (M. T. Burrows et al., 2011; Carroll et al., 2017; Dobrowski et al., 2013; Hamann et al., 2015; Loarie et al., 2009; Ohlemuller, 2011; Sandel et al., 2011). If climate velocity were a suitable predictor of the rate and direction white spruce needed to move to keep pace with post-glacial climate change, I should have seen the climate velocity estimates 1) predict similar rates and directions to each other and 2) correlate well with bioclimatic velocity speed and directions, even though this measure incorporates multiple climate factors and white spruce specific responses to climate change.

In this study I compared individual climate velocity metrics to "bioclimatic niche velocity" metrics which incorporate multivariate climate and species ecology to reveal species-specific responses to climate change not captured in climate velocity. Using bioclimatic niche velocity, I demonstrated that climate velocity is not well suited to assess species responses to climate change because it can use species-irrelevant climate variables, relying on simplistic univariate climate variables to derive complex migration responses, and estimating migration responses in areas where a species does not occur or has no climatic pressure to migrate.

2.6 REFERENCES

Abrahamson, I. L. (2014). Fire regimes of Alaskan white spruce communities. In: Fire Effects Information System, [Online]. Retrieved from https://www.fs.fed.us/database/feis/fire_regimes/AK_white_spruce/all.html

Ackerly, D. D., Loarie, S. R., Cornwell, W. K., Weiss, S. B., Hamilton, H., Branciforte, R., & Kraft, N. J. B. (2010). The geography of climate change: implications for conservation biogeography. *Diversity and Distributions, 16*(3), 476-487. doi:10.1111/j.1472-4642.2010.00654.x

Agostinelli, C., & Lund, U. (2013). R package 'circular': Circular Statistics (version 0.4-7).

Anderson, L. L., Hu, F. S., & Paige, K. N. (2011). Phylogeographic history of white spruce during the last glacial maximum: uncovering cryptic refugia. *Journal of heredity, 102*(2), 207-216.

Araujo, M. B., & Guisan, A. (2006). Five (or so) challenges for species distribution modelling. *Journal of Biogeography, 33*(10), 1677-1688. doi:10.1111/j.1365-2699.2006.01584.x

Austin, M. (2007). Species distribution models and ecological theory: a critical assessment and some possible new approaches. *Ecological modelling, 200*(1-2), 1-19.

Austin, M. P., & Van Niel, K. P. (2011). Improving species distribution models for climate change studies: variable selection and scale. *Journal of Biogeography, 38*(1), 1-8.

Buckley, L. B., Urban, M. C., Angilletta, M. J., Crozier, L. G., Rissler, L. J., & Sears, M. W. (2010). Can mechanism inform species' distribution models? *Ecology Letters, 13*(8), 1041-1054. doi:10.1111/j.1461-0248.2010.01479.x

Burrows, M. T., Schoeman, D. S., Buckley, L. B., Moore, P., Poloczanska, E. S., Brander, K. M., . . . Richardson, A. J. (2011). The Pace of Shifting Climate in Marine and Terrestrial Ecosystems. *Science, 334*(6056), 652-655. doi:10.1126/science.1210288

Burrows, M. T., Schoeman, D. S., Richardson, A. J., Molinos, J. G., Hoffmann, A., Buckley, L. B., . . . Duarte, C. M. (2014). Geographical limits to species-range shifts are suggested by climate velocity. *Nature, 507*(7493), 492.

Cade, B. S., & Noon, B. R. (2003). A gentle introduction to quantile regression for ecologists. *Frontiers in Ecology and the Environment, 1*(8), 412-420. doi:Doi 10.2307/3868138

Carroll, C., Roberts, D., Michalak, J., Lawler, J., Nielsen, S., Stralberg, D., . . . Wang, T. (2017). Scale-dependent complementarity of climatic velocity and environmental diversity for identifying priority areas for conservation under climate change. *Global change biology.*

Chen, I. C., Hill, J. K., Ohlemuller, R., Roy, D. B., & Thomas, C. D. (2011). Rapid Range Shifts of Species Associated with High Levels of Climate Warming. *Science, 333*(6045), 1024-1026. doi:10.1126/science.1206432

Clark, J. S., Lewis, M., & Horvath, L. (2001). Invasion by extremes: population spread with variation in dispersal and reproduction. *The American Naturalist, 157*(5), 537-554.

Clearinghouse, A. S. G.-S. D. (1990). *Alaska Major Lakes*. Retrieved from: http://www.asgdc.state.ak.us/#168

Clearinghouse, A. S. G.-S. D. (1998). *Alaska Major Rivers*. Retrieved from: http://www.asgdc.state.ak.us/#30

Colwell, R. K., Brehm, G., Cardelus, C. L., Gilman, A. C., & Longino, J. T. (2008). Global warming, elevational range shifts, and lowland biotic attrition in the wet tropics. *Science, 322*(5899), 258-261. doi:10.1126/science.1162547

Crimmins, S. M., Dobrowski, S. Z., Greenberg, J. A., Abatzoglou, J. T., & Mynsberge, A. R. (2011). Changes in Climatic Water Balance Drive Downhill Shifts in Plant Species' Optimum Elevations. *Science, 331*(6015), 324-327. doi:10.1126/science.1199040

Cubasch, U., Wuebbles, D., Chen, D., Facchini, M. C., Frame, D., Mahowald, N., & Winther, J.-G. (2013). Introduction: Climate Change 2013: The Physical Science Basis. Contribution of Working Group I to the Fifth Assessment Report of the Intergovernemtnal Panel on Climate Change. In. Cambridge, United Kingdom, New York, NY, USA: Cambridge University Press.

Dobrowski, S. Z., Abatzoglou, J., Swanson, A. K., Greenberg, J. A., Mynsberge, A. R., Holden, Z. A., & Schwartz, M. K. (2013). The climate velocity of the contiguous United States during the 20th century. *Global change biology, 19*(1), 241-251. doi:10.1111/gcb.12026

Dobrowski, S. Z., Abatzoglou, J. T., Greenberg, J. A., & Schladow, S. G. (2009). How much influence does landscape-scale physiography have on air temperature in a mountain environment? *Agricultural and Forest Meteorology, 149*(10), 1751-1758. doi:10.1016/j.agrformet.2009.06.006

Fastie, C. L. (1995). Causes and ecosystem consequences of multiple pathways of primary succession at Glacier Bay, Alaska. *Ecology, 76*(6), 1899-1916.

Franklin, J., Davis, F. W., Ikegami, M., Syphard, A. D., Flint, L. E., Flint, A. L., & Hannah, L. (2013). Modeling plant species distributions under future climates: how fine scale do climate projections need to be? *Global change biology, 19*(2), 473-483. doi:10.1111/gcb.12051

Gavin, D. G., Fitzpatrick, M. C., Gugger, P. F., Heath, K. D., Rodríguez-Sánchez, F., Dobrowski, S. Z., . . . Bartlein, P. J. (2014). Climate refugia: joint inference from fossil records, species distribution models and phylogeography. *New Phytologist, 204*(1), 37-54.

Greenberg, J. A., Santos, M. J., Dobrowski, S. Z., Vanderbilt, V. C., & Ustin, S. L. (2015). Quantifying Environmental Limiting Factors on Tree Cover Using Geospatial Data. *Plos One, 10*(2). doi:ARTN e0114648

10.1371/journal.pone.0114648

Guisan, A., & Thuiller, W. (2005). Predicting species distribution: offering more than simple habitat models. *Ecology Letters, 8*(9), 993-1009. doi:10.1111/j.1461-0248.2005.00792.x

Hamann, A., Roberts, D. R., Barber, Q. E., Carroll, C., & Nielsen, S. E. (2015). Velocity of climate change algorithms for guiding conservation and management. *Global change biology, 21*(2), 997-1004. doi:10.1111/gcb.12736

Hannah, L., Midgley, G. F., & Millar, D. (2002). Climate change-integrated conservation strategies. *Global Ecology and Biogeography, 11*(6), 485-495.

Helm, D., & Collins, W. (1997). Vegetation succession and disturbance on a boreal forest floodplain, Susitna River, Alaska. *Canadian Field-Naturalist, 111*(4), 553-566.

Huston, M. A. (2005). Introductory essay: critical issues for improving predictions. *Predicting species occurrences: issues of accuracy and scale*.

Hutchinson, G. (1957). Concluding remarks Cold ssring Harbor Symp. *Quant, 22*, 66-77.

Jackson, S. T., & Overpeck, J. T. (2000). Responses of plant populations and communities to environmental changes of the late Quaternary. *Paleobiology, 26*(4), 194-220. doi:Doi 10.1666/0094-8373(2000)26[194:Roppac]2.0.Co;2

Jammalamadaka, S. R., & Sarma, Y. (1988). A correlation coefficient for angular variables. *Statistical theory and data analysis II*, 349-364.

LANDFIRE. (2016). *LANDFIRE Existing Vegetation Cover*. Retrieved from: http://www.landfire.gov/

Littell, J. S., Peterson, D. L., & Tjoelker, M. (2008). Douglas-fir growth in mountain ecosystems: water limits tree growth from stand to region. *Ecological Monographs, 78*(3), 349-368.

Loarie, S. R., Duffy, P. B., Hamilton, H., Asner, G. P., Field, C. B., & Ackerly, D. D. (2009). The velocity of climate change. *Nature, 462*(7276), 1052-U1111. doi:10.1038/nature08649

Manley, W. F., & Kaufman, D. S. (2002). *Alaska PaleoGlacier Atlas: Institute of Arctic and Alpine Research (INSTARR)*. Retrieved from: http://instaar.colorado.edu/QGISL/ak_paleoglacier_atlas

Marion, J. L. (1991). *Developing a natural resource inventory and monitoring program for visitor impacts on recreation sites: A procedural manual*: US Department of the Interior, National Park Service.

Mawdsley, J. R., O'malley, R., & Ojima, D. S. (2009). A review of climate-change adaptation strategies for wildlife management and biodiversity conservation. *Conservation biology, 23*(5), 1080-1089.

Murphy, J. M., Sexton, D. M., Barnett, D. N., Jones, G. S., Webb, M. J., Collins, M., & Stainforth, D. A. (2004). Quantification of modelling uncertainties in a large ensemble of climate change simulations. *Nature, 430*(7001), 768.

Ohlemuller, R. (2011). Running Out of Climate Space. *Science, 334*(6056), 613-614. doi:10.1126/science.1214215

Parmesan, C., & Yohe, G. (2003). A globally coherent fingerprint of climate change impacts across natural systems. *Nature, 421*(6918), 37-42.

Pereira, H. M., Leadley, P. W., Proenca, V., Alkemade, R., Scharlemann, J. P. W., Fernandez-Manjarres, J. F., . . . Walpole, M. (2010). Scenarios for Global Biodiversity in the 21st Century. *Science, 330*(6010), 1496-1501. doi:10.1126/science.1196624

Pinsky, M. L., Worm, B., Fogarty, M. J., Sarmiento, J. L., & Levin, S. A. (2013). Marine taxa track local climate velocities. *Science, 341*(6151), 1239-1242.

Provan, J., & Bennett, K. (2008). Phylogeographic insights into cryptic glacial refugia. *Trends in Ecology & Evolution, 23*(10), 564-571.

Rehfeldt, G. E., Crookston, N. L., Warwell, M. V., & Evans, J. S. (2006). Empirical analyses of plant-climate relationships for the western United States. *International Journal of Plant Sciences, 167*(6), 1123-1150.

Sandel, B., Arge, L., Dalsgaard, B., Davies, R. G., Gaston, K. J., Sutherland, W. J., & Svenning, J. C. (2011). The Influence of Late Quaternary Climate-Change Velocity on Species Endemism. *Science, 334*(6056), 660-664. doi:10.1126/science.1210173

Sankaran, M., Hanan, N. P., Scholes, R. J., Ratnam, J., Augustine, D. J., Cade, B. S., . . . Zambatis, N. (2005). Determinants of woody cover in African savannas. *Nature, 438*(7069), 846-849. doi:10.1038/nature04070

Serra-Diaz, J. M., Franklin, J., Ninyerola, M., Davis, F. W., Syphard, A. D., Regan, H. M., & Ikegami, M. (2014). Bioclimatic velocity: the pace of species exposure to climate change. *Diversity and Distributions, 20*(2), 169-180.

Smith, W. B. (2002). Forest inventory and analysis: a national inventory and monitoring program. *Environmental pollution, 116*, S233-S242.

Soberon, J., & Peterson, A. T. (2005). Interpretation of models of fundamental ecological niches and species' distributional areas. *Biodiversity Informatics, 2*(0), 12. doi:10.17161/bi.v2i0.4

Thomson, J. D., Weiblen, G., Thomson, B. A., Alfaro, S., & Legendre, P. (1996). Untangling multiple factors in spatial distributions: lilies, gophers, and rocks. *Ecology, 77*(6), 1698-1715.

Urban, D. L., Miller, C., Halpin, P. N., & Stephenson, N. L. (2000). Forest gradient response in Sierran landscapes: the physical template. *Landscape Ecology, 15*(7), 603-620. doi:Doi 10.1023/A:1008183331604

USGS. (2016). *The National Map*. Retrieved from: http://nationalmap.gov/3DEP/3dep_prodserv.html

USGS-GAP. (2018). ***U.S. Geologic Survey Gap Analysis Program*** Retrieved from: USGS national Gap Analysis Program

Vandermeer, J. H. (1972). Niche Theory. *Annual review of Ecology and Systematics, 3*, 29.

Warnes, G. R., Bolker, B., & Lumley, T. (2014). gtools: Various R programming tools. *R package version, 3*(1).

Wiens, J. A. (1989). Spatial scaling in ecology. *Functional ecology, 3*(4), 385-397.

Wiens, J. A., Stralberg, D., Jongsomjit, D., Howell, C. A., & Snyder, M. A. (2009). Niches, models, and climate change: assessing the assumptions and uncertainties. *Proceedings of the National Academy of Sciences, 106*(Supplement 2), 19729-19736.

Williams, J. W., Jackson, S. T., & Kutzbacht, J. E. (2007). Projected distributions of novel and disappearing climates by 2100 AD. *Proceedings of the National Academy of Sciences of the United States of America, 104*(14), 5738-5742. doi:10.1073/pnas.0606292104

Woodward, F. I. (1987). *Climate and plant distribution*: Cambridge University Press.

Zazula, G., Telka, A., Harington, C., Schweger, C., & Mathewes, R. (2006). New spruce (Picea spp.) macrofossils from Yukon Territory: implications for Late Pleistocene refugia in Eastern Beringia. *Arctic*, 391-400.

CHAPTER 3: CALIFORNIA FOREST COMMUNITY MIGRATION RESPONSES TO 21ST CENTURY CLIMATE CHANGE

3.1 ABSTRACT

Conservation strategies aim to protect Earth's biodiversity from environmental change, however, community-centric conservation efforts assume modern communities protected today will continue to persist in the future and commonly employ static protected-area techniques based on the assumption climate will remain stable in the future. Static and stable assumptions of community dynamics assume that species will migrate with each other in response to climate change and form similar community assemblages in the future. I calculated the bioclimatic niche direction for 72 of California's native tree species derived from habitat suitability maps calibrated to high-resolution downscaled climate data for the modern (1985-2015) and future (2070-2100) eras and estimated the directions each species must migrate to keep pace with end-of-century climate change. Using each species' modern habitat suitability maps, I identified and classified the different forest community types that occurred throughout California during the modern era, and identified whether the species of a community, at a location, displayed uniform (anisotropic) migration directions, or random (isotropic) migration directions in response to climate change. A vast majority of California forest community types displayed isotropic species migration directions. My results suggest that community conservation strategies should not assume modern communities will exist as they are today at the end of the century as different species will migrate in different directions in response to climate change which may lead to the destabilization of extent community assemblages at the end of the 21st century.

3.2 INTRODUCTION

Many modern species have persisted through previous long-term natural climate cycles by shifting their ranges in order to remain within suitable habitat (Davis & Shaw, 2001; Huntley & Webb III, 1989; McGlone, 1996; Schoonmaker & Foster, 1991). As has occurred in the past, modern climate

change can be expected to lead to shifts in the geographic distribution of organisms (Chen, Hill, Ohlemuller, Roy, & Thomas, 2011; Hickling, Roy, Hill, Fox, & Thomas, 2006; Parmesan & Yohe, 2003; Thomas, 2010), however the rate and magnitude of modern climate change raises concerns as to whether species will be able to track climate change through migration and establishment with potentially serious implications for biological communities if they cannot (Davis, 1992; Walther et al., 2002). Assessing the vulnerability of individual species to climate change over the next 100 years is highly uncertain and complex (Serra-Diaz et al., 2014). Limited time and resources, as well as the ever increasing number of species affected by climate change, challenge our ability to preserve biodiversity, leading conservation strategies to focus on entire biological communities, rather than individual species (Olden, 2003).

Community-level conservation strategies have been perceived as a suitable and practical approach to biodiversity conservation (Franklin, 1993; Urbanska, 2000; Young, 2000) since communities provide habitat for individual target species and can be used to gauge ecosystem function and diversity (Jewell, 2000). However, community conservation is characteristically concerned with protecting current communities under the notion that modern community types will continue to exist in the future (Hannah, Midgley, & Millar, 2002), as highly structured, repeatable, and identifiable associations of species controlled by climate in space and time (Clements, 1916; Collins, Glenn, & Roberts, 1993). This is surprising as it is well accepted that individual species have unique fundamental niches that cause independent responses to climate change (Gleason, 1926; Hutchinson, 1957; Jackson & Overpeck, 2000), making it possible for modern community assemblages to disappear and give rise to new communities (Hannah, Midgley, & Millar, 2002; Williams & Jackson, 2007).

Conservation efforts seeking to protect communities from climate change as they currently exist may become obsolete if species moving independently of one another lead to the formation of novel communities with no modern analogs. This has two implications for the success of climate-oriented community conservation: first, most conservation strategies employ the static conservation paradigm, disregarding changing patterns of communities over time, with most reserves being established as static protected-areas (Hannah, Midgley, Lovejoy, et al., 2002). This makes dynamic conservation strategies,

75

that are necessary to protect biodiversity from climate change, impossible (Noss & Harris, 1986). Few reserve strategies have been set up with reference to climate change, under the unspoken assumption that climate, and therefore communities, will remain stable (Hannah, Midgley, Lovejoy, et al., 2002).

Second, conservation strategies aimed at protecting representative examples of modern community types will fail if the protected community disappears through the arrival of novel community assemblages regardless of protected areas. Similarly, if the focus of conservation is on modern communities, many possible no-analogue communities will be excluded from future conservation efforts (Hannah, Midgley, & Millar, 2002). It is well accepted that individual species have their own unique multi-dimensional fundamental niche that controls their capacity to migrate and survive in an area (Hutchinson, 1957; Jackson & Overpeck, 2000), not all realized combinations of climate fall within the full fundamental niche of a species, resulting in different portions of the fundamental niche realized through time (Figure 3.1) (Jackson & Overpeck, 2000). As a result, species vary in their timing, magnitude, and direction of response to climate change, with communities migrating as continuous, independent units (Gleason, 1926; Jackson & Overpeck, 2000; Williams & Jackson, 2007). When climate change leads to new combinations of climate, new portions of a species' fundamental niche become available, leading to potentially novel associations of species as well as the disappearance of modern community assemblages (Figure 3.1) (Williams & Jackson, 2007).
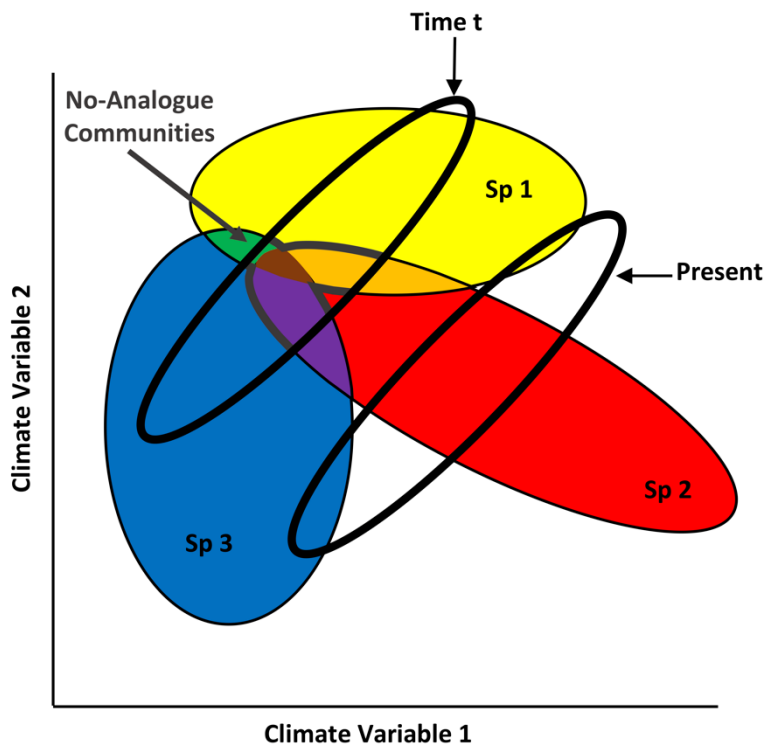
Figure 3.1: Niche-based conceptual diagram explaining how novel communities can arise from climate change. The realized environment will change as climate change occurs (open black ellipses, present and time t). The fundamental niches of 3 different species are represented in the 2-dimensional climate space by the red, yellow, and blue ellipses. At each time period, the realized niche is represented by the overlap between the realized climate environment and a species niche. During the present time frame, each species dominants a forest community, with no possible overlap of the realized niche with the other two species. Therefore, at present, only communities dominated by species 1 (yellow), 2 (red), or 3 (blue) exist. However, if the right climate arises, the realized environment intersected each species fundamental niche where each species niche overlaps with portions of all other species fundamental niche. Therefore, at time t, available communities of species 1, 2, and 3 occur, as well as the arrival of 4 novel community assemblages (1&2 (orange), 1&3 (green), 2&3 (purple), and 1&2&3 (brown). Adapted from Figure 5 Jackson and Overpeck (2000).

California is an appropriate region to investigate how forest communities may respond to future climate change as land areas within the state are biodiversity hotspots, contain sensitive biomes to climate change (Sala et al., 2000; Underwood, Klausmeyer, Morrison, Bode, & Shaw, 2009), and California's Natural Community Conservation Planning Act mandates the conservation of ecological communities (California Department of Fish and Game, 2003). Additionally, the United States Department of

Agriculture, Forest Service (USFS) has focused on California forest types to inform economic and forest management planning (Christensen, Waddell, Stanton, & Kuegler, 2016).

In this analysis I identified whether the tree species comprised of California forest communities will migrate in response to 21st century climate change in similar directions or migrate independent of one another. Anisotropic migration responses suggests the species of a community migrate together in response to climate change together, thus the community shifts together, (Clements, 1916) and supports the benefits of community-level conservation efforts. Isotropic migration responses suggests the species of a community migrate indecently of each other in response to climate change, thus the community will not shift together (Gleason, 1926), and suggests community-based conservation efforts may be in vain. Therefore, in this analysis I ask: Are species in modern Californian forest communities moving in a singular direction with respect to climate change or are they moving independent of one another?

To address these questions, I use similar methods to Serra-Diaz et al. (2014)'s bioclimatic niche velocity model, using species distribution models (SDMs) of 72 Californian tree species applied to modern (1985-2015) and future (2070-2100) climates to examine species-specific directional responses to climate change and identify the directions each species would need to migrate to keep pace with future climate change, summarized by their current community type.

3.3 METHODS

My goal was to first estimate species' migration directions with response to 21st century climate change, and then to summarize these changes by community type to determine whether species in these communities are expected to move together or move independent of one another. I downscaled climate rasters to 30 m resolution and used this data with USFS Forest Inventory Analysis (FIA) sample plot data to derive fine-scale habitat suitability maps of 72 tree species that exist in California during the modern era (1985-2015) and projected their distributions for the end of the 21st century (2070-2100). Using my modern and future SDMs, I derived the bioclimatic niche velocity of each species to identify the direction each species would need to migrate at a location to keep pace with climate change. The modern habitat

suitability maps were also used to classify and identify unique California forest community types throughout the state by the most dominant tree species present at a site. I then identified whether the species of California forest communities will migrate together (anisotropic) or independent of each other (isotropic) by determining if each species of a community, at a location, displayed random or uniform directional distributions.

3.3.1. Bioclimatic niche direction:

Input data:

<u>Climate data:</u> I downscaled California climate to produce 30 m resolution modern (1985-2015) and future (2070-2100) monthly climate normals for minimum temperature (T_{min}), maximum temperature (T_{max}), average temperature (T_{ave}), shortwave radiation, rain, snow, actual evapotranspiration, potential evapotranspiration, and water deficit using similar methods described in Chapter 1 and S. Z. Dobrowski et al. (2013). I collected spatially explicit monthly weather station data from N=1,919 weather stations across California from the National Oceanic and Atmospheric Administration's (NOAA) Global Historical Climatology Network (GHCND) (Menne, Durre, Vose, Gleason, & Houston, 2012) for T_{min}, T_{max}, T_{ave}, and total monthly precipitation. I acquired fine-scale topography of California from the United States Geologic Survey's (USGS) 1 arc-second (~30 m) digital elevation maps (DEM) (USGS, 2016). To represent the coarse-scale, time-varying climate, I acquired 1° general circulation model (GCM) monthly climate grids from the National Center for Atmospheric Research's (NCAR) Community Earth System Model (CESM, v. CCSM4), Coupled Atmospheric Model (CAM2), modern historical, and future RCP 8.5 model runs for near-surface, monthly T_{min}, T_{max}, T_{ave}, precipitation, short-wave downwelling surface radiation I_{could}, wind (U, V), and relative humidity (Gent et al., 2011; Kluzek, 2011).

My temperature and precipitation downscale models follow the same general form as my downscaled models from Chapter 1, with additional variables added to my precipitation model, as the variables in Chapter 1 for Alaskan precipitation were not acceptable to predict high resolution California precipitation patterns (Table 3.1).

Table 3.1: Input predictor surfaces for temperature and precipitation downscale models.

Variable	Unit	Resolution
Temperature Downscale Input Surfaces		
Temperature (Min, Max, or Average)	°C	100 km
Radiation	W/m^2	30 m
TCI	Unitless	30 m
Elevation	m.a.s.l.	30 m
Precipitation Downscale Surfaces		
Precipitation	mm	100 km
T$_{ave}$	°C	30 m
Relative Humidity	mm	100 km
Elevation	m.a.s.l.	5 km
Slope	Degrees	500 m
TCI	Unitless	30 m
Orographic Effect Proxy	Degrees	500 m
Distance to Ocean	m	30 m

My downscaled climatic evaporative demand products, actual and potential evapotranspiration (AET and PET), and water deficit, were computed using the Penman-Monteith equation (Allen, Pereira, Raes, & Smith, 1998) for PET. A snowmelt model (Dingman, 2002; Solomon Z Dobrowski, 2011) was used to compute rain and snow. AET and water deficit were computed using PET, rain, and snow to determine the previous months available water supply. If there is an excess of soil water, AET is the same as PET because evapotranspiration is not limited by water availability. However, if available water is less than the site's maximum potential available water, AET will be less than PET (AET = PET – DEF), because maximum water evaporative demand cannot be met by the available amount of water present at the site (S. Z. Dobrowski et al., 2013; Stephenson, 1998).

Forest Inventory Analysis Data: I used Forest Inventory and Analysis (FIA) plot locations of all available tree species in California provided by the United States Department of Agriculture, Forest Service (USFS) (Smith, 2002). The FIA dataset consists of a set of field sample locations distributed across the United States and contains, among other measurements, species presence for all species found in a plot. While 86 tree species were identified in the FIA database (Christensen et al., 2016), I removed 14 species

from the analysis that were either not native to California, ornamental, reported only by genus, or was a wide-ranged species with less than five observations that is commonly found in more than 10 counties in California (USDA NRCS National Plant Data Team) (Table 3.2). The remaining 72 species were the focus of my analysis. Absence locations for all species were considered any plot sites that did not report the species as present.

I created a species-climate database for each species using the N=5,617 unique FIA presence-absence sites and extracted the climate at each site from all nine downscaled climate surfaces. I built a validation dataset for each species-climate database by randomly selecting 20% of the original database for each species. The number of observed presences for each species varied from each other. To calibrate each SDM, I applied a stratified sampling technique to the remaining 80% of each original species-climate database to insure equal representation of presence-to-absence points for modeling purposes. Step 1: Produce SDMs:

I developed a unique empirical SDM model for each tree species in California using all nine of my downscaled climate surfaces for each species model and assumed my SDMs reflect the bioclimatic niche of each species. I used the general equation to model all tree species:

$$\textit{EQ 3.1: } P_{x,y,t} = f(T_{min}+T_{max}+T_{ave+}Rain+Snow+Radiation+AET+PET+Water\ Deficit)_{x,y,t}$$

where $P_{x,y,t}$ is the probability of occurrence at location (x,y) at time (t), and my nine climate predictors at location (x,y) at time (t). I used a random forest regression (Breiman, 2001; Cutler et al., 2007) to model the relationship between species occurrence and climate across California. To reduce computational complexity, I optimized the number of trees in each model by stopping the model at 100 trees beyond number of trees needed to achieve a minimum error.

My validation species databases were used to quantify the model performance of each SDM. I computed the kappa value for each SDM model to transform predicted continuous probability of occurrence (0 to 1) from my validation dataset to predicted binary probability of occurrence (0 or 1) (Allouche, Tsoar, & Kadmon, 2006; Hijmans, Phillips, Leathwick, Elith, & Hijmans, 2017; Liu, Berry, Dawson, & Pearson, 2005). I then computed the correlation coefficient, root mean squared error (RMSE),

and percent bias for each model. I also recorded the percent increase in mean square error (%IncMSE)

variable importance for each SDM to identify which climate variables were most important in estimating

each SDM, and computed the mean %IncMSE for each climate variable to rank and identify which

climate variables were generally the most important predictors across all species. Once an SDM model

was created for each California tree species, I applied the models to my downscaled climate predictor

surfaces, resulting in 144 SDM maps, 2 for each species, with one surface estimating modern

distributions and the other estimating future distributions based on climatically suitable regions within

California.

Step 2: Calculation of bioclimatic niche directions:

I calculated bioclimatic niche using identical methods reported in Chapter 2 for each California

tree species between the modern and future eras using the following equation:

$$EQ\ 3.2:\ V_{p,x,y} = \left(\frac{d_p/d_t}{d_p/d_x}, \frac{d_p/d_t}{d_p/d_y} \right) = \left(\frac{|Modern_{p,x,y} - Future_{p,x,y}|/100\ years}{atan(slope(Modern_{p,x,y}))} \right) = \frac{meters}{year}$$

where d_p/d_t is the change in a species' probability of occurrence over time (temporal gradient, p/yr) and

$d_p/d_{x,y}$ is the change in a species' probability of occurrence over a distance (spatial gradient, p/m). The

spatial gradient of each bioclimatic niche variable was derived using each species modern distributions,

therefore bioclimatic niche represents the rate and direction a species would need to migrate to keep pace

with climate change and remain within a similar, suitable habitat among its modern range. I masked all

bioclimatic niche velocities using a shapefile of California lakes, with a buffer of 100 m along lake, river,

and ocean boundaries to remove velocity artifacts over water. I then removed pixels greater than the 95th

percentile from each tree bioclimatic niche velocity to remove outliers and artifacts (e.g. water bodies)

that produce impossibly high speeds ($<10^8$ m yr^{-1}) where the spatial gradient was essentially flat (i.e.

slope=0), but not zero. Additionally, I masked all pixels where the habitat suitability increased for each

species by 2100, as these are regions where the climate has become more suitable, placing no pressure on

species at that location to emigrate.

I computed the mean and standard deviation of each species' bioclimatic niche direction and direction between each species to quantify the similarities and differences between species' responses to climate change in California. Similarly, I computed the standard deviation of each species direction by pixel to identify the mean difference in migration direction at the same location.

3.3.2. Defining potential forest communities:

To summarize species migrations by community types, I classified each pixel from my modern SDM output habitat suitability maps by forest type/alliance using formalized definitions of forest dominance types described by Greenberg, Dobrowski, Ramirez, Tuil, and Ustin (2006), which was based on the USFS forest community type definition (Christensen et al., 2016). If the top ranked species (by relative habitat suitability) had > 0.10 suitability than the second ranked species, the pixel was classified as single-species dominant. If the top two ranked species had < 0.10 difference in habitat suitability, but the second species had > 0.10 habitat suitability than the third ranked species, the pixel was classified as dual-species dominant. If the top 3 ranked species had < 0.10 habitat suitability from each other, the pixel was classified as multi-species dominant. Multi-species dominant pixels were further classified as multi-species montane if the elevation of the pixel was ≤2,133.6 m, and multi-species subalpine if the elevation was >2,133.6 m. If no tree species were present at a location, the pixel was assigned NA (Greenberg et al., 2006).

3.3.3. Analysis of anisotropy:

Tests of directional uniformity (also known as anisotropy) is a measure that can be used to detect whether data has a significant concentration in a single direction (Fisher, 1995). For all locations with at least 3 species present, I tested whether species at a location (i.e. pixel) move together in a uniform, anisotropic direction with climate change, or migrate in a random, isotropic direction from one another in

response to climate change using the kuiper.uniform.test function using the "uniftest" R package (Melnik & Pusev, 2015) with a circular transformation (Fisher, 1995; Kuiper, 1960).

Anisotropy was summarized by forest community type by computing the mean Kuiper p-value by community and the fraction of significantly anisotropic pixels throughout the community's distribution. A community is considered moving together in response to climate change if the mean Kuiper p-value of a forest community type is ≤0.15 (anisotropic), and conversely, species of a community are considered moving independently of each other if the mean Kuiper p-value is >0.15 (isotropic) (Fisher, 1995).

3.4 RESULTS

3.4.1 California climate change:

Future California climate estimates were warmer than the modern era for T_{ave}, T_{max}, and T_{min}, and drier for rain and snow (Table 3.3). Modern and future radiation climates differed from each other, however negligible at $7.40E^{-06}$ w/m^2 (Table 3.3). Future climatic water balance estimates showed greater potential evapotranspiration (PET) and water deficit from increased energy (e.g. temperature) and reduced available water (i.e. rain, snow), resulting in lower future climatic AET (Table 3.2).

Table 3.2: Summary of mean differences between all California climate variables from the modern era (1985-2015) to future RCP 8.5 era (2070-2100).

Variable	Unit	Mean Difference	Status
AET	mm	-51.4	Reduced Water Balance
Water deficit	mm	+102.4	Greater Water Demand
PET	mm	+50.9	Greater Evaporative Demand
Radiation	W m^{-2}	0.0	Negligible Change
Rain	mm	-532.7	Drier
Snow	mm	-141.5	Drier
T_{ave}	°C	+2.2	Hotter
T_{max}	°C	+2.6	Hotter
T_{min}	°C	+2.1	Hotter

3.4.2 Species distribution models:

The SDMs for each of the 72 California tree species performed well. Correlation coefficients for all models had strong positive correlations that ranged from 0.76 to 1.00 (Appendix A), with a mean correlation of 0.96 and standard deviation of 0.06. RMSE values ranged from 0.00 to 28.13 (Appendix A), with a mean RMSE of 3.89 and standard deviation of 6.50, indicating relatively low error in the probability of occurrence across all SDMs. Some SDMs had a slight positive bias and ranged from 0.00 to 0.37 (Appendix A), with a mean bias of 0.10 and standard deviation of 0.09.

Each SDM varied in what climate variables were estimated to be the most important (Appendix B). Mean %IncMSE across all climate variables ranged from 0.11 to 0.18, with snow generally playing the least important role in a species' distribution, and temperature (T_{ave}, T_{max}, T_{min}) playing the most important roles in a species' distributions (Figure 3.2, Appendix B). T_{ave} was the most important primary variable for 17 species, followed by T_{max} for 13 species, T_{min}, rain, and PET for 8 species, and AET for 7 species (Appendix B, Figure 3.2).
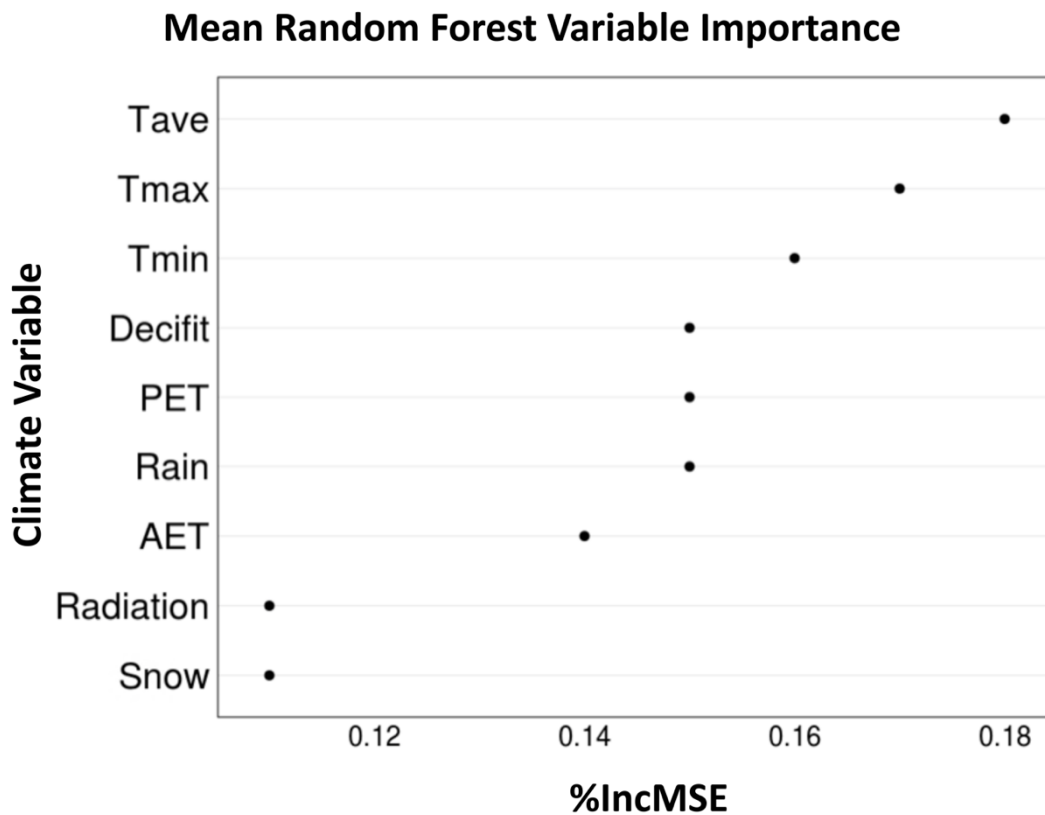
Figure 3.2: Ranked %IncMSE variable importance summary statistics for each climate variable across all species. Higher %IncMSE indicate greater model importance.

3.4.3 Forest community type migration trends:

<u>Species migration directions:</u> The direction of bioclimatic niche velocity varied considerably among the 72 species considered. The mean direction of movement for each individual species varied in direction, with models predicting 47 species moving northward (0-45°, 315-360°), 13 species eastward (45-135°), 4 species southward (135-225°), and 8 species westward (225-315°) (Table 3.3). The bioclimatic niche direction for pixels within an individual species varied little, with a mean standard deviation of 2.8° (Table 3.3).

Table 3.3: Summary mean and standard deviation statistics for each species bioclimatic niche velocity direction.

Common Name	Scientific Name	Mean Direction (°)	Stdev Direction (°)	Increased Suitability by 2100
Arizona Cypress	*Cupressus arizonica*	7.5	3.3	14.0%
Baker or Modoc Cypress	*Cupressus bakeri*	327.3	3.4	22.6%
Bigcone Douglas Fir	*Pseudotsuga macrocarpa*	341.1	2.9	37.3%
Bigleaf Maple	*Acer macrophyllum*	343.3	3.1	41.2%
Bishop Pine	*Pinus muricata*	323.5	3.5	21.3%
Bitter Cherry	*Prunus emarginata*	63.8	3.6	29.6%
Black Cottonwood	*Populus balsamifera*	169.8	4.1	31.3%
Blue Oak	*Quercus douglasii*	46.2	3.4	51.5%
Boxelder	*Acer negundo*	350.7	3.2	17.7%
Brewer Spruce	*Picea breweriana*	354.2	3.3	17.8%
California Black Oak	*Quercus kelloggii*	9.9	3.1	52.1%
California Buckeye	*Aesculus californica*	78.1	3.2	34.9%
California Juniper	*Juniperus californica*	224.7	3.7	42.2%
California Laurel	*Umbellularia californica*	350.7	3.2	47.2%
California Live Oak	*Quercus agrifolia*	2.9	3.8	35.4%
California Red Fir	*Abies magnifica*	307.5	3.5	35.8%
California Sycamore	*Platanus racemosa*	53.1	3.2	27.8%
California Torreya (Nutmeg)	*Torreya californica*	24.3	3.3	41.6%
California White Oak	*Quercus lobata*	170.0	3.6	39.6%
Canyon Live Oak	*Quercus chrysolepis*	50.6	3.6	51.8%
Chokecherry	*Prunus virginiana*	331.6	2.8	35.3%
Coulter Pine	*Pinus coulteri*	356.8	2.9	24.1%
Curlleaf Mountain Mahogany	*Cercocarpus ledifolius*	351.1	3.0	40.2%
Desert Ironwood	*Olneya tesota*	355.4	2.7	14.9%
Douglas Fir	*Pseudotsuga menziesii*	328.7	2.9	50.1%

Table 3.3 Continued (2)

Common Name	Scientific Name	Mean Direction (°)	Stdev Direction (°)	Increased Suitability by 2100
Engelmann Oak	*Quercus engelmannii*	16.5	2.8	16.3%
Engelmann Spruce	*Picea engelmannii*	33.0	2.1	29.6%
Foxtail Pine	*Pinus balfouriana*	352.3	2.5	25.6%
Fremont Cottonwood	*Populus fremontii*	326.4	3.4	14.7%
Giant Chinkapin, Golden Chinkapin	*Chrysolepis chrysophylla*	349.9	2.9	46.4%
Giant Sequoia	*Sequoiadendron giganteum*	350.6	2.9	29.3%
Grand Fir	*Abies grandis*	200.3	3.4	30.8%
Gray or California Foothill Pine	*Pinus sabiniana*	352.2	3.1	40.8%
Great Basin Bristlecone Pine	*Pinus longaeva*	283.5	3.4	26.9%
Honey Mesquite	*Prosopis glandulosa*	85.7	3.4	16.2%
Incense Cedar	*Calocedrus decurrens*	356.0	3.1	46.7%
Interior Live Oak	*Quercus wislizeni*	7.3	3.1	54.0%
Jeffrey Pine	*Pinus jeffreyi*	356.4	3.2	48.3%
Knobcone Pine	*Pinus attenuata*	349.3	3.0	36.1%
Limber Pine	*Pinus flexilis*	347.9	3.0	28.3%
Lodgepole Pine	*Pinus contorta*	9.3	3.1	30.8%
Monterey Cypress	*Cupressus macrocarpa*	16.1	2.2	20.2%
Monterey Pine	*Pinus radiata*	312.8	2.6	36.4%
Mountain Hemlock	*Tsuga mertensiana*	63.1	2.7	27.8%
Noble Fir	*Abies procera*	0.0	3.1	20.0%
Oregon Ash	*Fraxinus latifolia*	91.2	3.7	27.3%
Oregon White Oak	*Quercus garryana*	56.5	3.4	33.7%
Pacific Dogwood	*Cornus nuttallii*	337.6	2.9	41.6%
Pacific Madrone	*Arbutus menziesii*	8.7	3.0	31.6%
Pacific Silver Fir	*Abies amabilis*	26.0	2.6	43.4%

Table 3.3 Continued (3)

Common Name	Scientific Name	Mean Direction (°)	Stdev Direction (°)	Increased Suitability by 2100
Pacific Yew	*Taxus brevifolia*	352.1	2.5	47.2%
Ponderosa Pine	*Pinus ponderosa*	6.0	3.1	23.3%
Port Orford Cedar	*Chamaecyparis lawsoniana*	7.5	2.9	27.8%
Quaking Aspen	*Populus tremuloides*	284.1	3.1	29.0%
Red Alder	*Alnus rubra*	310.7	3.2	32.1%
Redwood	*Sequoia sempervirens*	17.9	3.0	20.7%
Sargent's Cypress	*Cupressus sargentii*	65.2	2.6	33.6%
Shasta Red Fir	*Abies shastensis*	119.6	3.2	37.2%
Singleleaf Pinyon	*Pinus monophylla*	354.6	2.8	11.7%
Sitka Spruce	*Picea sitchensis*	244.6	3.0	35.7%
Subalpine Fir	*Abies lasiocarpa*	63.5	2.0	19.2%
Sugar Pine	*Pinus lambertiana*	44.7	3.3	55.8%
Sweetgum	*Liquidambar styraciflua*	349.1	2.7	15.7%
Tanoak	*Lithocarpus densiflorus*	333.8	3.2	32.5%
Utah Juniper	*Juniperus osteosperma*	330.5	3.1	29.1%
Washoe Pine	*Pinus washoensis*	91.1	3.0	25.4%
Western Hemlock	*Tsuga heterophylla*	346.1	2.6	26.6%
Western Juniper	*Juniperus occidentalis*	343.7	3.1	37.5%
Western White Pine	*Pinus monticola*	31.4	3.4	42.7%
White Alder	*Alnus rhombifolia*	255.4	3.4	21.7%
Whitebark Pine	*Abies concolor*	43.6	3.1	36.6%
White Fir	*Pinus albicaulis*	313.1	3.2	69.1%

California anisotropy analysis: Different species at the same location displayed different migration directions with response to climate change, with a mean standard deviation in direction of 99.2°, and mean Kuiper p-value of 0.504 across all locations, indicating that while the directions of migration within a species is similar, the direction of migration among different species diverge (Figure 3.3). Only 14.6% (by area) of forest communities of California exhibited anisotropic migration.
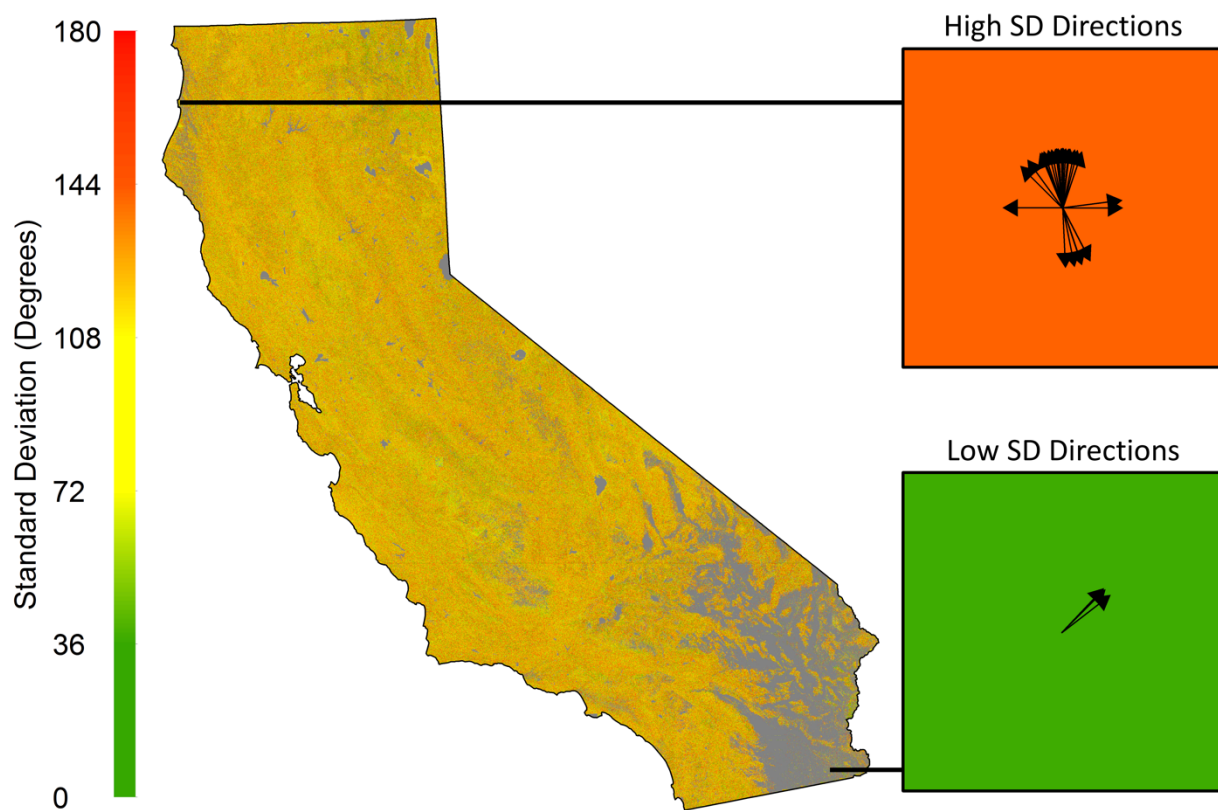
Figure 3.3: The standard deviation of bioclimatic niche velocity species direction by pixel. The upper right inset map demonstrations a location where 39 different species survive and a standard deviation of 156.1°. The lower right inset map demonstrates a location where 9 different species survive and a standard deviation of 2.5°. Grey land areas in the map indicate locations where none of the 72 species were predicted to occur during the modern era or always exhibited increased habitat suitability for all species present.

Forest community anisotropy summary: I identified 881 potential forest community types across California from the modern to future era, with 875 of communities displaying independent species migration within a forest community type (isotropic), covering 99.9% of California's forested land area.

Of all possible California forest community types, 8.7% California's forested land area contained pixels where <3 species occurred at the same location and had no Kuiper p-value to report (Table 3.4). Generally, the mean Kuiper p-value across all forest community types was 0.51, covering on average 14.0% of each forest types' distribution with dependent species migration directions (anisotropic), and 86.0% displaying independent species migration directions (isotropic) (Table 3.4).

Table 3.4: Summary of Kuiper and Clark-Evans statistics for all of California and the top 25 Californian forest community types, forest community types with significant mean Kuiper V values, and forest community types where significantly isotropic pixels are clustered. % cover is the fractional area of a forest community type over all of California's forest/woodland land areas. V p-value is the mean p-value from the Kuiper V test for each forest community type. % Isotropic is the fraction of pixels for a forest community type that had a significant Kuiper p-value (<=0.15), indicating the species within the forest classification are moving together.

Forest Type	% Cover	Mean V p-value	% Anisotropic	% Removed
California Summary				
Total California	100%	0.504	14.60%	8.70%
Top 25 CA Forest Types				
Multi-Montane	30.20%	0.503	14.70%	2.40%
Blue Oak	10.40%	0.501	15.00%	0.10%
California Live Oak	7.20%	0.499	15.50%	1.70%
Honey Mesquite	5.60%	0.504	14.50%	52.70%
California Juniper	3.30%	0.497	15.20%	2.00%
Singleleaf Pinyon	3.00%	0.502	14.60%	0.70%
Western Juniper	2.60%	0.523	13.40%	0.40%
Utah Juniper	2.50%	0.505	14.40%	2.60%
Jeffrey Pine	1.80%	0.51	13.60%	0.50%
Ponderosa Pine	1.70%	0.512	14.10%	0.70%
White Fir	1.70%	0.502	14.20%	0.70%
Coulter Pine	1.60%	0.509	13.90%	3.10%
Multi-Subalpine	1.60%	0.508	13.70%	1.30%
California White Oak	1.50%	0.519	12.70%	0.90%
Boxelder	1.40%	0.501	14.60%	0.00%
Desert Ironwood	1.10%	0.513	14.60%	51.70%
Interior Live Oak	1.00%	0.497	15.80%	0.60%
Canyon Live Oak	1.00%	0.496	15.50%	0.60%
Lodgepole Pine	0.90%	0.51	13.20%	1.10%
Douglas Fir	0.80%	0.503	15.10%	0.50%
California Black Oak	0.80%	0.493	15.60%	0.80%
Whitebark Pine	0.70%	0.511	14.00%	10.20%
Jeffrey Pine/White Fir	0.70%	0.505	14.00%	0.70%
Tanoak	0.60%	0.496	15.30%	9.60%
Singleleaf Pinyon/Utah Juniper	0.60%	0.507	14.20%	0.70%
Anisotropic Forest Types				
California Laurel/Monterey Pine	0.00%	0.144	50.00%	0.00%
California Buckeye/Chokecherry	0.00%	0.028	100.00%	0.00%
Giant Chinkapin/Pacific Dogwood	0.00%	0.136	100.00%	0.00%
Singleleaf Pinyon/Sweetgum	0.00%	0.123	100.00%	0.00%
California White Oak/White Alder	0.00%	0.022	100.00%	0.00%

3.5 DISCUSSION

3.5.1 Migration pressures: complex dynamics in space and time.

In this study, I showed that bioclimatic niche velocity direction vectors over the 21st century for 72 California tree species were estimated to have complex and individualized directional responses to climate change through time (Figure 3.3, Table 3.3). My directional estimates of potential species migration between the modern (1985-2015) and future (2070-2100) eras suggest that 65% of Californian tree species will generally respond to end-of-century climate change by moving in northern directions to cooler climates (0-45°, 315-360°) (Table 3.2, Figure 3.2) and is consistent with previous studies expecting plants will respond to warming climates by shifting to cooler, higher latitudes or elevations (Chen et al., 2011; Hughes, 2000; McCarty, 2001; Parmesan & Yohe, 2003).

However, I also demonstrated that species will not always respond to climate change by migrating to cooler environments at higher latitudes or elevations. My results support previous studies that have stressed the importance of not assuming species will move uphill or to higher latitudes in response to warming temperatures (Table 3.3, Figure 3.3). For example, Crimmins, Dobrowski, Greenberg, Abatzoglou, and Mynsberge (2011) found 64 Sierra Nevada tree species have shifted their optimal elevation downhill into warmer climates in response to increased regional water deficit. Zhu, Woodall, and Clark (2012) found of 94 eastern United States tree species, 58.7% of species underwent range contraction at their southern and northern ranges, with only 20.7% of species shifting north, and 16.3% of species shifting south. Similarly, while not a direct estimate of species migration, S. Z. Dobrowski et al. (2013) demonstrated how different climate variables can shift in different directions as climate changes, with climatic water balance velocities commonly pointing in opposing directions to temperature velocity, and that these differences in climate variables will have varying or opposing influences on biota from temperature. My results and these studies are reminders that species will respond according to their most limiting climate factors.

Individual species at a location commonly migrated independent of each other (Figure 3.3, Table 3.4). This suggests that as species move in response to end-of-century climate change, they may not migrate with each other, leading to shifts in the distributions of current forest communities, and consequently promoting the formation of novel forest communities in the future (community assemblages not seen during the modern era). Distributional and compositional changes in California forest communities have already occurred during modern climate change in the 20th century (1900-2009), where forest composition shifted towards more oak dominated communities, rather than pines, as a result of warming and increased water stress (McIntyre et al., 2015). Novel species' associations have been well documented in the paleorecord as well. For example, a carbon dating analysis identified unique communities of late Pleistocene micromammals (i.e. no-analogue communities) (Stafford et al., 1999) or early time periods (Wing et al., 2005). Similarly, high latitude terrestrial plant communities have shown changes in community composition during the Last Glacial Maximum (Jackson & Overpeck, 2000).

3.5.2: Implications of independent migration for community conservation:

Community conservation needs to incorporate updated climate change information, such as the results of this analysis, into existing and future conservation strategies and activities (Hannah, Midgley, Lovejoy, et al., 2002; Mawdsley, O'malley, & Ojima, 2009). As demonstrated by my analysis, the species of Californian forest communities will likely not remain stable relative to their modern distributions and species composition (Figure 3.3, Table 3.3, 3.4). Reserves developed under the assumption that modern communities will remain stable will ultimately fail if species within the reserve migrate outside of the static, protected-area (Hannah, Midgley, Lovejoy, et al., 2002; Noss & Harris, 1986). Similarly, conservation strategies based on the assumption that modern communities will continue to exist in the future will ultimately fail to protect biodiversity at risk from climate change, as current communities may not be capable of existing in future climates, and future no-analogue communities may not be recognized and included in future conservation efforts (Figure 3.1) (Hannah, Midgley, & Millar, 2002).

Recent adaptation strategies for conservation efforts have been proposed to help reduce the effects of climate change on biodiversity. These new methods tend to focus on managing and restoring ecosystem function over specific components (e.g. species, community, etc.) or revising and updating current conservation strategies by incorporating climate change information (Mawdsley et al., 2009). Likewise, the development of dynamic landscape conservation plans has been proposed as a possible new approach to conserve biodiversity by specifically including desired future habitat conditions based on anticipated shifts in the distribution of species or ecosystems, while intermediate conditions species may need to transition between current and future conditions and climate change (Hannah, Midgley, & Millar, 2002). Over recent decades, ecologists' investigations into climate change, and its influence on Earth's biota, have greatly increased my understanding of biodiversity-climate change interactions through advancements such as statistical downscaling (Easterling, 1999), climate velocity (Ackerly et al., 2010; S. Z. Dobrowski et al., 2013; Loarie et al., 2009; Sandel et al., 2011), species distribution models (Elith & Leathwick, 2009; Guisan et al., 2013; Thuiller et al., 2008), and much more. Therefore, current conservation strategies should be revised and updated, and/or new and dynamic conservation plans that reflect ecologists' current understanding of biodiversity-climate change interactions should be created and employed to ensure conservation management, strategies, and activities are as effective as possible.

3.5.3 Conclusions:

In this study I show how California forest communities, and the species that comprise those communities, migrate in directions independent of one another in response to climate change. While a majority of tree species are estimated to migrate in a northward direction as the climate warms over the coming century, a large number of tree species are expected to migrate in non-northern directions, highlighting that species will not always respond to temperature change alone, and it should not be assumed species will migrate northwards or up in elevation. Similarly, species occurring in the same locations do not necessarily migrate in the same direction as one another, indicating that each species

migrates independently of one another, and will likely form novel community assemblages by the end of the 21st century.

3.6 REFERENCES

Ackerly, D. D., Loarie, S. R., Cornwell, W. K., Weiss, S. B., Hamilton, H., Branciforte, R., & Kraft, N. J. B. (2010). The geography of climate change: implications for conservation biogeography. *Diversity and Distributions, 16*(3), 476-487. doi:10.1111/j.1472-4642.2010.00654.x

Allen, R. G., Pereira, L. S., Raes, D., & Smith, M. (1998). *Crop evapotranspiration-Guidelines for computing crop water requirements-FAO Irrigation and drainage paper 56* (Vol. 300): Irrigation and Drainage.

Allouche, O., Tsoar, A., & Kadmon, R. (2006). Assessing the accuracy of species distribution models: prevalence, kappa and the true skill statistic (TSS). *Journal of Applied Ecology, 43*(6), 1223-1232.

Breiman, L. (2001). Random forests. *Machine learning, 45*(1), 5-32.

California Fish and Game Code: section 2800–2835, Natural Community Conservation Planning Act, (2003).

Chen, I. C., Hill, J. K., Ohlemuller, R., Roy, D. B., & Thomas, C. D. (2011). Rapid Range Shifts of Species Associated with High Levels of Climate Warming. *Science, 333*(6045), 1024-1026. doi:10.1126/science.1206432

Christensen, G. A., Waddell, K. L., Stanton, S. M., & Kuegler, O. (2016). California's forest resources: Forest Inventory and Analysis, 2001–2010. *Gen. Tech. Rep. PNW-GTR-913. Portland, OR: US Department of Agriculture, Forest Service, Pacific Northwest Research Station. 293 p., 913*.

Clements, F. E. (1916). *Plant succession: an analysis of the development of vegetation*: Carnegie Institution of Washington.

Collins, S. L., Glenn, S. M., & Roberts, D. W. (1993). The hierarchical continuum concept. *Journal of Vegetation Science, 4*(2), 149-156.

Crimmins, S. M., Dobrowski, S. Z., Greenberg, J. A., Abatzoglou, J. T., & Mynsberge, A. R. (2011). Changes in Climatic Water Balance Drive Downhill Shifts in Plant Species' Optimum Elevations. *Science, 331*(6015), 324-327. doi:10.1126/science.1199040

Cutler, D. R., Edwards Jr, T. C., Beard, K. H., Cutler, A., Hess, K. T., Gibson, J., & Lawler, J. J. (2007). Random forests for classification in ecology. *Ecology, 88*(11), 2783-2792.

Davis, M. B. (1992). Changes in geographical range resulting from greenhouse warming: effects on biodiversity in forests. *Global warming and biological diversity*, 297-308.

Davis, M. B., & Shaw, R. G. (2001). Range shifts and adaptive responses to Quaternary climate change. *Science, 292*(5517), 673-679.

Dingman, S. (2002). Water in soils: infiltration and redistribution. Physical hydrology. In: upper saddle river, New Jersey: Prentice-Hall, Inc.

Dobrowski, S. Z. (2011). A climatic basis for microrefugia: the influence of terrain on climate. *Global change biology, 17*(2), 1022-1035.

Dobrowski, S. Z., Abatzoglou, J., Swanson, A. K., Greenberg, J. A., Mynsberge, A. R., Holden, Z. A., & Schwartz, M. K. (2013). The climate velocity of the contiguous United States during the 20th century. *Global change biology, 19*(1), 241-251. doi:10.1111/gcb.12026

Easterling, D. R. (1999). Development of regional climate scenarios using a downscaling approach. *Climatic Change, 41*(3-4), 615-634.

Elith, J., & Leathwick, J. R. (2009). Species Distribution Models: Ecological Explanation and Prediction Across Space and Time. *Annual Review of Ecology Evolution and Systematics, 40*, 677-697. doi:10.1146/annurev.ecolsys.110308.120159

Fisher, N. I. (1995). *Statistical analysis of circular data*: Cambridge University Press.

Franklin, J. F. (1993). Preserving biodiversity: species, ecosystems, or landscapes? *Ecological Applications, 3*(2), 202-205.

Gent, P. R., Danabasoglu, G., Donner, L. J., Holland, M. M., Hunke, E. C., Jayne, S. R., . . . Zhang, M. H. (2011). The Community Climate System Model Version 4. *Journal of Climate, 24*(19), 4973-4991. doi:10.1175/2011jcli4083.1

Gleason, H. A. (1926). The individualistic concept of the plant association. *Bulletin of the Torrey botanical club*, 7-26.

Greenberg, J. A., Dobrowski, S. Z., Ramirez, C. M., Tuil, J. L., & Ustin, S. L. (2006). A bottom-up approach to vegetation mapping of the Lake Tahoe Basin using hyperspatial image analysis. *Photogrammetric Engineering & Remote Sensing, 72*(5), 581-589.

Guisan, A., Tingley, R., Baumgartner, J. B., Naujokaitis-Lewis, I., Sutcliffe, P. R., Tulloch, A. I., . . . Mantyka-Pringle, C. (2013). Predicting species distributions for conservation decisions. *Ecology Letters, 16*(12), 1424-1435.

Hannah, L., Midgley, G., Lovejoy, T., Bond, W., Bush, M., Lovett, J., . . . Woodward, F. (2002). Conservation of biodiversity in a changing climate. *Conservation biology, 16*(1), 264-268.

Hannah, L., Midgley, G. F., & Millar, D. (2002). Climate change-integrated conservation strategies. *Global Ecology and Biogeography, 11*(6), 485-495.

Hickling, R., Roy, D. B., Hill, J. K., Fox, R., & Thomas, C. D. (2006). The distributions of a wide range of taxonomic groups are expanding polewards. *Global change biology, 12*(3), 450-455.

Hijmans, R. J., Phillips, S., Leathwick, J., Elith, J., & Hijmans, M. R. J. (2017). Package 'dismo'. *Circles, 9*(1).

Hughes, L. (2000). Biological consequences of global warming: is the signal already apparent? *Trends in Ecology & Evolution, 15*(2), 56-61.

Huntley, B., & Webb III, T. (1989). Migration: species' response to climatic variations caused by changes in the earth's orbit. *Journal of Biogeography*, 5-19.

Hutchinson, G. (1957). Concluding remarks Cold ssring Harbor Symp. *Quant, 22*, 66-77.

Jackson, S. T., & Overpeck, J. T. (2000). Responses of plant populations and communities to environmental changes of the late Quaternary. *Paleobiology, 26*(4), 194-220. doi:10.1666/0094-8373(2000)26[194:Roppac]2.0.Co;2

Jewell, S. D. (2000). Multi-species recovery plans. *Endangered Species, 25*(3), 31.

Kluzek, E. (2011). CCSM research tools: CLM4. 0 user's guide documentation. In.

Kuiper, N. H. (1960). *Tests concerning random points on a circle.* Paper presented at the Nederl. Akad. Wetensch. Proc. Ser. A.

Liu, C., Berry, P. M., Dawson, T. P., & Pearson, R. G. (2005). Selecting thresholds of occurrence in the prediction of species distributions. *Ecography, 28*(3), 385-393.

Loarie, S. R., Duffy, P. B., Hamilton, H., Asner, G. P., Field, C. B., & Ackerly, D. D. (2009). The velocity of climate change. *Nature, 462*(7276), 1052-U1111. doi:10.1038/nature08649

Mawdsley, J. R., O'malley, R., & Ojima, D. S. (2009). A review of climate-change adaptation strategies for wildlife management and biodiversity conservation. *Conservation biology, 23*(5), 1080-1089.

McCarty, J. P. (2001). Ecological consequences of recent climate change. *Conservation biology, 15*(2), 320-331.

McGlone, M. S. (1996). When history matters: scale, time, climate and tree diversity. *Global Ecology and Biogeography Letters*, 309-314.

McIntyre, P. J., Thorne, J. H., Dolanc, C. R., Flint, A. L., Flint, L. E., Kelly, M., & Ackerly, D. D. (2015). Twentieth-century shifts in forest structure in California: Denser forests, smaller trees, and increased dominance of oaks. *Proceedings of the National Academy of Sciences, 112*(5), 1458-1463.

Melnik, M., & Pusev, R. (2015). Package 'uniftest' (Version 1.1). Retrieved from https://cran.r-project.org/web/packages/uniftest/uniftest.pdf

Menne, M. J., Durre, I., Vose, R. S., Gleason, B. E., & Houston, T. G. (2012). An Overview of the Global Historical Climatology Network-Daily Database. *Journal of Atmospheric and Oceanic Technology, 29*(7), 897-910. doi:10.1175/Jtech-D-11-00103.1

Noss, R. F., & Harris, L. D. (1986). Nodes, networks, and MUMs: preserving diversity at all scales. *Environmental management, 10*(3), 299-309.

Olden, J. D. (2003). A species-specific approach to modeling biological communities and its potential for conservation. *Conservation biology, 17*(3), 854-863.

Parmesan, C., & Yohe, G. (2003). A globally coherent fingerprint of climate change impacts across natural systems. *Nature, 421*(6918), 37-42.

Sala, O. E., Chapin, F. S., Armesto, J. J., Berlow, E., Bloomfield, J., Dirzo, R., . . . Kinzig, A. (2000). Global biodiversity scenarios for the year 2100. *Science, 287*(5459), 1770-1774.

Sandel, B., Arge, L., Dalsgaard, B., Davies, R. G., Gaston, K. J., Sutherland, W. J., & Svenning, J. C. (2011). The Influence of Late Quaternary Climate-Change Velocity on Species Endemism. *Science, 334*(6056), 660-664. doi:10.1126/science.1210173

Schoonmaker, P. K., & Foster, D. R. (1991). Some implications of paleoecology for contemporary ecology. *The Botanical Review, 57*(3), 204-245.

Serra-Diaz, J. M., Franklin, J., Ninyerola, M., Davis, F. W., Syphard, A. D., Regan, H. M., & Ikegami, M. (2014). Bioclimatic velocity: the pace of species exposure to climate change. *Diversity and Distributions, 20*(2), 169-180.

Smith, W. B. (2002). Forest inventory and analysis: a national inventory and monitoring program. *Environmental pollution, 116*, S233-S242.

Stafford, J. T. W., Semken, J. H. A., Graham, R. W., Klippel, W. F., Markova, A., Smirnov, N. G., & Southon, J. (1999). First accelerator mass spectrometry 14C dates documenting contemporaneity of nonanalog species in late Pleistocene mammal communities. *Geology, 27*(10), 903-906.

Stephenson, N. L. (1998). Actual evapotranspiration and deficit: biologically meaningful correlates of vegetation distribution across spatial scales. *Journal of Biogeography, 25*(5), 855-870. doi:DOI 10.1046/j.1365-2699.1998.00233.x

Thomas, C. D. (2010). Climate, climate change and range boundaries. *Diversity and Distributions, 16*(3), 488-495.

Thuiller, W., Albert, C., Araujo, M. B., Berry, P. M., Cabeza, M., Guisan, A., . . . Zimmermann, N. E. (2008). Predicting global change impacts on plant species' distributions: Future challenges. *Perspectives in Plant Ecology Evolution and Systematics, 9*(3-4), 137-152. doi:10.1016/j.ppees.2007.09.004

Underwood, E. C., Klausmeyer, K. R., Morrison, S. A., Bode, M., & Shaw, M. R. (2009). Evaluating conservation spending for species return: A retrospective analysis in California. *Conservation Letters, 2*(3), 130-137.

Urbanska, K. M. (2000). Environmental conservation and restoration ecology: two facets of the same problem. *Web Ecology, 1*(1), 20-27.

USGS. (2016). *The National Map*. Retrieved from: http://nationalmap.gov/3DEP/3dep_prodserv.html

Walther, G.-R., Post, E., Convey, P., Menzel, A., Parmesan, C., Beebee, T. J., . . . Bairlein, F. (2002). Ecological responses to recent climate change. *Nature, 416*(6879), 389.

Williams, J. W., & Jackson, S. T. (2007). Novel climates, no-analog communities, and ecological surprises. *Frontiers in Ecology and the Environment, 5*(9), 475-482. doi:10.1890/070037

Wing, S. L., Harrington, G. J., Smith, F. A., Bloch, J. I., Boyer, D. M., & Freeman, K. H. (2005). Transient floral change and rapid global warming at the Paleocene-Eocene boundary. *Science, 310*(5750), 993-996.

Young, T. P. (2000). Restoration ecology and conservation biology. *Biological conservation, 92*(1), 73-83.

Zhu, K., Woodall, C. W., & Clark, J. S. (2012). Failure to migrate: lack of tree range expansion in response to climate change. *Global change biology, 18*(3), 1042-1052. doi:10.1111/j.1365-2486.2011.02571.x

CONCLUSIONS

In my dissertation, I addressed the following major topics: 1) the effects of spatial resolution on climate change estimates, 2) the suitability of climate velocity as a species migration estimate, and 3) the direction species will migrate in response to climate change relative to community dynamics. The three studies presented in this dissertation contain important findings towards understanding how species may have, or will, respond to climate change. The models, particularly bioclimatic niche velocity, are applicable to many ecological analyses, from local to global. As with all research, further developments are necessary to reduce uncertainties, better validate the approaches, and understand biological responses to climate change.

Chapter 1, "Spatial scale affects novel and disappeared climate change projections in Alaska" produced eight novel and disappeared climate maps for 10 different climate variables ranging in spatial resolutions from 60 m to 12 km in Alaska from the LGM to modern era. Results suggest that as the spatial resolution of gridded climate data becomes coarser, the fraction of novel and disappeared climate estimated increases, although it is possible for the fractional area of novel and disappeared climates to decrease or have no apparent relationship with spatial resolution. Disappeared climates occurred through Alaska, although generally appeared more within interior and northern Alaska, resulting from extremely cold LGM temperatures warming into the modern era, and reduced modern evaporative demand. Novel climates were primarily restricted to the southern, coastal regions of Alaska where modern climate has warmed significantly, resulting in more precipitation falling as rain, rather than snow. My investigation into how the spatial resolution of gridded climate affects the amount of novel and disappeared climates reinforces the importance of downscaling coarse climate data and suggest that studies analyzing the effects of climate change on ecosystems may overestimate or underestimate their conclusions when utilizing coarse climate data.

Chapter 2, "Is climate velocity an adequate measure of species migration responses to climate change?" produced climate velocities surfaces for eight climate variables as well as the bioclimatic niche

velocity of white spruce from the LGM to modern era in Alaska using my downscaled climate data presented in Chapter 1. My results demonstrate that climate velocity alone does not provide suitable estimates of species migration responses to climate change due to climate velocity not accounting for species ecology and climatic tolerances that affect migration responses. These results may help explain unexpected or conflicting observational evidence of climate-driven species range shifts presented in previous climate velocity analyses and other migration studies, as well as provide an efficient and less time-consuming approach to estimate, predict, and manage future species migration in light of climate change.

Finally, Chapter 3, "California forest community migration responses to 21st century climate change" produced estimates of the direction 72 native California tree species will migrate in response to end-of-century climate change. My results suggest that many California tree species will migrate in Northern directions, however, multiple species will migrate in non-northern or uphill directions in response to climate change, re-emphasizing the importance that many species may not responds to future temperature change. Similarly, my results demonstrated that species of a California forest community type, at the same location, migrate independent of one another, in different directions, suggesting that modern forest communities are not stable and may form novel community assemblages with future climate change. I hope these results encourage community conservation managers to revise and update their current methods to include more dynamic reserve strategies that support independent species migration and unstable community assemblages through time as the climate continues to shift into the future.

Appendix A: SDM validation statistics for all California tree species.

Common Name	Correlation	% Bias	RMSE	# Present
Arizona Cypress	1.00	0.00	0.00	1
Baker or Modoc Cypress	1.00	0.00	0.00ß	2
Bigcone Douglas Fir	1.00	0.43	0.04	26
Bigleaf Maple	0.96	4.52	0.15	276
Bishop Pine	1.00	0.20	0.03	11
Bitter Cherry	1.00	0.50	0.05	28
Black Cottonwood	1.00	0.29	0.04	16
Blue Oak	0.94	6.29	0.17	554
Boxelder	1.00	0.09	0.02	6
Brewer Spruce	1.00	0.18	0.03	10
California Black Oak	0.83	19.56	0.31	1136
California Buckeye	0.98	2.66	0.11	145
California Juniper	0.99	1.34	0.08	129
California Laurel	0.95	5.88	0.17	349
California Live Oak	0.96	4.74	0.15	336
California Red Fir	0.93	8.08	0.19	463
California Sycamore	1.00	0.38	0.04	23
California Torreya (Nutmeg)	0.99	0.58	0.05	30
California White Oak	0.98	1.84	0.09	123
Canyon Live Oak	0.84	17.69	0.29	1053
Chokecherry	1.00	0.09	0.02	5
Coulter Pine	1.00	0.44	0.05	38
Curlleaf Mountain Mahogany	0.96	4.33	0.14	247

Appendix A Continued (2)

Common Name	Correlation	% Bias	RMSE	*# Present*
Desert Ironwood	1.00	0.00	0.00	8
Douglas Fir	0.76	29.13	0.37	1790
Engelmann Oak	1.00	0.16	0.03	10
Engelmann Spruce	1.00	0.02	0.01	2
Foxtail Pine	1.00	0.29	0.04	24
Fremont Cottonwood	1.00	0.18	0.03	11
Giant Chinkapin, Golden Chinkapin	0.99	1.47	0.08	88
Giant Sequoia	1.00	0.13	0.03	7
Grand Fir	0.99	0.94	0.07	47
Gray or California Foothill Pine	0.94	6.08	0.17	372
Great Basin Bristlecone Pine	1.00	0.00	0.00	6
Honey Mesquite	1.00	0.00	0.00	8
Incense Cedar	0.83	19.87	0.30	1068
Interior Live Oak	0.93	7.23	0.18	416
Jeffrey Pine	0.88	13.11	0.25	782
Knobcone Pine	0.99	1.58	0.09	99
Limber Pine	1.00	0.34	0.04	20
Lodgepole Pine	0.94	6.30	0.17	403
Monterey Cypress	1.00	0.02	0.01	7
Monterey Pine	1.00	0.16	0.03	7
Mountain Hemlock	0.98	1.63	0.09	86
Noble Fir	1.00	0.04	0.02	5
Oregon Ash	0.99	0.56	0.05	33
Oregon White Oak	0.96	3.96	0.14	245
Pacific Dogwood	0.98	2.19	0.10	119
Pacific Madrone	0.91	10.05	0.22	613

Common Name	Correlation	% Bias	RMSE	# *Present*
Pacific Silver Fir	1.00	0.09	0.02	1
Pacific Yew	0.99	0.63	0.05	33
Ponderosa Pine	0.80	22.65	0.33	1441
Port Orford Cedar	1.00	0.31	0.04	19
Quaking Aspen	0.99	0.72	0.06	40
Red Alder	0.98	1.77	0.09	113
Redwood	0.95	5.40	0.16	297
Sargent's Cypress	1.00	0.13	0.03	7
Shasta Red Fir	0.99	0.90	0.06	57
Singleleaf Pinyon	0.97	3.49	0.13	288
Sitka Spruce	1.00	0.27	0.04	21
Subalpine Fir	1.00	0.09	0.02	2
Sugar Pine	0.86	16.55	0.28	972
Sweetgum	1.00	0.00	0.00	1
Tanoak	0.91	9.45	0.21	603
Utah Juniper	0.99	0.98	0.07	57
Washoe Pine	1.00	0.00	0.00	6
Western Hemlock	0.99	0.76	0.06	44
Western Juniper	0.95	5.53	0.16	467
Western White Pine	0.95	5.07	0.15	279
White Alder	0.99	1.39	0.08	76
Whitebark Pine	0.99	1.08	0.07	82
White Fir	0.79	24.01	0.34	1492

APPENDIX B: SDM Variable Importance of CA Trees

Appendix B: Random forest model variable importance for all species and each climate variable. Importance are reported as % increase in MSE.

Common Name	AET	DEF	PET	RAD	Rain	Snow	T_{ave}	T_{max}	T_{min}
Arizona Cypress	0.060	0.110	0.060	0.000	0.030	0.030	0.050	0.150	0.040
Baker or Modoc Cypress	0.050	0.220	0.050	0.120	0.050	0.090	0.160	0.210	0.070
Bigcone Douglas Fir	0.160	0.170	0.300	0.070	0.140	0.140	0.180	0.140	0.200
Bigleaf Maple	0.190	0.180	0.150	0.220	0.170	0.120	0.210	0.170	0.170
Bishop Pine	0.120	0.080	0.100	0.110	0.150	0.050	0.250	0.200	0.260
Bitter Cherry	0.180	0.200	0.290	0.220	0.140	0.150	0.190	0.220	0.210
Black Cottonwood	0.160	0.190	0.230	0.210	0.140	0.120	0.160	0.180	0.240
Blue Oak	0.110	0.130	0.110	0.050	0.130	0.120	0.200	0.200	0.130
Boxelder	0.140	0.110	0.200	0.220	0.100	0.020	0.220	0.240	0.210
Brewer Spruce	0.090	0.170	0.080	0.220	0.140	0.090	0.130	0.240	0.140
California Black Oak	0.060	0.060	0.070	0.040	0.080	0.070	0.120	0.090	0.090
California Buckeye	0.180	0.190	0.200	0.240	0.180	0.130	0.220	0.240	0.170
California Juniper	0.170	0.150	0.180	0.100	0.170	0.130	0.210	0.190	0.160
California Laurel	0.170	0.260	0.300	0.090	0.180	0.130	0.250	0.240	0.200
California Live Oak	0.170	0.140	0.150	0.160	0.150	0.090	0.250	0.150	0.210
California Red Fir	0.150	0.120	0.180	0.090	0.140	0.050	0.270	0.110	0.210
California Sycamore	0.110	0.140	0.130	0.060	0.100	0.170	0.210	0.240	0.170
California Torreya (Nutmeg)	0.170	0.190	0.210	0.110	0.220	0.030	0.280	0.180	0.230
California White Oak	0.140	0.140	0.230	0.300	0.150	0.110	0.190	0.210	0.200
Canyon Live Oak	0.190	0.200	0.190	0.140	0.210	0.080	0.240	0.280	0.220
Chokecherry	0.060	0.060	0.070	0.050	0.070	0.080	0.130	0.080	0.110
Coulter Pine	0.090	0.150	0.110	0.200	0.070	0.070	0.140	0.230	0.100

Appendix B Continued (2)

Common Name	AET	DEF	PET	RAD	Rain	Snow	T_{ave}	T_{max}	T_{min}
Curlleaf Mountain Mahogany	0.180	0.270	0.300	0.090	0.150	0.090	0.230	0.190	0.180
Desert Ironwood	0.180	0.200	0.200	0.110	0.180	0.230	0.180	0.190	0.260
Douglas Fir	0.020	0.180	0.040	0.010	0.040	0.000	0.120	0.110	0.010
Engelmann Oak	0.030	0.040	0.020	0.000	0.050	0.020	0.020	0.030	0.020
Engelmann Spruce	0.080	0.210	0.260	0.100	0.180	0.010	0.170	0.230	0.160
Foxtail Pine	0.090	0.210	0.060	0.210	0.150	0.020	0.050	0.140	0.060
Fremont Cottonwood	0.100	0.220	0.100	0.040	0.220	0.180	0.160	0.210	0.040
Giant Chinkapin, Golden Chinkapin	0.160	0.200	0.190	0.190	0.110	0.030	0.230	0.260	0.230
Giant Sequoia	0.230	0.190	0.160	0.130	0.270	0.150	0.200	0.250	0.170
Grand Fir	0.230	0.200	0.180	0.090	0.200	0.190	0.170	0.110	0.150
Gray or California Foothill Pine	0.270	0.220	0.180	0.120	0.190	0.030	0.240	0.240	0.260
Great Basin Bristlecone Pine	0.210	0.050	0.210	0.060	0.180	0.210	0.140	0.110	0.150
Honey Mesquite	0.150	0.110	0.050	0.060	0.140	0.010	0.080	0.220	0.050
Incense Cedar	0.050	0.060	0.060	0.040	0.070	0.090	0.120	0.050	0.120
Interior Live Oak	0.130	0.140	0.160	0.080	0.140	0.100	0.210	0.200	0.190
Jeffrey Pine	0.090	0.110	0.100	0.070	0.110	0.160	0.140	0.120	0.110
Knobcone Pine	0.230	0.250	0.210	0.140	0.270	0.120	0.180	0.240	0.210
Limber Pine	0.170	0.130	0.260	0.070	0.230	0.270	0.170	0.150	0.130
Lodgepole Pine	0.160	0.130	0.150	0.080	0.160	0.170	0.230	0.230	0.170
Monterey Cypress	0.110	0.040	0.010	0.100	0.070	0.000	0.090	0.020	0.120
Monterey Pine	0.070	0.110	0.150	0.120	0.110	0.020	0.240	0.130	0.220
Mountain Hemlock	0.110	0.160	0.120	0.100	0.140	0.160	0.270	0.270	0.200
Noble Fir	0.190	0.070	0.210	0.080	0.160	0.200	0.120	0.070	0.140
Oregon Ash	0.190	0.190	0.200	0.200	0.160	0.100	0.280	0.260	0.240
Oregon White Oak	0.210	0.230	0.180	0.110	0.210	0.130	0.190	0.190	0.170

Appendix B Continued (3)

Common Name	AET	DEF	PET	RAD	Rain	Snow	T_{ave}	T_{max}	T_{min}
Pacific Dogwood	0.190	0.190	0.180	0.220	0.250	0.160	0.220	0.200	0.220
Pacific Madrone	0.170	0.160	0.120	0.070	0.190	0.120	0.130	0.100	0.130
Pacific Silver Fir	0.040	0.020	0.040	0.010	0.030	0.110	0.080	0.050	0.140
Pacific Yew	0.180	0.150	0.200	0.230	0.160	0.190	0.250	0.200	0.220
Ponderosa Pine	0.050	0.050	0.070	0.020	0.030	0.060	0.080	0.050	0.060
Port Orford Cedar	0.240	0.140	0.160	0.150	0.180	0.080	0.150	0.240	0.130
Quaking Aspen	0.130	0.170	0.180	0.120	0.250	0.190	0.230	0.250	0.290
Red Alder	0.270	0.100	0.220	0.140	0.220	0.090	0.230	0.190	0.160
Redwood	0.190	0.120	0.150	0.070	0.150	0.040	0.200	0.150	0.230
Sargent's Cypress	0.130	0.200	0.210	0.120	0.220	0.030	0.200	0.120	0.210
Shasta Red Fir	0.150	0.250	0.200	0.060	0.130	0.180	0.250	0.250	0.150
Singleleaf Pinyon	0.230	0.270	0.200	0.050	0.140	0.160	0.130	0.150	0.130
Sitka Spruce	0.230	0.080	0.230	0.090	0.160	0.010	0.190	0.130	0.210
Subalpine Fir	0.020	0.020	0.120	0.050	0.010	0.050	0.080	0.290	0.020
Sugar Pine	0.070	0.090	0.090	0.050	0.090	0.090	0.150	0.100	0.130
Sweetgum	0.020	0.020	0.050	0.120	0.020	0.000	0.040	0.140	0.100
Tanoak	0.180	0.130	0.100	0.060	0.150	0.120	0.130	0.130	0.120
Utah Juniper	0.300	0.240	0.120	0.080	0.210	0.160	0.100	0.120	0.140
Washoe Pine	0.200	0.130	0.150	0.060	0.200	0.170	0.120	0.160	0.170
Western Hemlock	0.240	0.130	0.180	0.140	0.250	0.040	0.220	0.210	0.190
Western Juniper	0.130	0.200	0.150	0.070	0.150	0.180	0.140	0.150	0.200
Western White Pine	0.120	0.140	0.150	0.060	0.110	0.160	0.240	0.290	0.180
White Alder	0.190	0.190	0.220	0.250	0.170	0.160	0.220	0.180	0.210
Whitebark Pine	0.030	0.030	0.030	0.010	0.030	0.060	0.100	0.060	0.080
White Fir	0.120	0.090	0.190	0.040	0.150	0.220	0.290	0.200	0.100